https://www.mdc-berlin.de/de/veroeffentlichungstypen/clinical-journal-club

Als gemeinsame Einrichtung von MDC und Charité fördert das Experimental and Clinical Research Center die Zusammenarbeit zwischen Grundlagenwissenschaftlern und klinischen Forschern. Hier werden neue Ansätze für Diagnose, Prävention und Therapie von Herz-Kreislauf- und Stoffwechselerkrankungen, Krebs sowie neurologischen Erkrankungen entwickelt und zeitnah am Patienten eingesetzt. Sie sind eingeladen, uns beizutreten. Bewerben Sie sich!

A 56-year-old woman with rheumatoid arthritis presented to the dermatology clinic with a 2-month history of an extremely itchy rash. She had been treated with tofacitinib and methotrexate for the previous 4 years. On physical examination, large patches of erythematous skin with overlying scales, crusting, and deep fissures were seen on the chest, upper arms, neck, abdomen, buttocks, and thighs. Similar findings were noted on the hands, with sparing of the nails. Which of the following is the most likely diagnosis?

Atopic Dermatitis

Crusted Scabies

Cutaneous T-cell lymphoma

Erythroderma

Psoriasis

Crusted scabies is a severe and highly contagious variant of scabies that most commonly affects immunocompromised persons. The diagnosis is made by identifying mites and eggs in microscopic examination of skin scrapings, as were seen in this case. Management of crusted scabies includes systemic therapy with ivermectin plus a topical agent.

Crusted scabies, also known as Norwegian scabies, is a severe and highly contagious form of scabies characterized by thick, scaly, crusty skin and a massive infestation of mites (often millions). Unlike typical scabies, it may not cause intense itching, and the rash may be less obvious. Crusted scabies is most common in individuals with weakened immune systems, the elderly, or those with disabilities.

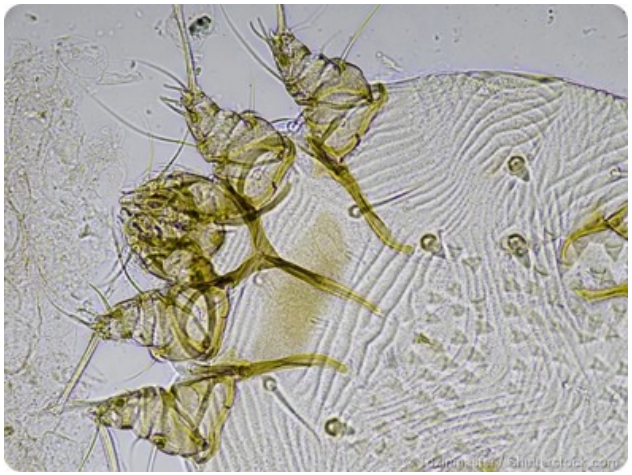

Das Multiple Myelom, kurz MM, ist eine maligne Erkrankung, die zu den B-Zell-Lymphomen gerechnet wird. Sie ist durch eine monoklonale Vermehrung von Plasmazellen im Knochenmark charakterisiert. In der Folge kommt es zu einer vermehrten Produktion kompletter oder inkompletter Immunglobuline, die als Paraproteine bezeichnet werden. Die genaue Ätiologie ist bislang (2023) unklar. Nach WHO-Definition lautet die Bezeichnung Plasmazellmyelom.

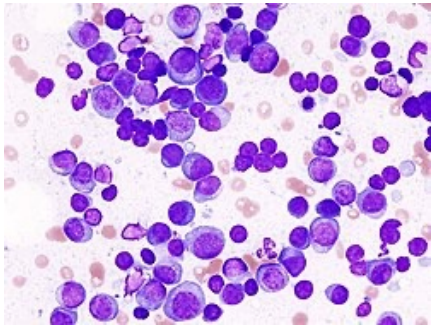

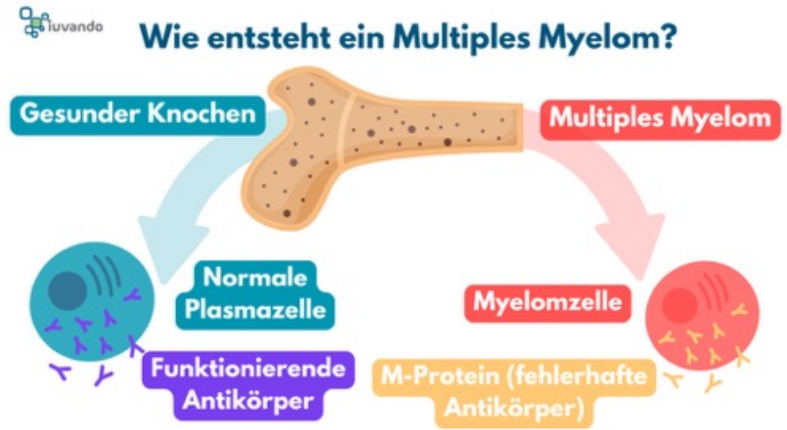

Um asymptomatische Patienten mit einem hohen Risiko für eine schnelle Progression der Erkrankung zu identifizieren, wurden die CRAB-Kriterien 2014 durch die International Myeloma Working Group aktualisiert und um Biomarker erweitert.

Current treatment of multiple myeloma

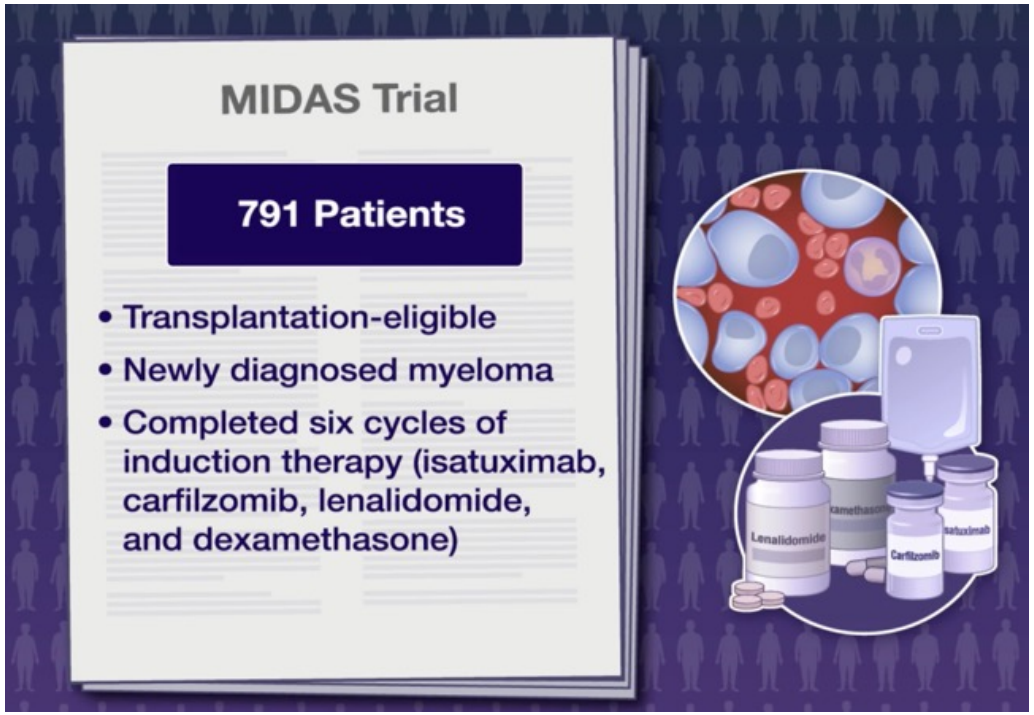

Isatuximab = anti CD38

Carfilzomib = Proteosome inhibitor

Lenalidomide = Molecular „glue“ immune modulator

Dexamethasone = Glucocorticoid

Abbreviated IsaKRD

Then sequencing is done to determine minimal residual disease + or -

ASCT steht für autologe Stammzelltransplantation (autologous stem cell transplantation). Im Deutschen wird dies als autologe Stammzelltransplantation bezeichnet. Es ist ein medizinisches Verfahren, bei dem patienteneigene Stammzellen verwendet werden, um das Knochenmark nach einer Hochdosis-Chemotherapie zu ersetzen.

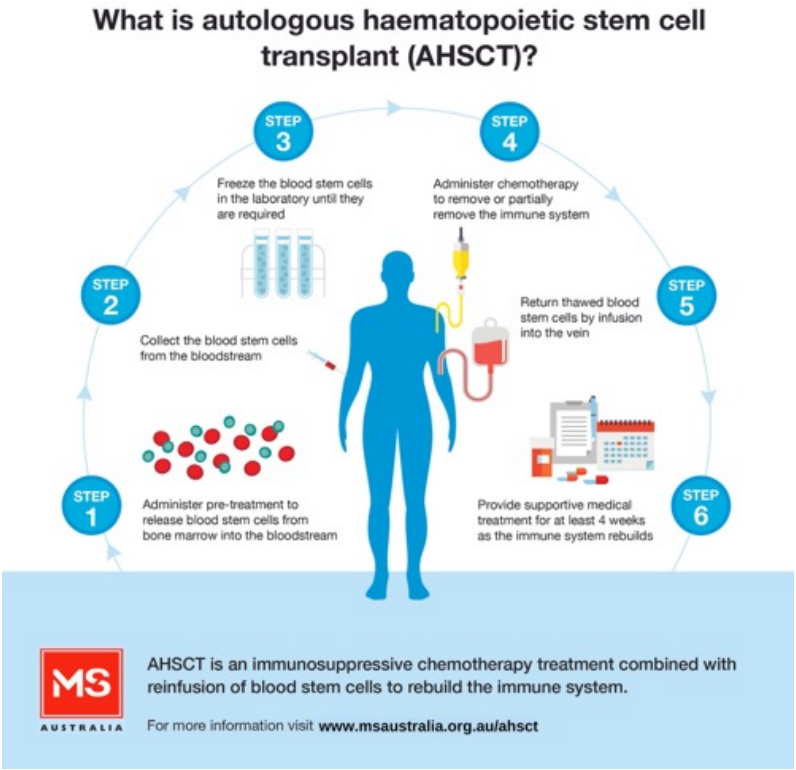

4 treatment regimens were used
In Minimum-Residual-Dissease + or –
Patients.

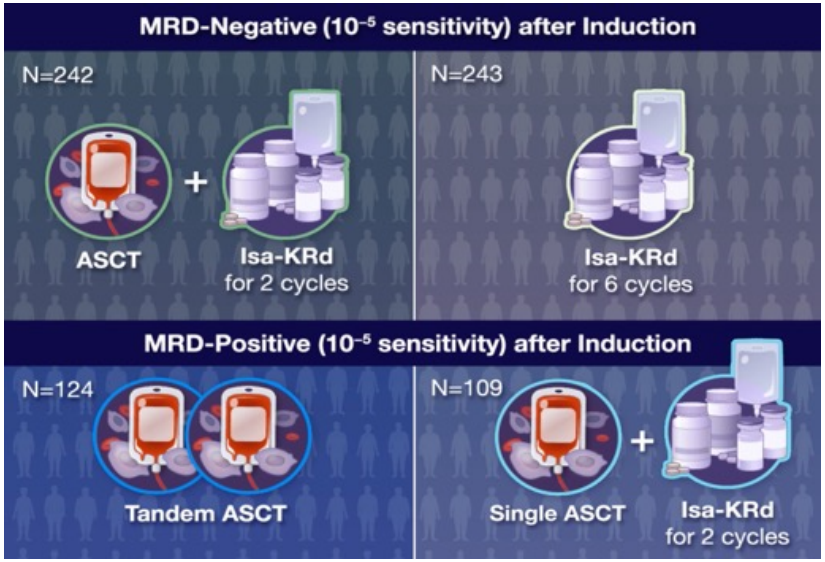

Next-Generation Sequencing (NGS):
NGS analyzes the unique DNA sequences of myeloma cells to identify and quantify residual cancer cells. It also achieves high sensitivity, reaching levels of 1 in 1,000,000 cells or even higher.

Measurable Residual Disease–Guided Therapy in Newly Diagnosed Myeloma

Measurable residual disease (MRD) is a major prognostic factor in newly diagnosed multiple myeloma. An assessment of an MRD-guided consolidation strategy in patients who are eligible for autologous stem-cell transplantation (ASCT) may be useful. In this phase 3 trial, we randomly assigned transplantation-eligible patients with newly diagnosed myeloma who had completed induction therapy with isatuximab, carfilzomib, lenalidomide, and dexamethasone (Isa-KRd). Patients who were MRD-negative at 10^{-5} sensitivity (i.e., <1 cancer cell per 100,000 normal cells, as assessed by next-generation sequencing) were assigned to undergo ASCT and receive Isa-KRd for two cycles (ASCT group) or to receive Isa-KRd for six cycles (Isa-KRd group). Patients who were MRD-positive at 10^{-5} sensitivity were assigned to undergo tandem ASCT (two ASCTs within a short period; tandem ASCT group) or to undergo ASCT and receive Isa-KRd for two cycles (single ASCT group). The primary end point was an MRD-negative status at 10^{-6} sensitivity before maintenance therapy.

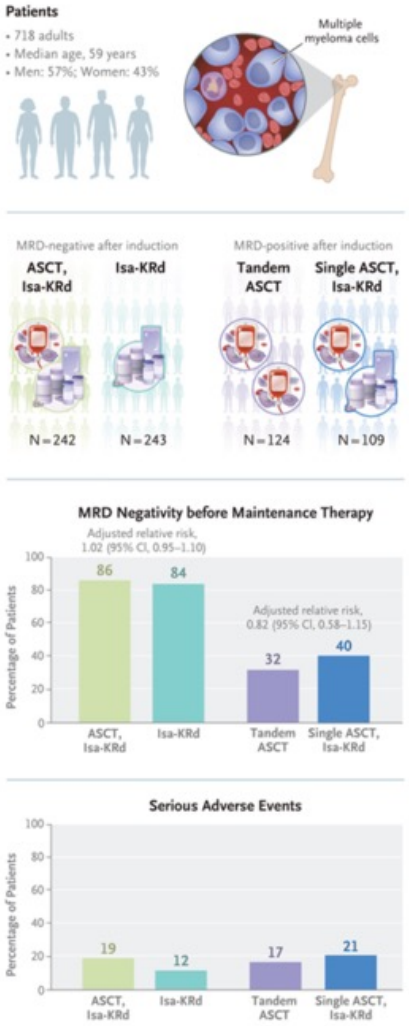

Quadruplet induction therapy followed by autologous stem-cell transplantation (ASCT) is the new standard care for transplantation-eligible patients with newly diagnosed multiple myeloma. In several phase 3 trials in which progression-free survival was evaluated in such patients, bortezomib–thalidomide–dexamethasone (VTd) plus daratumumab was superior to VTd alone, and bortezomib–lenalidomide–dexamethasone (VRd) plus either daratumumab or isatuximab was superior to VRd alone. Quadruplet regimens made up of an anti-CD38 monoclonal antibody, carfilzomib, lenalidomide, and dexamethasone also showed a high level of efficacy in transplantation-eligible patients with newly diagnosed myeloma, particularly those with high-risk disease.

Measurable residual disease (MRD) is an independent prognostic factor that has been shown to be a predictor of both progression-free survival and overall survival in patients with newly diagnosed myeloma.

We conducted the MIDAS (Minimal Residual Disease Adaptive Strategy) trial to address these issues. Patients who had received quadruple induction therapy (isatuximab, carfilzomib, lenalidomide, and dexamethasone [Isa-KRd]) for six cycles were randomly assigned to one of four consolidation therapy groups according to MRD status after induction. Here, we report the results from an analysis of this MRD-adapted consolidation strategy.

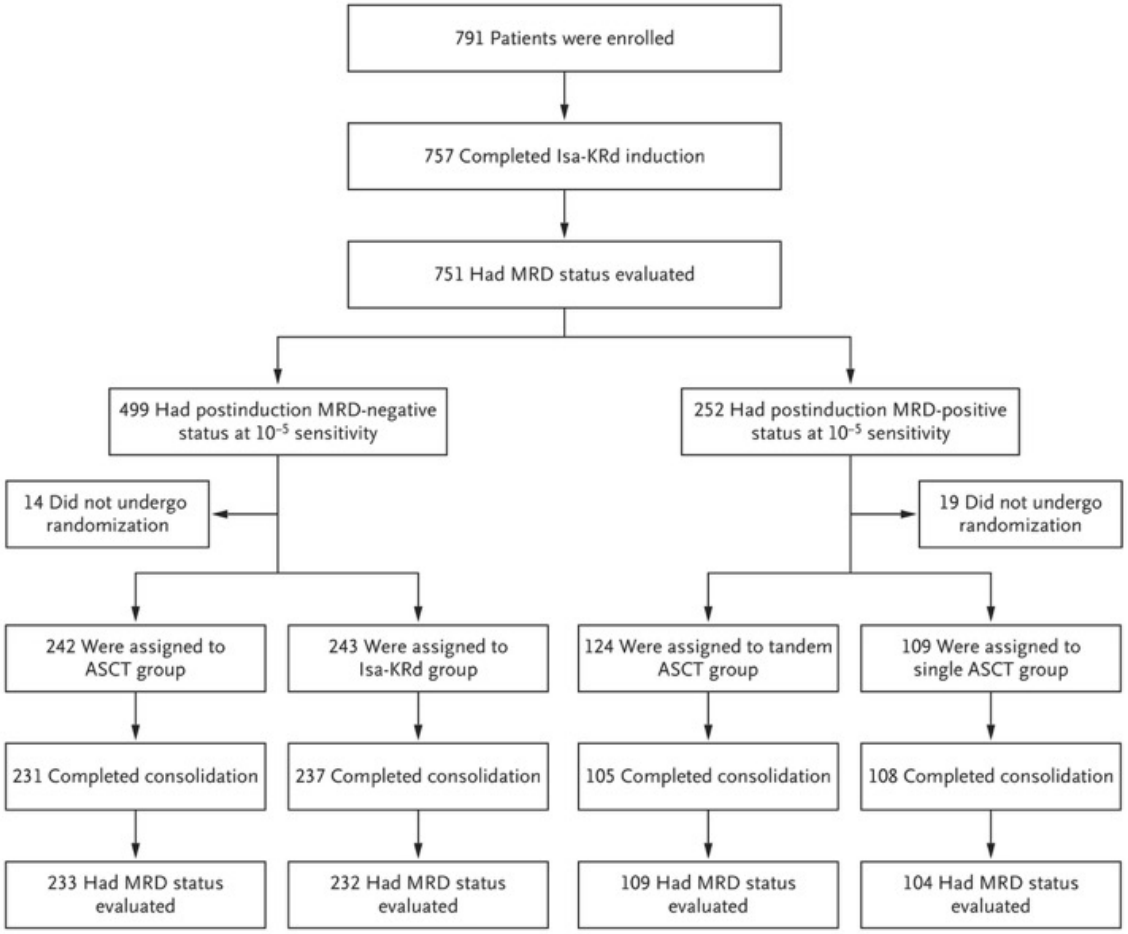

Enrollment, Randomization, and Follow-up.

All the patients received induction therapy with isatuximab, carfilzomib, lenalidomide, and dexamethasone (Isa-KRd) for six cycles. Patients with a postinduction minimal residual disease (MRD)–negative status at 10^{-5} sensitivity (i.e., <1 cancer cell per 100,000 normal cells, as assessed by next-generation sequencing) were randomly assigned to undergo autologous stem-cell transplantation (ASCT) and receive Isa-KRd for two cycles (ASCT group) or to receive Isa-KRd for six more cycles (Isa-KRd group) as consolidation therapy. Patients with a postinduction MRD-positive status at 10^{-5} sensitivity (i.e., ≥1 cancer cell per 100,000) were randomly assigned to undergo tandem ASCT (two ASCTs within a short period; tandem ASCT group) or to undergo ASCT and receive Isa-KRd for two cycles (single ASCT group) as consolidation therapy.

Characteristic	ASCT (N=242)	Isa-KRd (N=243)	Tandem ASCT (N=124)	Single ASCT (N=109)
Age				
Median (range) — yr	57.8 (25–66)	59.8 (36–66)	58.3 (33–65)	57.5 (36–65)
>60 yr — no. (%)	92 (38)	118 (49)	47 (38)	35 (32)
Male sex — no. (%)	142 (59)	143 (59)	75 (60)	58 (53)
ECOG performance-status score — no. (%)†				
0 or 1	216 (89)	206 (85)	111 (90)	100 (92)
2	26 (11)	37 (15)	12 (10)	9 (8)
ISS stage — no. (%)‡				
I or II	210 (87)	210 (86)	113 (91)	100 (92)
III	32 (13)	33 (14)	11 (9)	9 (8)
R-ISS stage — no. (%)§				
I or II	226 (93)	229 (94)	120 (97)	105 (96)
III	16 (7)	13 (5)	4 (3)	4 (4)
R2-ISS stage — no. (%)¶				
I or II	141 (58)	141 (58)	75 (60)	75 (69)
III or IV	91 (38)	96 (40)	46 (37)	32 (29)
Not available	10 (4)	6 (2)	3 (2)	2 (2)
Cytogenetic abnormality — no. (%)				
t(4;14)	20 (8)	29 (12)	8 (6)	3 (3)
t(11;14)	46 (19)	32 (13)	59 (48)	43 (39)
t(14;16)	5 (2)	1 (<1)	5 (4)	2 (2)
Del(17p)	10 (4)	10 (4)	12 (10)	6 (6)
TP53 mutation	9 (4)	7 (3)	5 (4)	3 (3)
1q gain	60 (25)	55 (23)	33 (27)	27 (25)
Del(1p32)	23 (10)	18 (7)	7 (6)	2 (2)
Double del(1p32)	4 (2)	2 (1)	1 (1)	0
High-risk cytogenetic feature — no. (%)‖				
IFM linear predictor score >1	18 (7)	19 (8)	13 (10)	5 (5)
IMS–IMWG definition of high-risk disease	55 (23)	58 (24)	29 (23)	18 (17)
Results of induction — no. (%)				
MRD-negative status at 10^{-6} sensitivity	177 (73)	185 (76)	0	0
Very good partial response or better	230 (95)	229 (94)	113 (91)	96 (88)

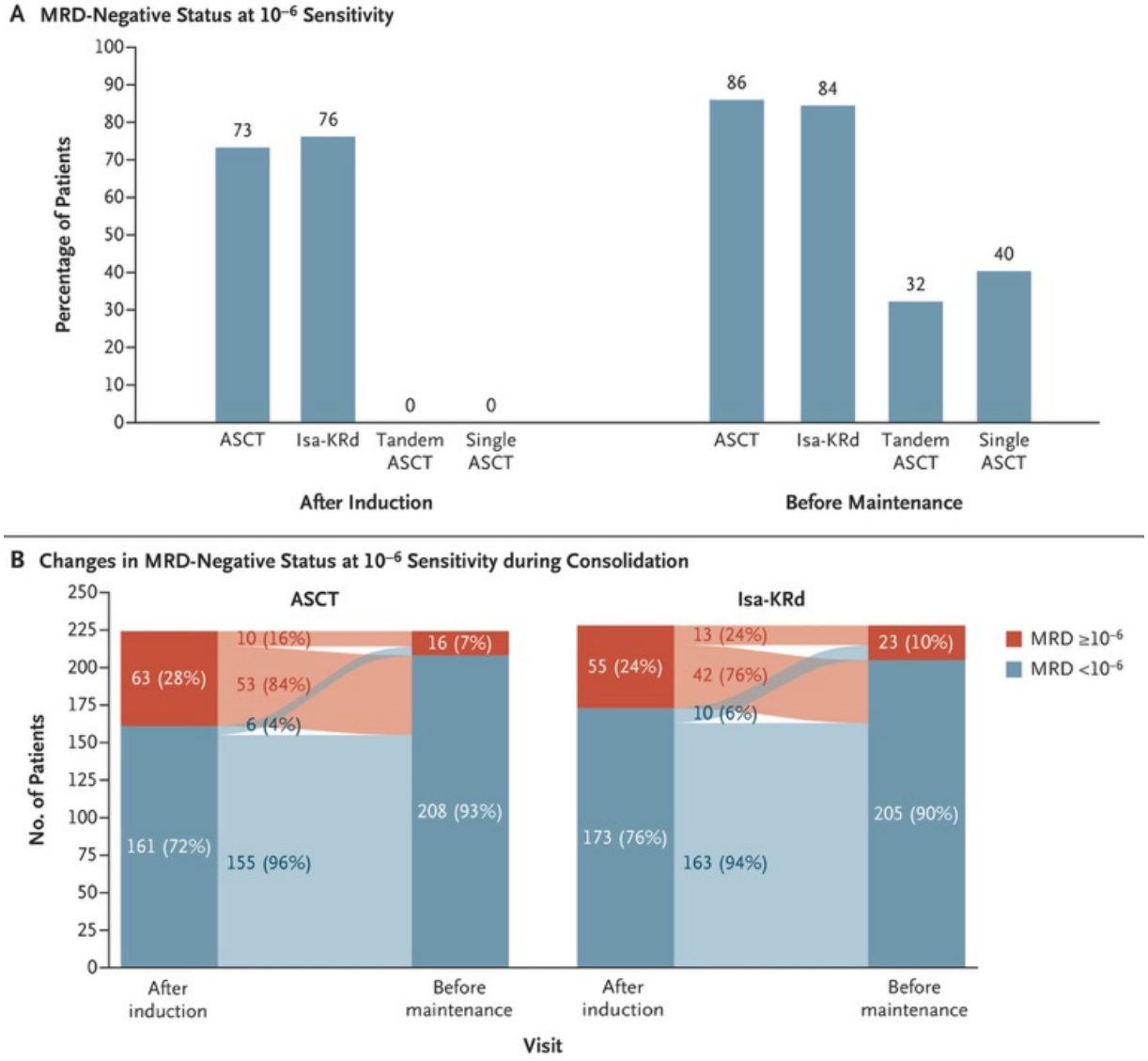

MRD-Negative Status after Induction Therapy and before Maintenance Therapy.

Panel A shows the percentages of patients with an MRD-negative status at 10^{-6} sensitivity (i.e., <1 cancer cell per million normal cells) at the end of induction and before the start of maintenance therapy according to trial group. Panel B shows Sankey diagrams of the changes in MRD status at 10^{-6} sensitivity between the visit at the end of induction and the visit before the start of maintenance therapy in the ASCT and Isa-KRd groups. Data are for the subset of patients (224 in the ASCT group and 228 in the Isa-KRd group) who had available data on MRD status from the visit before the start of maintenance therapy or who had disease progression or died during the consolidation phase. MRD 10^{-6} or higher indicates the presence of at least 1 cancer cell per million normal cells, and MRD less than 10^{-6} the presence of less than 1 cancer cell per million normal cells.

MRD-Negative Status and Treatment Response (Intention-to-Treat Population).

Variable	ASCT (N=242)	Isa-KRd (N=243)	Adjusted Relative Risk (95% CI)†	Tandem ASCT (N=124)	Single ASCT (N=109)	Adjusted Relative Risk (95% CI)‡
	no. of patients (%)			*no. of patients (%)*		
MRD-negative status before maintenance						
10^{-6} sensitivity: primary end point	208 (86)	205 (84)	1.02 (0.95–1.10)	40 (32)	44 (40)	0.82 (0.58–1.15)
10^{-5} sensitivity	228 (94)	225 (93)	1.02 (0.97–1.07)	76 (61)	73 (67)	0.93 (0.77–1.13)
Response						
IMWG criteria)						
Very good partial response or better	224 (93)	225 (93)	1.00 (0.95–1.05)	106 (85)	105 (96)	0.89 (0.82–0.97)
Complete response	42 (17)	40 (16)	1.06 (0.72–1.58)	24 (19)	17 (16)	1.25 (0.71–2.2)
Very good partial response	182 (75)	185 (76)	—	82 (66)	88 (81)	—
Partial response	1 (<1)	3 (1)	—	1 (1)	2 (2)	—
Stable disease	0	1 (<1)	—	1 (1)	0	—
Progressive disease	0	2 (1)	—	0	0	—
Not available	17 (7)	12 (5)	—	16 (13)	2 (2)	—
Near complete response or complete response according to NCI criteria	220 (91)	216 (89)	1.02 (0.96–1.09)	91 (73)	89 (82)	0.91 (0.80–1.05)
Near complete response or complete response according to GMMG criteria	220 (91)	217 (89)	1.02 (0.96–1.08)	92 (74)	90 (83)	0.91 (0.79–1.04)

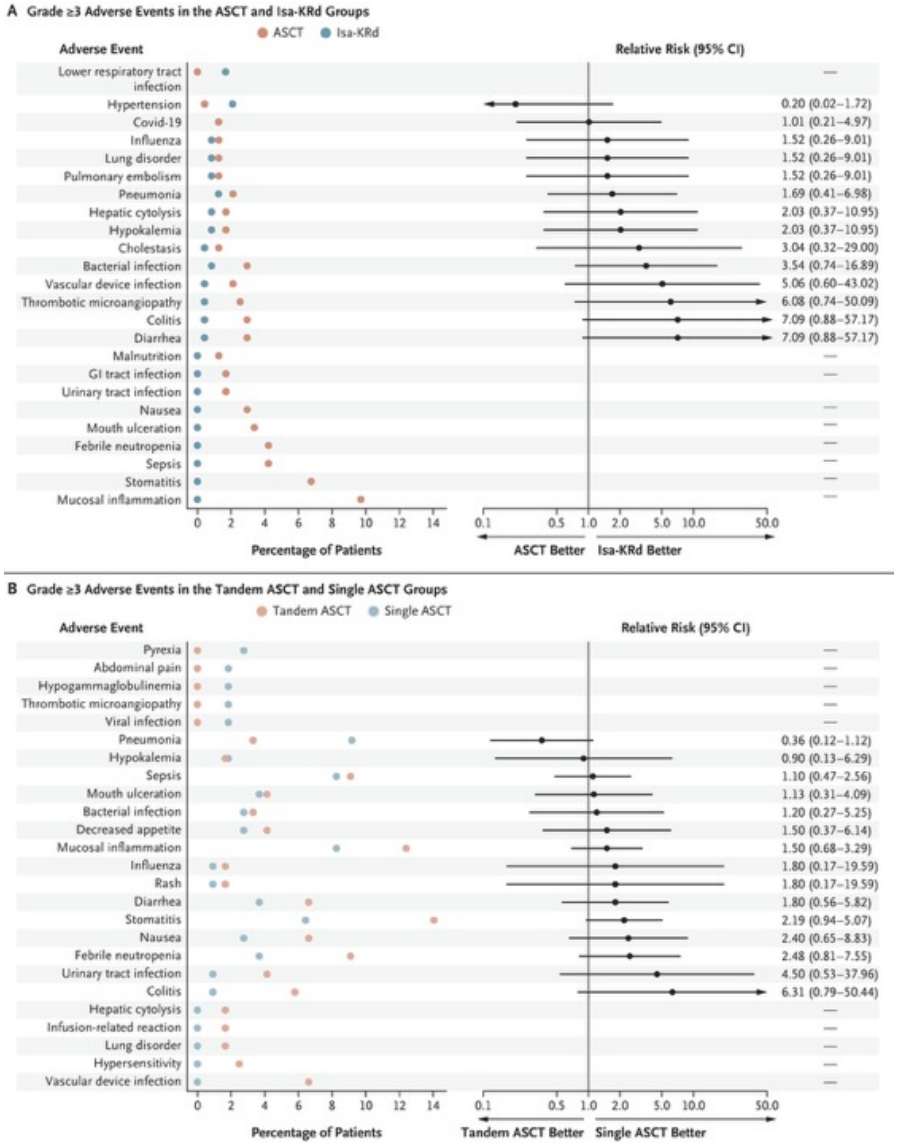

Adverse Events (Safety Population).

Panel A shows the frequency and relative risk of grade 3 or higher adverse events that occurred in at least 1% of the patients in the ASCT or Isa-KRd group. Panel B shows the frequency and relative risk of grade 3 or higher adverse events that occurred in at least 1% of the patients in the tandem ASCT or single ASCT group. The safety population included all the patients who received at least one dose of induction therapy. Adverse events were coded according to the *Medical Dictionary for Regulatory Activities*, version 24.1. Covid-19 denotes coronavirus disease 2019, and GI gastrointestinal.

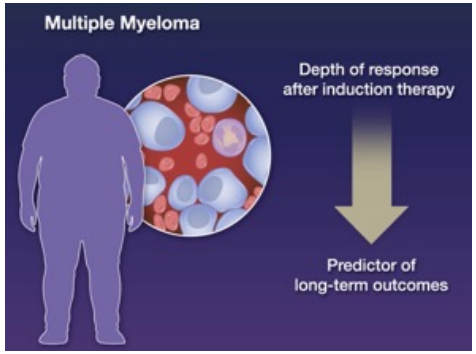

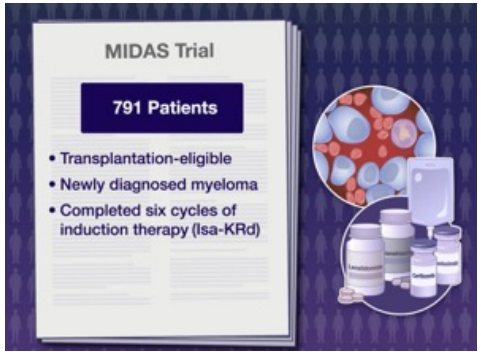

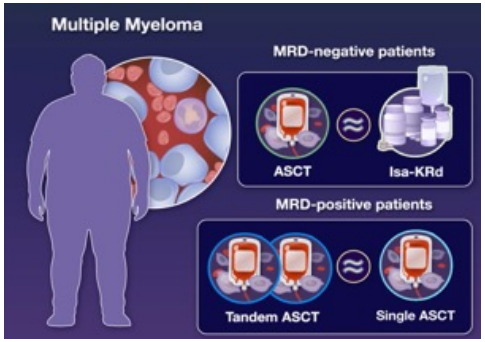

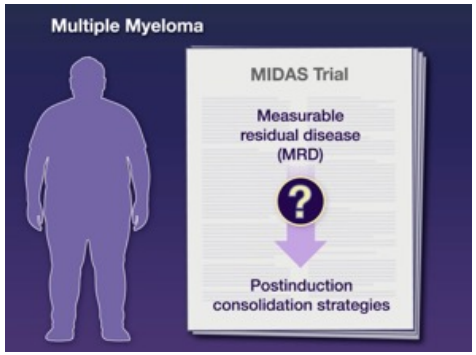

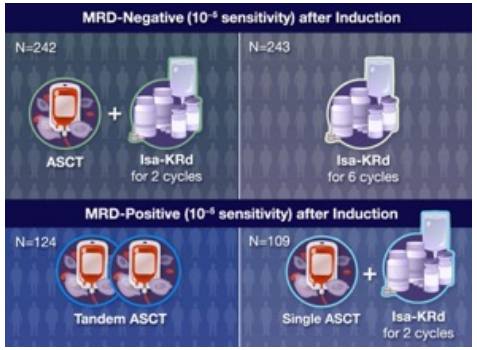

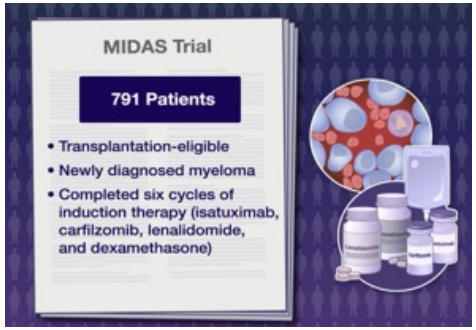

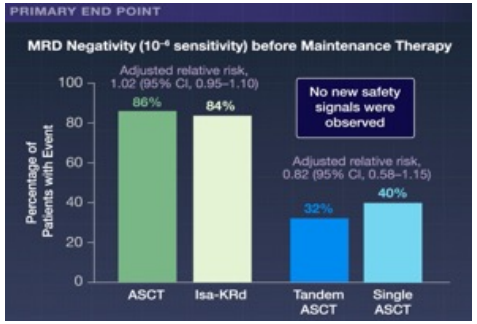

Conclusions

Among patients who were MRD-negative at 10^{-5} sensitivity after induction, the percentage with a premaintenance MRD-negative status at 10^{-6} sensitivity was not significantly higher with ASCT than with Isa-KRd.

Among patients who were MRD-positive status at 10^{-5} sensitivity after induction, the percentage with a premaintenance MRD-negative status at 10^{-6} sensitivity was not significantly higher with tandem ASCT than with single ASCT.

Mitochondriopathien sind Erkrankungen, die durch eine Fehlfunktion oder Schädigung der Mitochondrien verursacht werden. Da die Zellorganellen vor allem für die Bereitstellung der Energie (in Form von ATP) in den Körperzellen zuständig sind, machen sich diese Erkrankungen meist durch massive Schwäche, Müdigkeit und Ähnliches bemerkbar.
Es werden zwei Formen der Mitochondriopathien unterschieden: ererbte und durch Umwelteinflüsse erworbene Mitochondriopathien (auch sekundäre Mitochondriopathien genannt). Die Übergänge zwischen den beiden Formen der Mitochondriopathien können fließend sein: So kann eine ererbte Mitochondriopathie erst im Erwachsenenalter zum Tragen kommen, wenn sie zunächst wenig ausgeprägt war (subklinisch) und für den Patienten erst dann zu nicht mehr tolerierbaren Symptomen führt, wenn bestimmte Umweltfaktoren zusätzlich negativ einwirken. Es kann jedoch genauso eine erworbene Mitochondriopathie vererbt werden, wenn ein hoher Anteil der Mitochondrien der befruchteten Eizelle durch Umwelteinflüsse (irreversibel) geschädigt wurde.

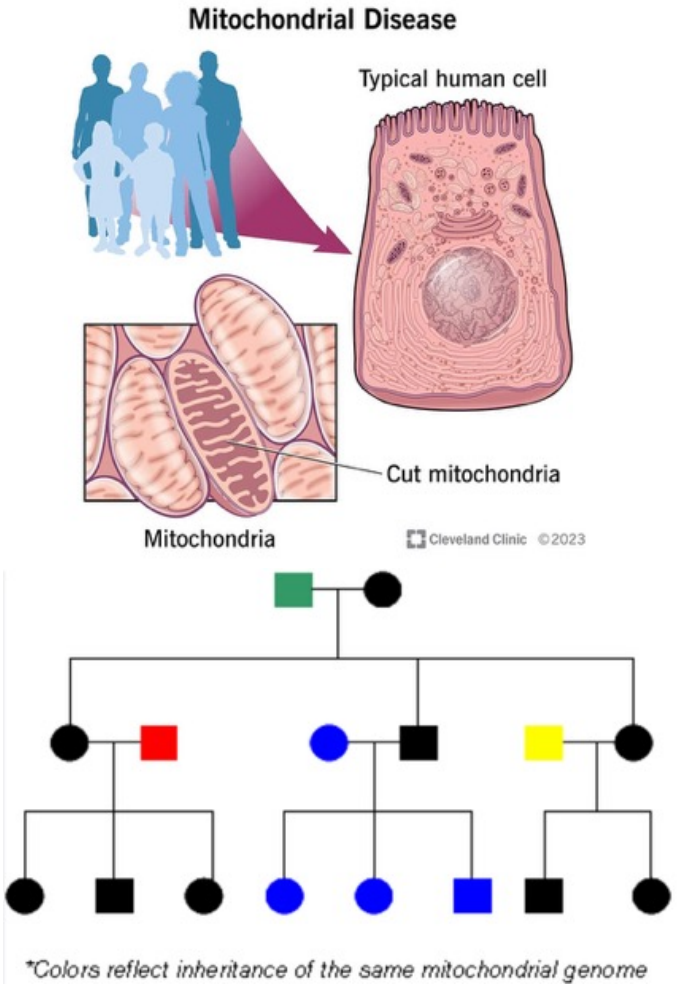


Mitochondrial disease in children
Encephalopathy – strokes, seizures, regression
Deafness
Blindness
Cardiomyopathy
Hormone deficiencies
Diabetes
Liver failure
Renal disease
Enteropathy
Anaemia
Myopathy
Neuropathy
JIM Journal of Internal Medicine
Founded in 1863

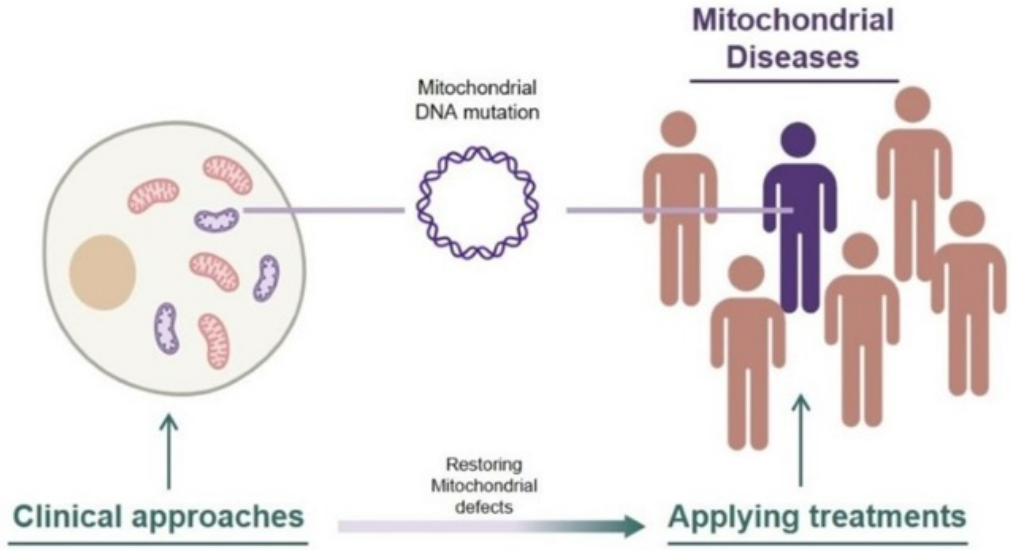
Mitochondrial Diseases
Mitochondrial DNA mutation
Clinical approaches
Restoring Mitochondrial defects
Applying treatments

Ein Pronukleus (Mehrzahl: Pronuklei) ist der haploide Zellkern einer Eizelle (weiblicher Pronukleus) oder eines Spermiums (männlicher Pronukleus) nach der Befruchtung, aber noch bevor sie zu einem einzigen diploiden Kern (Zygote) verschmelzen.

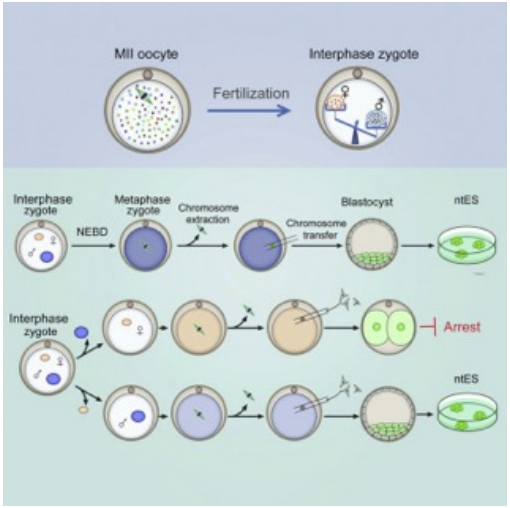

Pronuclei transplantation ist eine Technik, bei der die männlichen und weiblichen Zellkerne (Pronuklei) einer befruchteten Eizelle in eine andere, ebenfalls befruchtete, aber leere Eizelle übertragen werden. Dies geschieht, um genetische Defekte der ursprünglichen Eizelle zu umgehen und eine gesunde Entwicklung des Embryos zu ermöglichen. Die Technik wird auch als Drei-Eltern-Baby-Methode bezeichnet, da der Embryo genetisches Material von drei Individuen enthält.

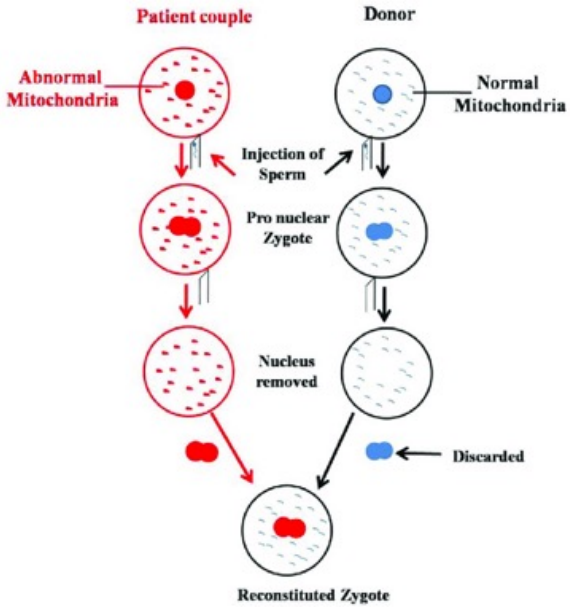

Mitochondrial Donation and Preimplantation Genetic Testing for mtDNA Disease

Children born to women who carry pathogenic variants in mitochondrial DNA (mtDNA) are at risk for a range of clinical syndromes collectively known as mtDNA disease. Mitochondrial donation by pronuclear transfer involves transplantation of nuclear genome from a fertilized egg from the affected woman to an enucleated fertilized egg donated by an unaffected woman. Thus, pronuclear transfer offers affected women the potential to have a genetically related child with a reduced risk of mtDNA disease.

Methods

We offered mitochondrial donation (by pronuclear transfer) or preimplantation genetic testing (PGT) to a series of women with pathogenic mtDNA variants who sought to reduce the transmission of these variants to their children. Patients with heteroplasmy (variants present in a proportion of copies of mtDNA) were offered PGT, and patients with homoplasmy (variants present in all copies of mtDNA) or elevated heteroplasmy were offered pronuclear transfer.

Conclusions

We found that mitochondrial donation through pronuclear transfer was compatible with human embryo viability. An integrated program involving pronuclear transfer and PGT was effective in reducing the transmission of homoplasmic and heteroplasmic pathogenic mtDNA variants.
(Funded by NHS England and others.)

The mitochondrial genome is inherited maternally, and children born to women who carry pathogenic mitochondrial DNA (mtDNA) variants are at risk for life-limiting mtDNA disease. Disorders resulting from pathogenic mtDNA variants have an estimated prevalence of 1 in 5000 births. Pathogenic variants can be either homoplasmic (present in all copies of mtDNA) or heteroplasmic (present in a proportion of copies of mtDNA). Homoplasmic variants are transmitted in full to all children, but the penetrance of homoplasmic variants varies. Transmission of heteroplasmic variants is subject to a genetic bottleneck. This mtDNA genetic bottleneck gives rise to a random shift in mtDNA heteroplasmy, which results in widely varying levels of heteroplasmy among oocytes from the same woman, making the risk of the development of severe disease in a child difficult to predict.

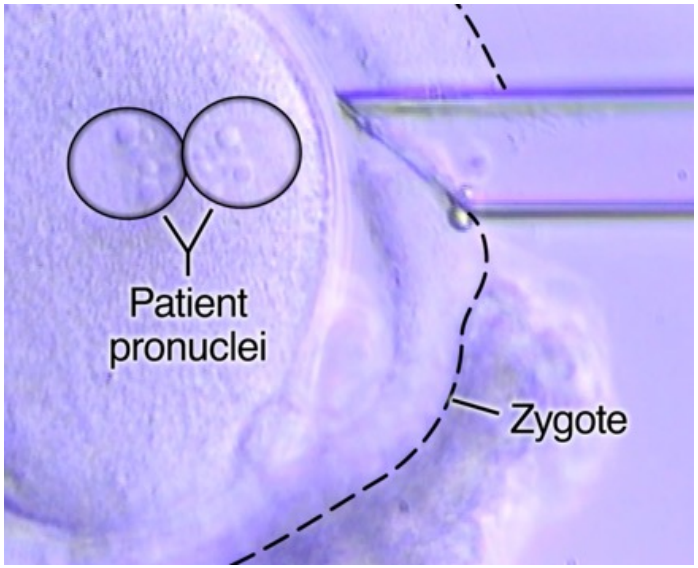

Removal of pronuclei
The pronuclei are removed separately. The video shows the enucleation pipette being inserted through the laser-drilled hole in the zona. The first pronucleus is aspirated in the form of a karyoplast surrounded by a small amount of cytoplasm and a fragment of the egg membrane. The enucleation pipette is reinserted through the hole in the zona, and the second pronucleus is aspirated into the pipette in a karyoplast.

Mitochondrial donation can be performed before fertilization during metaphase II arrest (maternal-spindle transfer) or after fertilization when the maternal and paternal haploid genomes are contained in pronuclei (pronuclear transfer). Both approaches can result in embryos with heteroplasmy for maternal mtDNA owing to cotransfer (carryover) of some mitochondria surrounding the transplanted pronuclei. For reasons that remain unclear, the small amount of maternal mtDNA increases to homoplasmic levels in approximately 20% of embryonic stem-cell lines derived from embryos obtained after a mitochondrial donation procedure. Moreover, an elevated level of heteroplasmy (40 to 60%) for maternal mtDNA has been reported in one of six babies born after maternal-spindle transfer for infertility treatment. These findings evoke questions about whether mitochondrial donation can reliably prevent transmission of pathogenic mtDNA variants. Here we describe the clinical application of a pronuclear-transfer procedure previously established for human zygotes. Pronuclear transfer and PGT were offered in an integrated program to reduce transmission of a range of heteroplasmic and homoplasmic pathogenic variants.

Replacement of Pronuclei. The video shows the two karyoplasts, each containing a pronucleus, being placed together under the zona of an enucleated donor egg by insertion of the enucleation pipette through the laser-drilled hole in the zona.

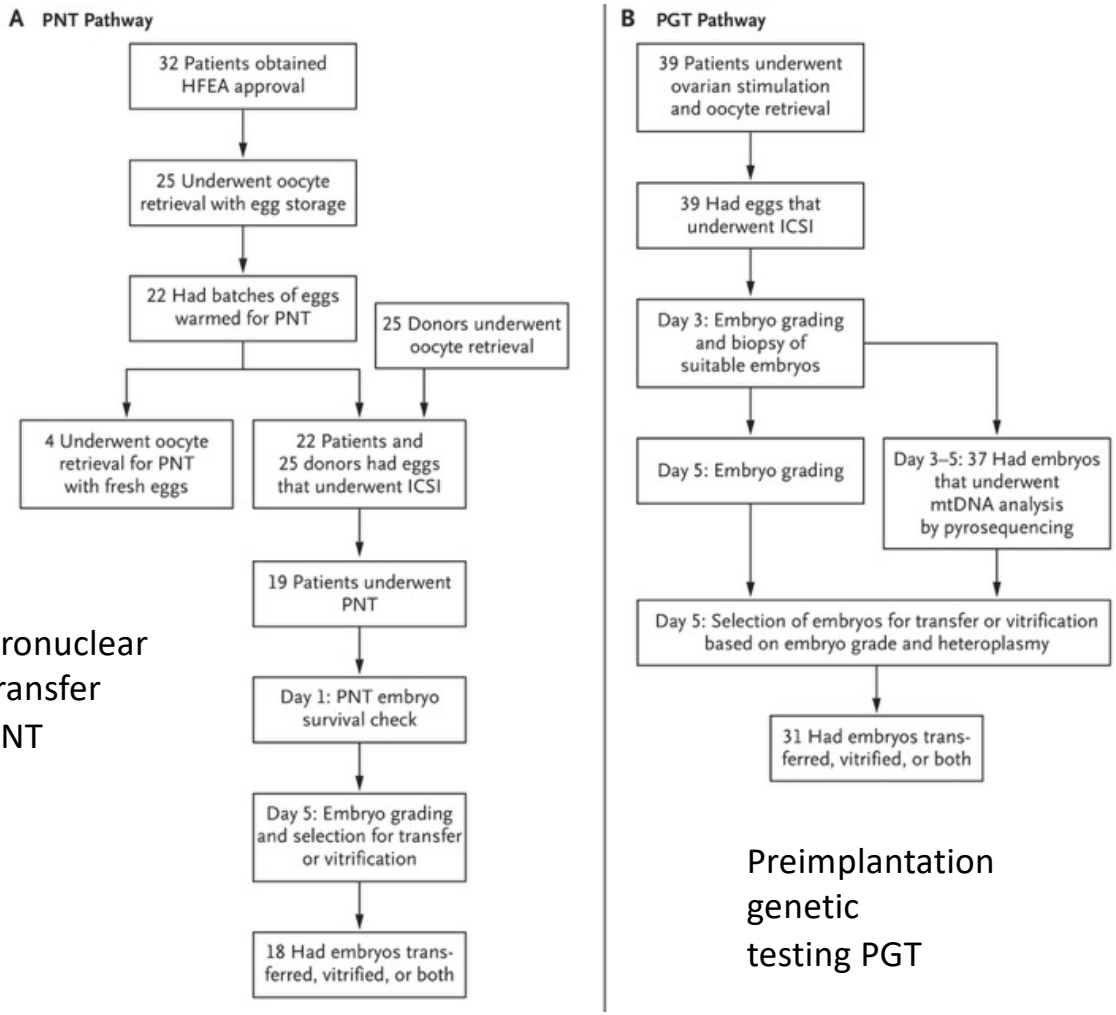

Pronuclear transfer PNT

Preimplantation genetic testing PGT

Pronuclear Transfer and Preimplantation Genetic Testing Treatment Pathways.

Panel A shows the pronuclear-transfer (PNT) pathway and the progression of the 32 patients approved for pronuclear transfer through the stages of egg storage, pronuclear transfer, and embryo transfer. Panel B shows the preimplantation genetic testing (PGT) pathway and the progression of the 39 patients through the stages of intracytoplasmic sperm injection (ICSI), embryo biopsy, and embryo transfer. HFEA denotes Human Fertilisation and Embryology Authority, and mtDNA mitochondrial DNA.

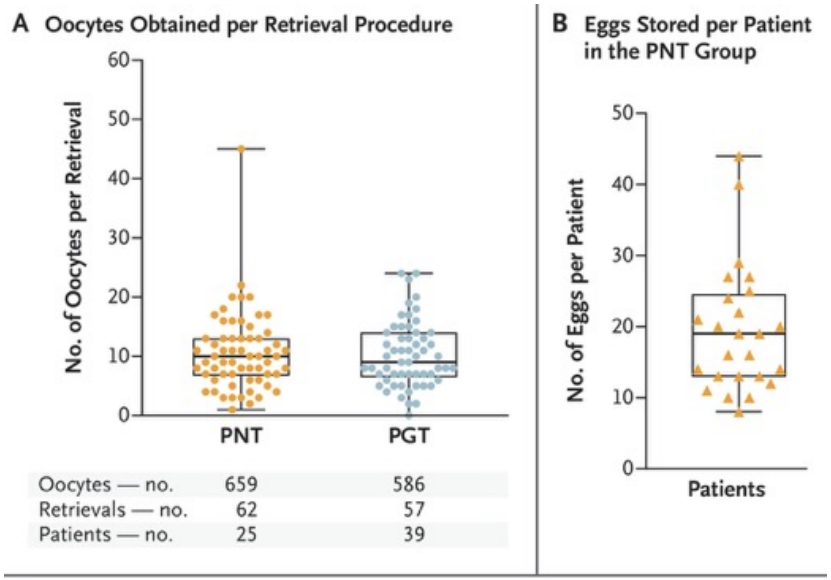

Oocyte Retrieval and Fertilization Outcomes.

Panel A shows the number of oocytes obtained per retrieval procedure among patients who underwent pronuclear transfer (PNT) and those who underwent PGT. Dots denote the retrieval procedures. Panel B shows the number of eggs stored per patient who underwent pronuclear transfer. Triangles denote patients. In Panels A and B, the horizontal line within each box indicates the median, the top and bottom of the box indicate the interquartile range, and the whiskers indicate the minimum and maximum values. Panel C shows the percentage of eggs with normal fertilization among patients in the pronuclear-transfer group as compared with those in the PGT group ($P<0.001$ by chi-square test) and egg donors ($P<0.001$ by chi-square test).

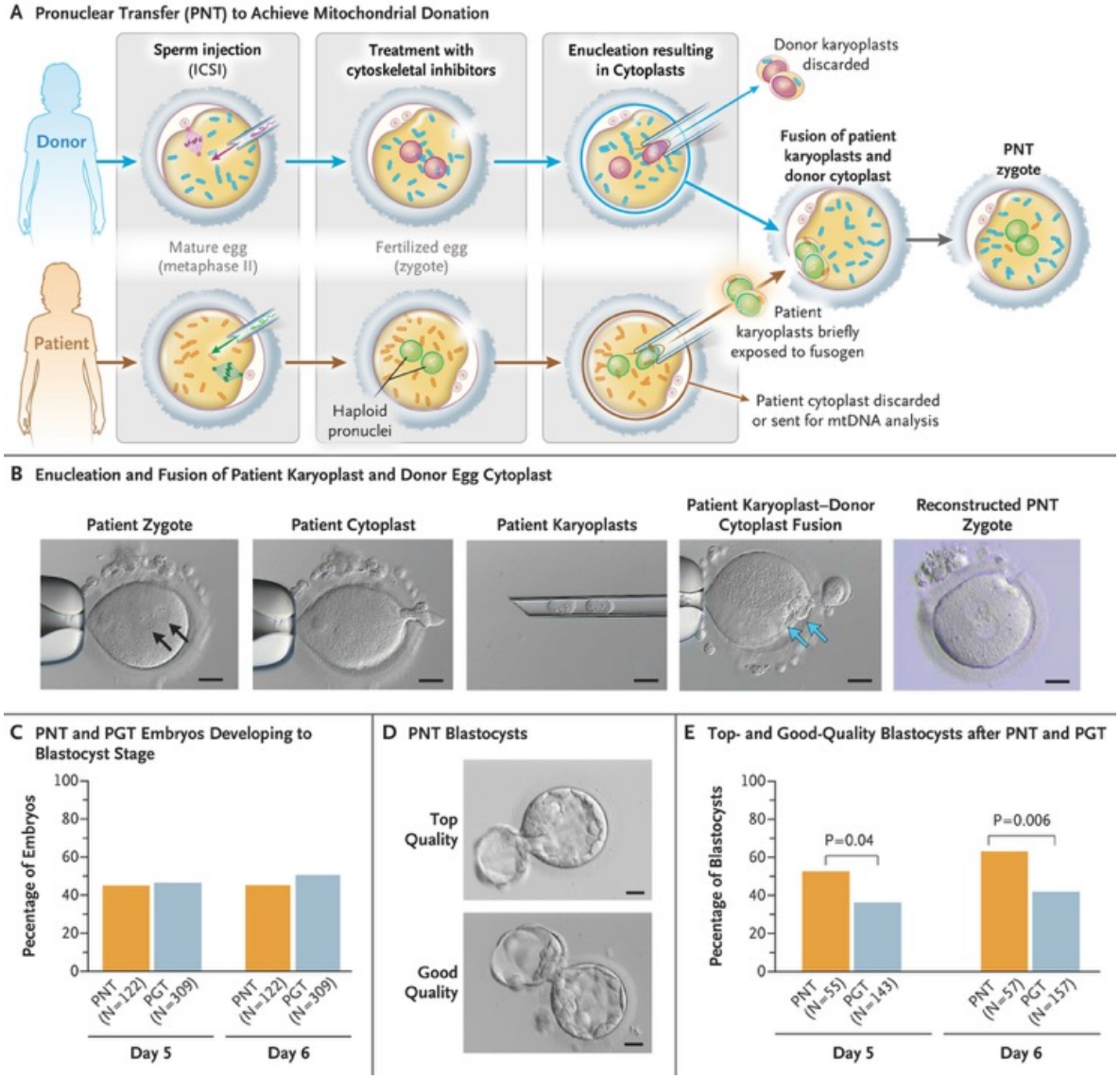

Pronuclear-Transfer Procedure and Comparison of Embryo Development with Pronuclear Transfer and with PGT.

Panel A shows the pronuclear-transfer procedure. The images in Panel B show the enucleation of patient karyoplasts and the fusion of patient karyoplasts with the donor egg cytoplast (scale bar, 20 μm). Arrows in the first image indicate the pronuclei, and arrows in the fourth image indicate the karyoplasts. Panel C shows a comparison of the percentage of embryos with blastocyst formation on days 5 and 6 after intracytoplasmic sperm injection in the pronuclear-transfer group and in the PGT group. The images in panel D show examples of top-quality and good-quality pronuclear-transfer blastocysts (scale bar, 20 μm). Panel E shows the percentage of blastocysts that were top quality or good quality after pronuclear transfer and after PGT on days 5 and 6. The percentage was higher in the pronuclear-transfer group than the PGT group on both day 5 (P=0.04 by chi-square test) and day 6 (P=0.006 by chi-square test).

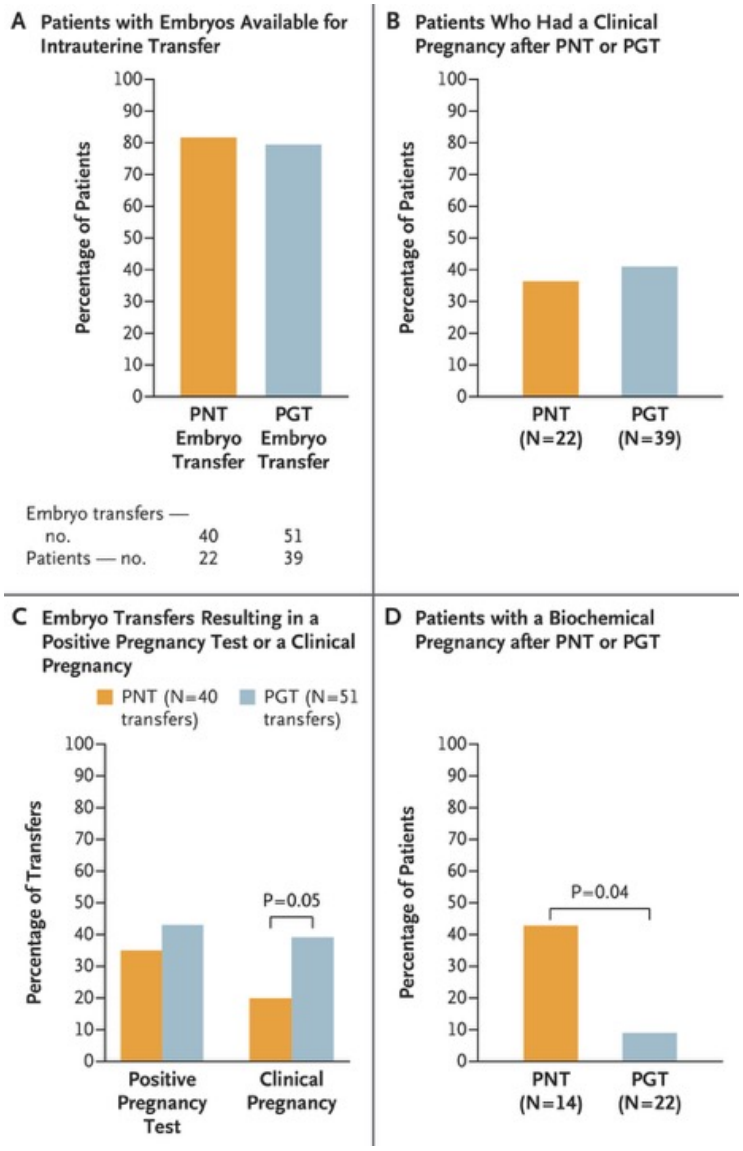

Clinical Outcomes after Pronuclear Transfer and PGT.

Panel A shows the percentage of patients who had embryos available for intrauterine transfer after intracytoplasmic sperm injection for pronuclear transfer or PGT. Panel B shows the overall percentage of patients who had a clinical pregnancy after pronuclear transfer or PGT. Panel C shows the percentage of embryo transfers (fresh and frozen) that resulted in a positive pregnancy test and those that resulted in a clinical pregnancy after pronuclear transfer or PGT. Patients who underwent pronuclear transfer had a lower incidence of clinical pregnancy than those who underwent PGT (P=0.05 by chi-square test). Panel D shows the percentage of patients with a biochemical pregnancy after pronuclear transfer or PGT. Patients who underwent pronuclear transfer had a higher incidence of biochemical pregnancy than those who underwent PGT (P=0.04 by Fisher's exact test).

Maternal Pathogenic Variant Heteroplasmy in Infants.

Assisted Reproductive Procedure and Maternal Variant	Reproductive History	Percent Heteroplasmy		Pronuclear-Transfer Procedure Score		Percent Heteroplasmy in Neonatal Blood		Infant Sex
		Maternal Urine	Enucleated Egg or Test Blastomere†	Cytoplasm Carryover‡	Cytoplasm Leakage§	Pyrosequencing	NGS	
Pronuclear transfer								
m.4300A→G	No pregnancies or births	Homoplasmic	—	2	2	5	—	Female
m.4300A→G	Live birth of affected child (deceased)	Homoplasmic	—	2	2	Not detected	0.06	Male
m.3260A→G	No pregnancies or births	79	68	2	1	16	—	Male
m.3460G→A	No pregnancies or births	89	99	2	4	Not detected	0.17	Female
m.11778G→A	No pregnancies or births	82	64	1	0	Not detected	0.09	Female
m.11778G→A	No pregnancies or births	Homoplasmic	—	3	1			
Identical twin 1						Not detected	—	Male
Identical twin 2						Not detected	—	Male
m.11778G→A	Live birth	Homoplasmic¶	99.9	1	3	12	—	Female
PGT								
m.10158T→C	Live birth of affected child (deceased)	33						
Child 1			Not detected			Not detected		Male
Child 2			Not detected			Not detected		Female
m.13094T→C	Live birth of affected child (deceased)	45	Not detected			Not detected		Male
m.3243A→G	No pregnancies or births	23	Not detected			Not detected		Female
m.3243A→G	No pregnancies or births	23	Not detected			Not detected		Male
m.3243A→G	No pregnancies or births	61	9 and 24‖					
Twin 1						Not tested		Female
Twin 2						Not detected		Male
m.3688G→A	Live birth of affected child (deceased)	50	Not detected and 5**			7		Female
m.8993T→G	Live birth of affected child (deceased)	Not detected						
Child 1			Not detected			Not detected		Female
Child 2			Not detected			Not detected		Male
m.8993T→C	Live birth of affected child	37	Not detected			Not detected		Female

Discussion

Building on our previous preclinical findings, we found in the current study that clinical translation of pronuclear transfer was compatible with human embryo viability and reduced transmission of pathogenic mtDNA variants; analyses of neonatal blood showed a reduction in levels of maternal pathogenic mtDNA variants by 95 to 100% in six newborns and by 77 to 88% in two others. These data indicate that pronuclear transfer was effective in reducing transmission of mtDNA disease.

Our results show that a program involving PGT and pronuclear transfer was effective in reducing transmission of a range of pathogenic mtDNA variants. The reduced levels of heteroplasmy in infants born to women carrying homoplasmic variants provides grounds for optimism. However, until more is known about its efficacy, mitochondrial donation should be regarded as a risk-reduction strategy. In addition, clinical follow-up of children born after mitochondrial donation will be essential for monitoring the safety and efficacy of this procedure.

Mitochondrial Donation in a Reproductive Care Pathway for mtDNA Disease

Summary

Pathogenic variants in mitochondrial DNA (mtDNA) are a common cause of severe, often fatal, inherited metabolic disease. A reproductive care pathway was implemented to provide women carrying pathogenic mtDNA variants with reproductive options. A total of 22 women with pathogenic mtDNA variants have commenced or completed pronuclear transfer (and thus receipt of a mitochondrial donation), and there have been 8 live births. All 8 children were healthy at birth, with no or low levels of mtDNA heteroplasmy in blood. Hyperlipidemia and cardiac arrhythmia developed in a child whose mother had hyperlipidemia during pregnancy; both of the child's conditions responded to treatment. Infant myoclonic epilepsy developed in another child, with spontaneous remission. At the time of this report, all the children have made normal developmental progress. (Funded by the U.K. National Health Service and others.)

Characteristics of Women with Pregnancies after Pronuclear Transfer.

mtDNA Variant (NC_012920.1)	Heteroplasmy				Age	Disease in Family	Outcome of Mitochondrial Donation
	Blood	Urine	Buccal	Muscle			
	percent				*yr*		
m.3260A→G	36	79	NA	94	27	Severe cardiomyopathy	Live birth
m.3460G→A	67	89	86	NA	31	Blindness	Live birth
m.4300A→G	Hom	Hom	Hom	NA	36	Fatal cardiomyopathy or child death	Live birth
m.4300A→G	Hom	Hom	NA	NA	34	Fatal cardiomyopathy or child death	Live birth
m.11778G→A	74	82	NA	81	35	Blindness	Live birth
m.11778G→A	Hom	Hom	Hom	NA	30	Blindness	Live births (twins)
m.11778G→A	94	Hom	Hom	NA	31	Blindness	Live birth
m.11778G→A	Hom	Hom	Hom	NA	33	Blindness	Ongoing pregnancy

Details of Pregnancy and Births of Infants after Pronuclear Transfer.

mtDNA Variant (NC_012920.1)	Max. Mat. Het.†	Sex	Antenatal Ultrasound	Gestation	Mode of Delivery	Birth Weight	Apgar Score‡			Neonatal Heteroplasmy	
							1 min	5 min	10 min	Blood	Urine
	%					*g*				%	
m.3260A→G	94	M	Normal	38 wk	EL LSCS	3220	—	9	10	16	20
m.3460G→A	89	F	Normal	38 wk 6 days	NVD	3090	—	9	10	ND	ND
m.4300A→G	>97	F	Abnormal§	38 wk	EL LSCS	2815	10	10	10	5	9
m.4300A→G	>97	M	Normal	38 wk 6 days	EL LSCS	3210	9	10	10	ND	ND
m.11778G→A	82	F	Normal	42 wk 2 days	EL LSCS	3665	5	7	9	ND	ND
m.11778G→A¶	>97	M	Normal	36 wk 1 day	EL LSCS	2460	5	9	10	ND	NA
m.11778G→A¶	>97	M	Normal	36 wk 1 day	EL LSCS	2190	5	9	10	ND	NA
m.11778G→A	>97	F	Normal	36 wk 2 days	NVD	3330	5	9	9	12	13

Discussion

Women at risk for transmitting severe mtDNA disease to their children should have the opportunity to make informed choices about their reproductive options: prenatal testing, PGT, mitochondrial donation, egg donation, adoption, and deciding not to have children. Multidisciplinary advice regarding the optimal choice for an individual woman is tailored to the specific mtDNA variant and the woman's own views on risk reduction. In this study, many of the women who were eligible for mitochondrial donation or PGT decided, after counseling, not to proceed in the pathway at this time. Because mitochondrial donation and PGT involve in vitro fertilization, the success of which is inversely correlated with age, we would encourage this type of early fact-finding discussion. Although this study involved women from the United Kingdom, we believe that the results are generalizable to other countries.

There is a theoretical risk of deterioration in health during pregnancy among women with pathogenic mtDNA variants, with an increased risk of pregnancy complications and early delivery. In seven pregnancies, including one that is ongoing, no complications have been reported, although one patient with hypertrophic cardiomyopathy had intermittent atrial fibrillation. This patient also had a clinically significant complication of severe hyperlipidemia during pregnancy.

Mitochondrial Replacement Therapy (MRT) in the United Kingdom.

Shown is a timeline of events beginning in 1981, including a change in U.K. regulations to allow clinical research on MRT, and ending with reports of eight children born after pronuclear transfer.

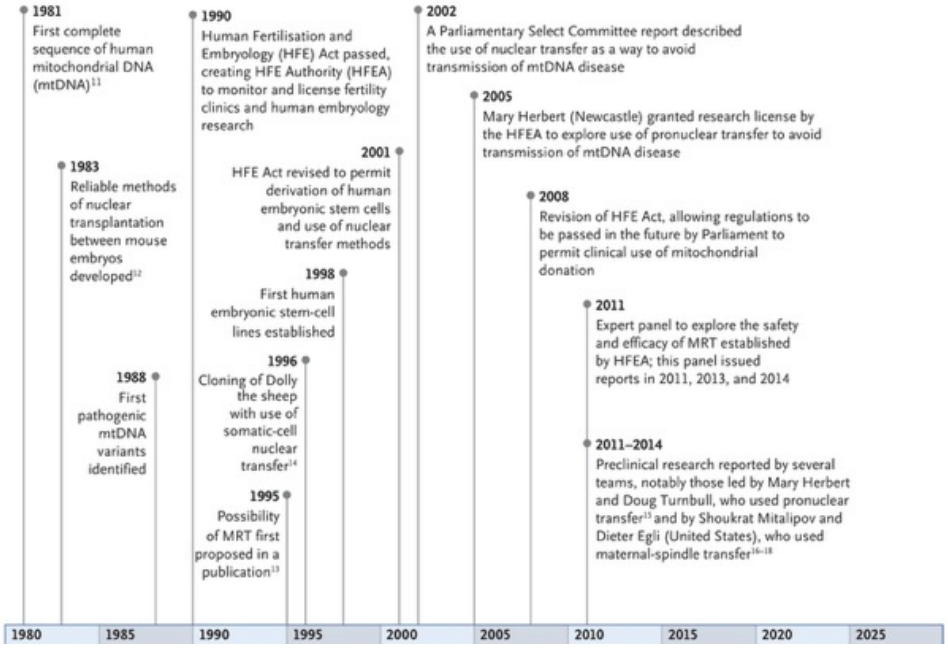

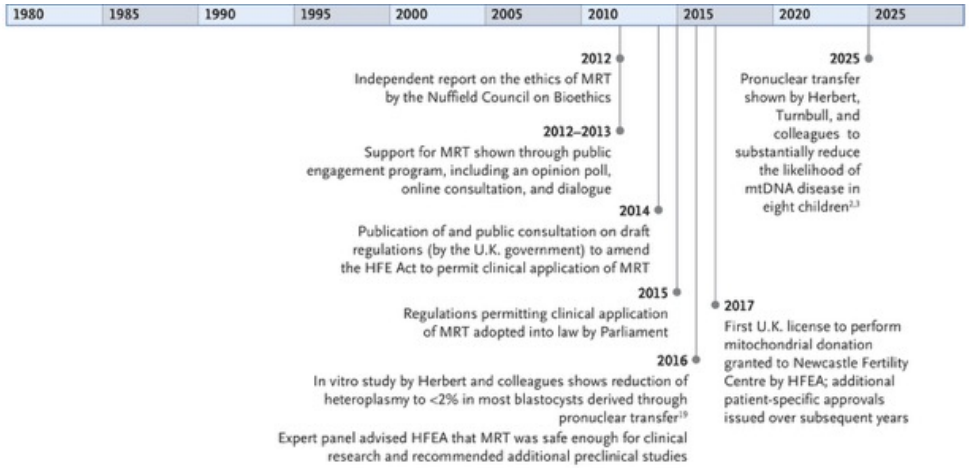

Intraoperative normovolemic hemodilution (ANH) is a blood conservation technique used during surgery where a patient's own blood is removed and replaced with a crystalloid or colloid solution to maintain normal blood volume (normovolemia). This reduces the concentration of red blood cells (hemodilution) but keeps the overall blood volume stable. The removed blood is stored and then reinfused later during the surgery, typically after significant blood loss, to help maintain the patient's red blood cell count. (Sounds like autologous blood donation in the OR.)

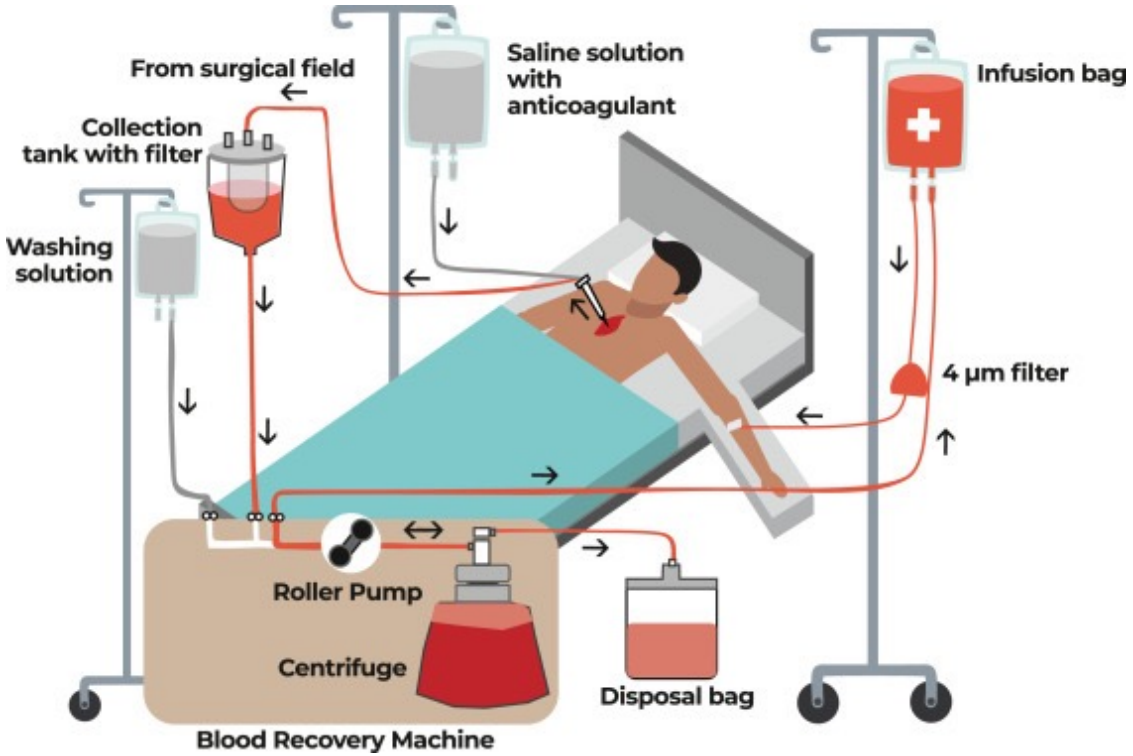

Eine Eigenblutspende ist eine Methode, bei der ein Patient vor einer geplanten Operation oder Therapie eigenes Blut spendet, um es später während oder nach dem Eingriff wieder transfundiert zu bekommen. Dies kann dazu beitragen, das Risiko von Transfusionen mit Fremdblut zu minimieren.

Eigenblutspende im OP

A Randomized Trial of Acute Normovolemic Hemodilution in Cardiac Surgery

Patients undergoing cardiac surgery often receive red-cell transfusions, along with the associated risks and costs. Early intraoperative normovolemic hemodilution (i.e., acute normovolemic hemodilution [ANH]) is a blood-conservation technique that entails autologous blood collection before initiation of cardiopulmonary bypass and reinfusion of the collected blood after bypass weaning. More data are needed on whether ANH reduces the number of patients receiving allogeneic red-cell transfusion.

In a multinational, single-blind trial, we randomly assigned adults from 32 centers and 11 countries who were undergoing cardiac surgery with cardiopulmonary bypass to receive ANH (withdrawal of ≥650 ml of whole blood with crystalloids replacement if needed) or usual care. The primary outcome was the transfusion of at least one unit of allogeneic red cells during the hospital stay. Secondary outcomes were death from any cause within 30 days after surgery or during the hospitalization for surgery, bleeding complications, ischemic complications, and acute kidney injury.

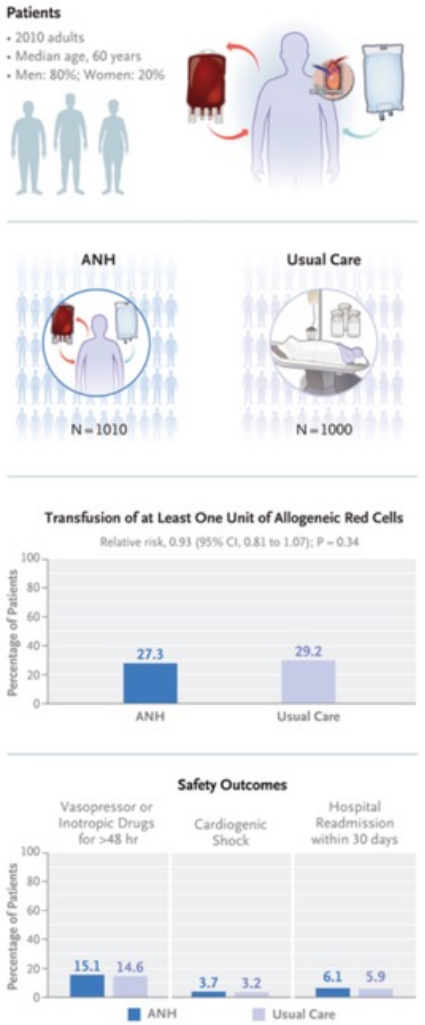

Red-cell transfusion is common in modern clinical practice, with one study estimating that more than 10 million red-cell units are transfused in the United States each year. However, this procedure is affected by three main concerns: costs, shortages, and transfusion-related complications. The median cost of red cells ranges from $150 to $634 per unit depending on the country, which results in substantial expenses for hospitals and health care systems. In addition, the availability of red cells fluctuates over time, with periods of shortage potentially leading to postponement of nonurgent surgeries. Such delays affect patients' health and, again, costs. Finally, red-cell transfusion carries risks spanning from mild fever, chills, and allergic reactions to more-severe side effects such as infections, transfusion-related lung injury, and transfusion-associated circulatory overload, which occurs in 1 to 5% of transfusions.

Patients who undergo cardiac surgery are at high risk for allogeneic red-cell transfusion. More than two million patients undergo cardiac surgery annually worldwide, and approximately 35% receive at least one unit of red cells. Transfusion during cardiac surgery is a risk factor for adverse perioperative outcomes and death. Early intraoperative normovolemic hemodilution (known as acute normovolemic hemodilution, or ANH) is a well-known technique that is performed in approximately 20% of cardiac surgery departments in the United States. It is also performed by 26.7% of cardiac anesthesiologists and in 13.7% of patients worldwide. ANH allows for the reinfusion of the patient's whole blood, which is withdrawn before the patient receives heparin and undergoes cardiopulmonary bypass. This technique improves the coagulation profile after cardiopulmonary bypass and reduces activation of inflammatory pathways, consumption of clotting factors and platelets owing to activation of circuit contacts, the need for allogeneic red-cell transfusion, and blood viscosity, thereby contributing to improved microcirculatory perfusion.

Trial Design

We conducted a phase 3, single-blind, randomized trial at 32 centers in 11 countries in North America, South America, Europe, and Asia.

Patients

All adult patients who were scheduled to undergo cardiac surgery with cardiopulmonary bypass underwent screening for eligibility. The main exclusion criteria were unstable coronary artery disease, critical perioperative state (e.g., hemodynamic instability or a need for mechanical ventilation), emergency surgery, or inadequate suspension of anticoagulant or antiplatelet therapy before surgery; the use of low-dose aspirin was permitted.

Primary and Secondary Outcomes

The primary outcome was the transfusion of at least one unit of allogeneic red cells from randomization until hospital discharge. Prespecified secondary outcomes were acute kidney injury, bleeding-related and ischemic complications, and death from any cause within 30 days after surgery or during the hospitalization in which the surgery was performed.

Prespecified Safety Outcomes

Prespecified intraoperative and postoperative safety outcomes included cardiogenic shock, inotropic drug use for more than 48 hours, mechanical circulatory support, sepsis, septic shock, lowest hematocrit level occurring in the ICU, and death.

Characteristics of Patients at Baseline.

Characteristic	ANH Group (N=1010)	Usual-Care Group (N=1000)
Median age (IQR) — yr	59 (52–66)	61 (53–68)
Female sex — no. (%)	219 (21.7)	186 (18.6)
Median body-mass index (IQR)†	26 (24–30)	27 (24–30)
Race — no. (%)‡		
White	792 (78.4)	778 (77.8)
Asian	195 (19.3)	198 (19.8)
Other	23 (2.3)	20 (2.0)
Median hemoglobin concentration (IQR) — g/dl	14 (14–15)	15 (14–15)
New York Heart Association class III or IV for heart failure — no. (%)	236 (23.4)	273 (27.3)
Medical condition — no. (%)		
Previous myocardial infarction	160 (15.8)	168 (16.8)
Atrial fibrillation	168 (16.6)	149 (14.9)
Arterial hypertension	626 (62.0)	668 (66.8)
Chronic kidney disease	65 (6.4)	64 (6.4)
Regular medications before surgery — no. (%)		
Aspirin	389 (38.5)	396 (39.6)
Beta-blockers	540 (53.5)	557 (55.7)
ACE inhibitors, ARB agents, or both	458 (45.3)	472 (47.2)
Diuretics	409 (40.5)	397 (39.7)
Surgery type — no./total no. (%)		
Valve§	619/1005 (61.6)	594/998 (59.5)
Coronary-artery bypass graft	384/1003 (38.3)	394/998 (39.5)
Ascending aorta or aortic arch	97/1004 (9.7)	109/997 (10.9)

Trial Interventions and Intraoperative Characteristics.

Variable	ANH Group (N=1010)	Usual-Care Group (N=1000)
Trial interventions		
Median volume of blood withdrawn during ANH (IQR) — ml†	650 (650–700)	0
Plasmapheresis instead of withdrawal of whole blood — no./total no. (%)	18/1003 (1.8)	0
Crystalloids administered before cardiopulmonary bypass — no./total no. (%)	976/1004 (97.2)	962/994 (96.8)
Median volume of crystalloids infused before cardiopulmonary bypass (IQR) — ml‡	1000 (500–1200)	700 (500–1000)
Other fluids administered before cardiopulmonary bypass — no./ total no. (%)§	2/1004 (0.2)	2/994 (0.2)
Intraoperative characteristics		
Median duration of cardiopulmonary bypass (IQR) — min¶	102 (75–134)	98 (71–131)
Hypotension — no./total no. (%)	114/1005 (11.3)	46/994 (4.6)
Tachyarrhythmia — no./ total no. (%)	27/1005 (2.7)	21/994 (2.1)

Clinical Outcomes.

Outcomes	ANH Group (N=1010)	Usual-Care Group (N=1000)	Relative Risk or Absolute Mean Difference (95% CI)*
Primary outcome			
Receipt of at least one allogeneic red-cell transfusion — no./total no. (%)	274/1005 (27.3)	291/997 (29.2)	0.93 (0.81 to 1.07)†
Secondary outcomes			
Death within 30 days after surgery or during hospitalization — no./total no. (%)	14/1008 (1.4)	16/997 (1.6)	0.87 (0.42 to 1.76)
Bleeding complications			
Surgical revision for bleeding — no./total no. (%)	38/1004 (3.8)	26/995 (2.6)	1.45 (0.89 to 2.37)
Median volume of blood drained from chest tubes at 12 hr after surgery (IQR) — ml‡	290 (190–423)	300 (200–450)	−11.66 (−35.54 to 12.22)
Ischemic complications — no./total no. (%)			
Myocardial infarction	10/1005 (1.0)	9/996 (0.9)	1.10 (0.45 to 2.70)
Stroke, transient ischemic attack, or both	11/1005 (1.1)	12/996 (1.2)	0.91 (0.40 to 2.05)
Thromboembolic event	5/1005 (0.5)	7/996 (0.7)	0.71 (0.23 to 2.22)
Acute kidney injury — no./total no. (%)	85/1005 (8.5)	89/996 (8.9)	0.95 (0.71 to 1.26)
Median no. of units of allogeneic blood component in patients receiving transfusion during hospital stay (IQR)			
Red cells	2 (1–4)	2 (1–3)	0.50 (−0.03 to 1.03)
Fresh frozen plasma	2 (1–4)	2 (1–4)	0.24 (−0.26 to 0.74)
Platelets	1 (1–3)	1(1–3)	0.17 (−0.59 to 0.93)

Safety Outcomes.

Outcome	ANH Group (N=1010)	Usual-Care Group (N=1000)	Relative Risk or Absolute Mean Difference (95% CI)†	P Value
Cardiogenic shock — no./total no. (%)	37/1006 (3.7)	32/995 (3.2)	1.14 (0.72 to 1.82)	0.57
Vasopressor or inotropic drugs for >48 hr — no./total no. (%)	152/1005 (15.1)	145/995 (14.6)	1.04 (0.84 to 1.28)	0.73
Mechanical circulatory support — no./total no. (%)‡	27/1006 (2.7)	23/996 (2.3)	1.16 (0.67 to 2.01)	0.59
Sepsis — no./total no. (%)	6/1006 (0.6)	5/995 (0.5)	1.19 (0.36 to 3.88)	0.99
Septic shock — no./total no. (%)	5/1006 (0.5)	3/995 (0.3)	1.65 (0.40 to 6.88)	0.73
Acute respiratory distress syndrome — no./total no. (%)	4/1003 (0.4)	2/995 (0.2)	1.98 (0.36 to 10.81)	0.69
Median lowest hematocrit level while in ICU (IQR) — %§	32 (28–36)	32 (29–36)	–0.04 (–0.50 to 0.43)	0.60
AKI with need for renal replacement therapy — no./total no. (%)	15/1005 (1.5)	14/996 (1.4)	1.06 (0.51 to 2.19)	0.87
Median duration of ventilation (IQR) — hr¶	7 (4–14)	7 (4–13)	3.26 (–0.31 to 6.82)	0.97
Median duration of ICU stay (IQR) — hr‖	38 (20–68)	40 (21–66)	6.23 (–0.02 to 12.47)	0.82
Died in the ICU — no./total no. (%)	11/1008 (1.1)	10/997 (1.0)	1.09 (0.46 to 2.55)	0.85
Median duration of hospital stay (IQR) — days**	8 (6–11)	8 (6–11)	0.50 (–0.20 to 1.20)	0.50
Died in the hospital — no./total no. (%)	14/1008 (1.4)	14/997 (1.4)	0.99 (0.47 to 2.06)	0.98
Hospital readmission within 30 days after randomization — no./total no. (%)	61/1008 (6.1)	59/997 (5.9)	1.02 (0.72 to 1.45)	0.90

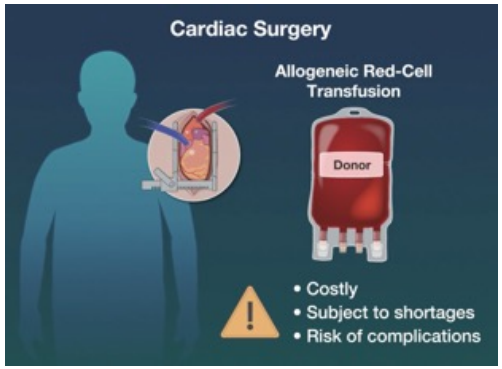
Cardiac Surgery
Allogeneic Red-Cell Transfusion
Donor
• Costly
• Subject to shortages
• Risk of complications

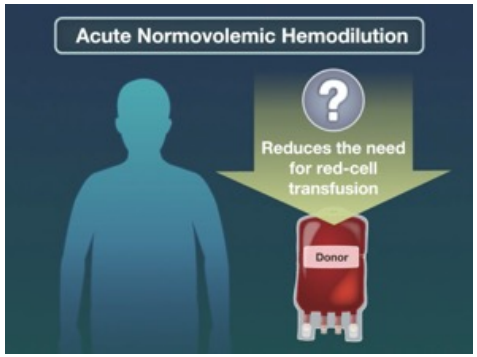
Acute Normovolemic Hemodilution
Reduces the need for red-cell transfusion
Donor

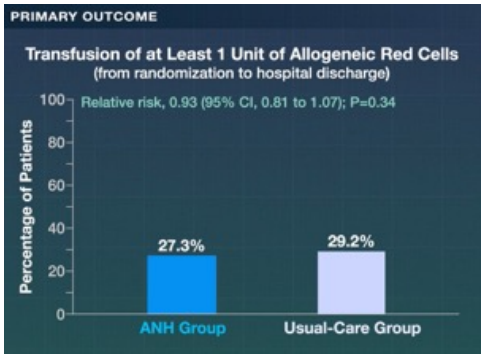
PRIMARY OUTCOME
Transfusion of at Least 1 Unit of Allogeneic Red Cells
(from randomization to hospital discharge)
Relative risk, 0.93 (95% CI, 0.81 to 1.07); P=0.34
Percentage of Patients
100
80
60
40
20
0
27.3%
29.2%
ANH Group
Usual-Care Group

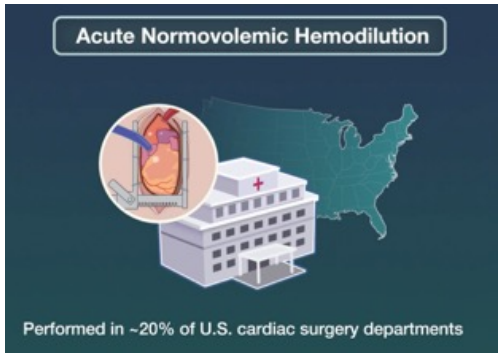
Acute Normovolemic Hemodilution
Performed in ~20% of U.S. cardiac surgery departments

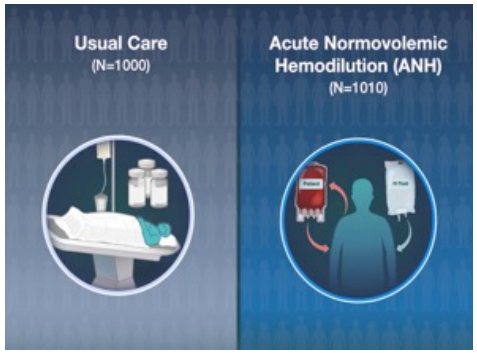
Usual Care
(N=1000)
Acute Normovolemic Hemodilution (ANH)
(N=1010)

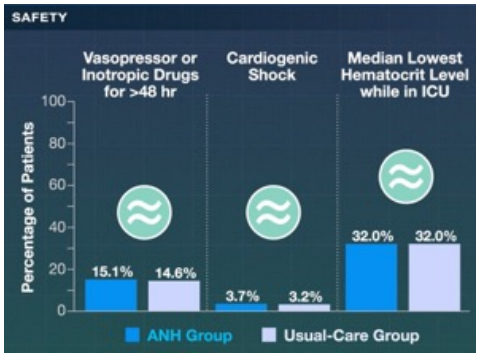
SAFETY
Vasopressor or Inotropic Drugs for >48 hr
Cardiogenic Shock
Median Lowest Hematocrit Level while in ICU
Percentage of Patients
100
80
60
40
20
0
15.1%
14.6%
3.7%
3.2%
32.0%
32.0%
ANH Group
Usual-Care Group

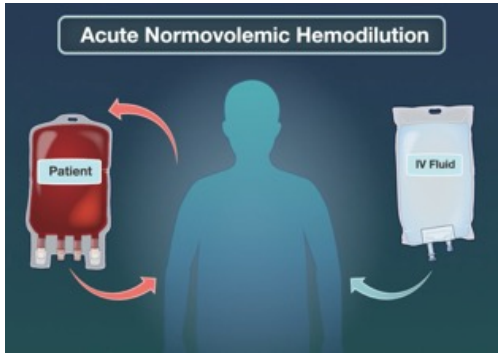
Acute Normovolemic Hemodilution
Patient
IV Fluid

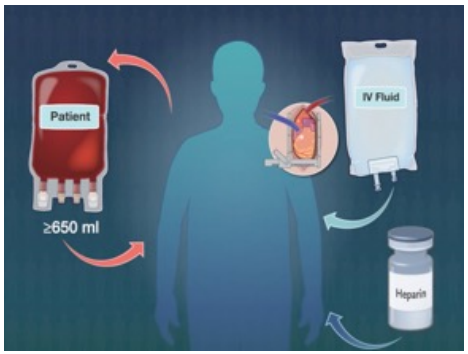
Patient
IV Fluid
≥650 ml
Heparin

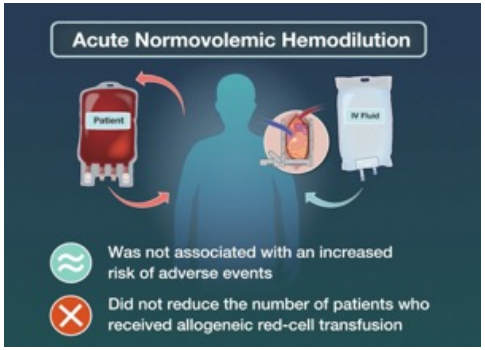
Acute Normovolemic Hemodilution
Patient
IV Fluid
Was not associated with an increased risk of adverse events
Did not reduce the number of patients who received allogeneic red-cell transfusion

A T cell receptor (TCR) is a protein complex located on the surface of T cells, specialized immune cells that play a crucial role in the adaptive immune response. TCRs are responsible for recognizing and binding to specific antigens, which are foreign substances or molecules that trigger an immune response. This recognition process is essential for activating T cells to fight infections, cancer, or other diseases.

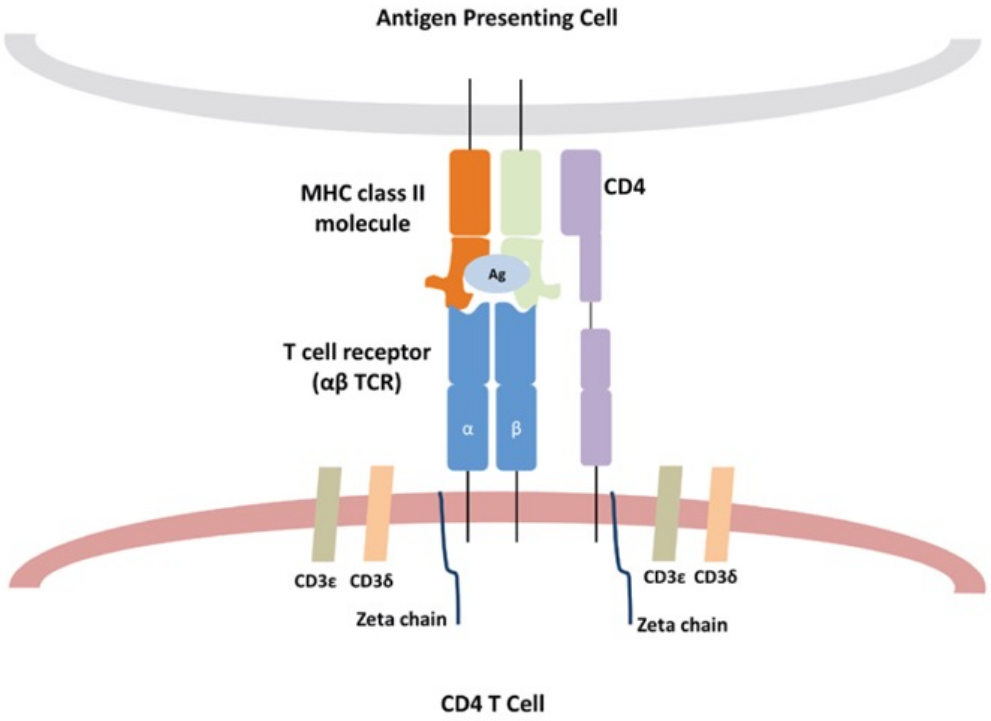

ZAP70 ist ein Protein, das eine Schlüsselrolle in der T-Zell-Signalübertragung spielt. Es ist eine Protein-Tyrosinkinase, die nach Aktivierung des T-Zell-Rezeptors (TCR) durch Bindung eines Antigens aktiviert wird. ZAP70 ist essentiell für die Weiterleitung des Signals vom TCR zu intrazellulären Signalwegen, die für die T-Zell-Aktivierung, Proliferation und Differenzierung verantwortlich sind.

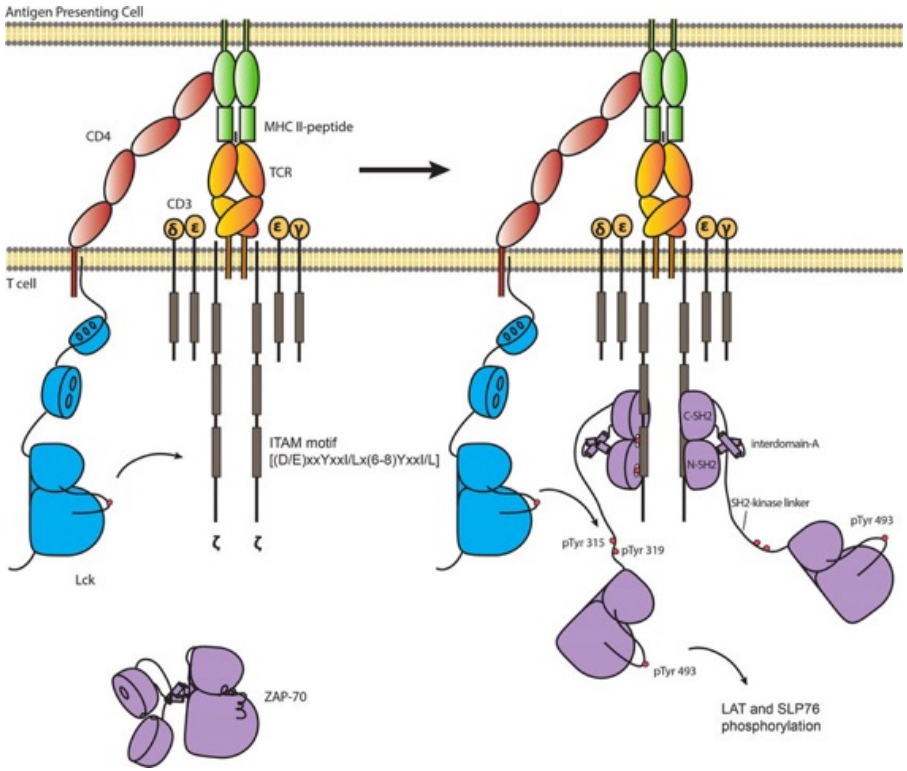

ZAP70 is a tyrosine kinase

Phosphorylation of ZAP-70 is required to initiate T cell receptor signaling. TCR signaling is initiated by two tyrosine kinases: the Src family kinase Lck and ZAP-70. Activated Lck phosphorylates ITAMs in the intracellular tails of chains of the TCR complex. Doubly phosphorylated ITAMs recruit ZAP-70 from the cytosol to the plasma membrane. Tyr 315, Tyr 319, and Tyr 493 of ZAP-70 are phosphorylated by Lck to fully activate ZAP-70, enabling ZAP-70 to phosphorylate two scaffold proteins, LAT and SLP-76, leading to the recruitment of effector proteins that stimulate T cell activation.

Resolution of Squamous-Cell Carcinoma by Restoring T-Cell Receptor Signaling

Summary

Cutaneous squamous-cell carcinoma (SCC) is primarily caused by oncogenesis mediated by ultraviolet radiation, and β-human papillomavirus (β-HPV) is believed to be a mere facilitator that is dispensable for the maintenance of cutaneous SCC. Here, we describe a woman with benign and malignant HPV-related diseases that include a recurrent, unresectable, invasive cutaneous SCC with β-HPV19 genomic integration in the context of germline pathogenic mutations in *ZAP70*, an adapter required for T-cell receptor (TCR) signal transduction. Restoration of the integrity of TCR signaling by allogeneic hematopoietic-cell transplantation led to the resolution of all HPV-related diseases, thereby revealing a direct role of β-HPV in skin carcinogenesis in hosts with defective adaptive T-cell responses. (Funded by the National Institutes of Health.)

Although the causative and prognostic roles of ultraviolet exposure, Fitzpatrick skin type, age, and sex in cutaneous SCC have been well defined and even incorporated into risk-prediction models, the contribution of immunosurveillance against cutaneous β-human papillomaviruses (β-HPVs) in the pathogenesis of cutaneous SCC remains unclear. Whereas a direct oncogenic role has been firmly established for mucosal α-HPVs that are integrated into the host genome in mucosal SCC (i.e., in the anogenital, oropharyngeal, or respiratory tract) and constitutively express the E6/E7 viral oncogenes, cutaneous β-HPVs are believed to have an indirect role as mere facilitators of skin carcinogenesis. In this so-called hit-and-run model, β-HPVs appear to be relevant at an early stage of carcinogenesis by enabling the accumulation of ultraviolet-induced DNA mutations. However, these β-HPVs have not been found to be stably transcribed in samples of established cutaneous SCC and, therefore, are considered to be dispensable in the maintenance of a frankly malignant phenotype. In addition, although the role of immunosurveillance in skin carcinogenesis is inferred by the high prevalence of cutaneous SCC in immunocompromised hosts and by the clinical response to checkpoint inhibitors in patients with a high mutational burden, the contribution of immunologic escape to viral or ultraviolet-mediated neoantigens in skin carcinogenesis remains uncertain.

Inborn errors of immunity can help to decipher the role of HPVs and specific immunologic functions in skin and mucosal carcinogenesis. Here, we report on the immunopathogenesis and management of recurrent, treatment-refractory, invasive cutaneous SCC associated with a β-HPV in the context of defective proximal T-cell receptor (TCR) signaling owing to germline variants in the gene encoding the zeta chain of the TCR-associated protein kinase 70 (*ZAP70*). The regression of multiple benign and recurrent malignant HPV-related lesions after restoration of HPV-specific T-cell responses following hematopoietic-cell transplantation (HCT) illustrates the role of adaptive T-cell functions and the implications of integrated ablative and immunotherapeutic approaches to severe HPV-related diseases.

Case Report

A 34-year-old woman with a history of cryptococcal meningitis with neuro-ophthalmic involvement had progressively worsening cutaneous and mucosal HPV-related diseases with oral condylomas, diffuse verrucous lesions, and multiple recurrent cutaneous SCCs in sun-exposed surfaces at 43 different biopsy-proven lesions or sites.

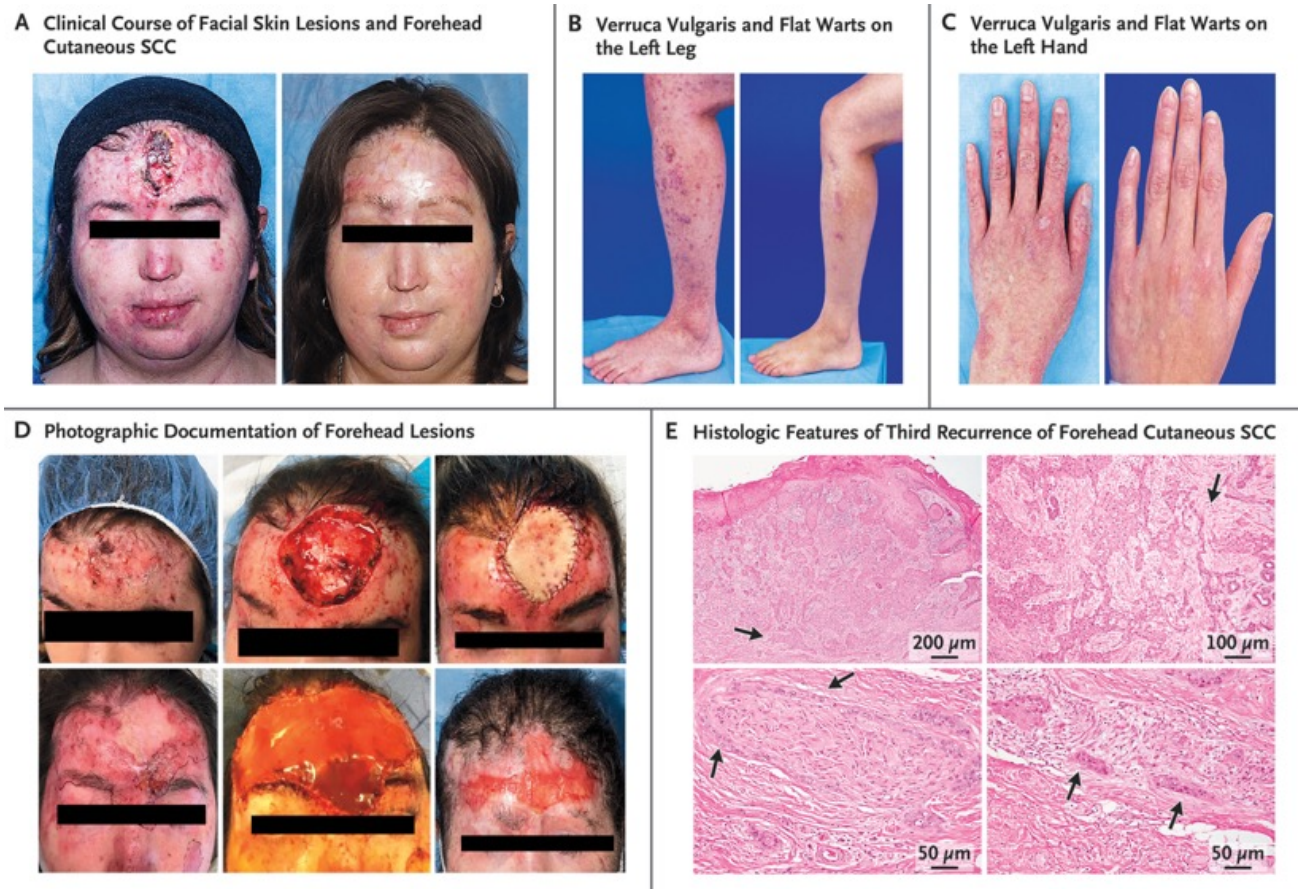

Clinical, Virologic, and Histologic Findings in the Study Patient with Recurrent Cutaneous Squamous-Cell Carcinoma (SCC).

Panel A shows the clinical course of facial skin lesions and the forehead cutaneous SCC in the study patient before and after hematopoietic-cell transplantation (HCT) (left and right panel, respectively).

Shown is the clinical course of verruca vulgaris and flat warts on the left leg (**Panel B**) and the left hand (**Panel C**) before and after HCT (left and right panels, respectively). **Panel D** shows clinical photographic documentation of the course of the forehead cutaneous SCC. **Panel E** shows the histologic features of the third recurrence of invasive cutaneous SCC.

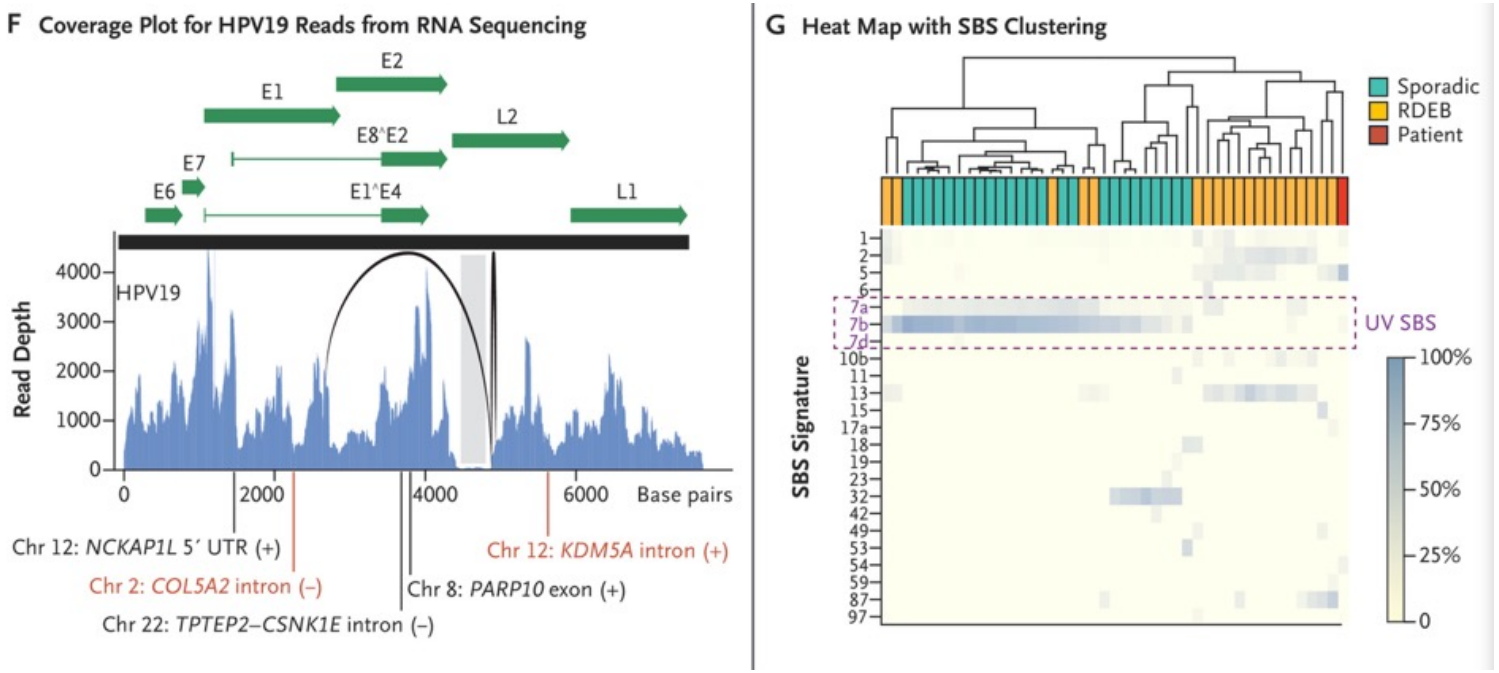

Panel F shows the coverage plot for HPV19 reads from RNA sequencing of a sample of paraffin-embedded tissue derived from the third recurrence of the forehead invasive cutaneous SCC. The different early (E) or late (L) transcribed open reading frames of HPV19, including the alternatively spliced E8^E2 and E1^E4, are shown in green above the coverage plots shaded in blue. The gray box indicates the low level of transcription in the proximal region of the L2 gene, which prompted the analysis of junction-spanning reads and identification of the recombination of regions of the viral genome junctions (black arcs). **Panel G** shows a heat-map display of the clustering of COSMIC single-base substitutions (SBSs) identified by DNA sequencing of the third recurrence of the forehead invasive cutaneous SCC alongside previously published cutaneous SCCs.

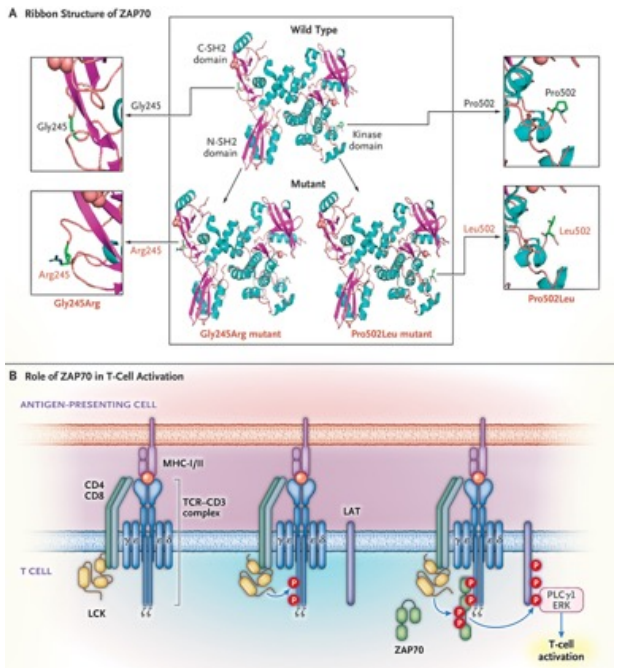

An immunoreceptor tyrosine-based activation motif (ITAM) is a conserved sequence of four amino acids that is repeated twice in the cytoplasmic tails of non-catalytic tyrosine-phosphorylated receptors, cell-surface proteins found mainly on immune cells.

Structure and Function of *ZAP70*.

Panel A shows the ribbon structure of *ZAP70*, the gene with germline variants that were identified as the cause of the underlying immunodeficiency that led to the HPV19-related cutaneous SCC in the study patient. The upper portion illustrates the wild-type ZAP70 protein (PBD identification code, 4K2R), highlighting the positions of Gly245 in the carboxy-terminal SH2 domain and the Pro502 in the kinase domain. The mutated alleles — c.1505C→T (p.Pro502Leu), ClinVar SCV005903646 and c.733G→A (p.Gly245Arg), and ClinVar SCV005903647 — are shown in the lower portion of the figure. The amino acid residues of these positions are shown as ball and stick with color according to atoms. The missense change resulting in Gly245Arg introduces a large positively charged side chain in place of a small nonpolar one and results in altered binding of the SH2 domain to the ITAM domain on the CD3 zeta chain. The Pro502Leu change results in the substitution in the kinase domain of a smaller side chain for a larger nonpolar amino acid with one with a smaller side chain. Such changes alter the autophosphorylation of ZAP70 and impair the phosphorylation of the downstream scaffold proteins LAT and SLP76, which ultimately compromises the transduction of TCR signaling T-cell activation, proliferation, and generation of HPV-antigen–specific T cells (as shown in Fig. 3). **Panel B** shows sequential modeling of the role of ZAP70 in T-cell activation. After successful recognition of major histocompatibility complex (MHC)–associated peptides (i.e., short fragments of proteins that bind to MHC molecules) and T-cell receptor (TCR) engagement, the coreceptor (CD4/CD8)–associated LCK can phosphorylate the CD3 zeta chain immunoreceptor tyrosine-based activation motif (ITAM; phosphorylation sites indicated by red circles marked P). In resting T cells, ZAP70 is present in an inactive cytoplasmic conformation, but the phosphorylated ITAMs allow the binding of the ZAP70 SH2 domains to the TCR complex. Such CD3 zeta-chain–bound form of ZAP70 can be phosphorylated by LCK, resulting in the activation of ZAP70 catalytic activity. Zeta-chain–bound ZAP70 in this active phosphorylated conformation can subsequently phosphorylate LAT, which functions as a scaffold protein to recruit other signaling proteins — phospholipase C gamma 1 (PLCγ1) and extracellular signal-regulated kinase (ERK). This process ultimately results in T-cell activation and consequent proliferation and differentiation.

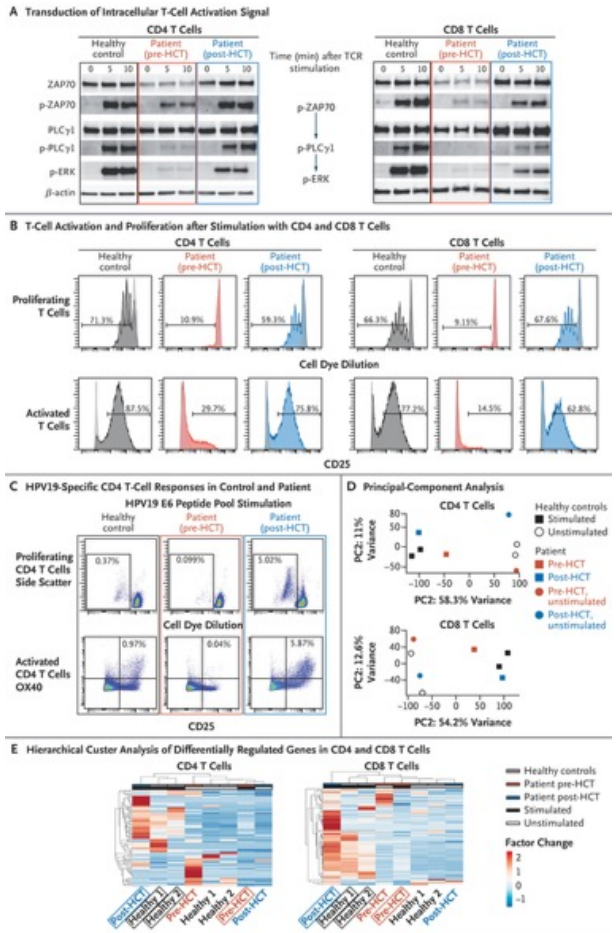

Genetic, Functional, and Immunologic Analysis of ZAP70 before and after Hematopoietic-Cell Transplantation (HCT). **Panel A** shows transduction of the intracellular T-cell activation signal in sorted CD4 and CD8 T cells from a healthy control and from the study patient before and after HCT. Cells are harvested and cellular proteins are extracted for Western blot analysis of TCR signaling before TCR stimulation with CD3/CD28 cross-linking antibodies and 5 minutes and 10 minutes after such analysis. Normal transduction of the TCR-engagement signal results in phosphorylation of ZAP70, PLCγ1, and ERK (healthy control, black rectangle). Such signal transduction is impaired in the study patient before HCT, as shown by the reduced amount of phosphorylated ZAP70, PLCγ1, and ERK after TCR stimulation (red rectangle shows before HCT). HCT restores the integrity of the transduction of TCR signaling (blue rectangle). **Panel B** shows T-cell activation and proliferation after stimulation with CD4 and CD8 T cells in a healthy control (black histogram) and in the study patient before and after HCT (red and blue histograms, respectively). Shown is the dilution of a cell dye during cell proliferation (upper panels) and the expression of the activation marker CD25 (lower panels) after TCR stimulation with anti–CD3/CD28 cross-linking antibodies as measured by flow cytometry. Normal T-cell activation results in the up-regulation of CD25 and dilution of the cell dye, whereas the impaired TCR signal transduction in the study patient before HCT results in poor T-cell proliferation (lack of cell dye dilution) and lack of up-regulation of CD25. By restoring the integrity of TCR signaling, HCT results in normal T-cell activation and proliferation. **Panel C** shows HPV19-specific CD4 T-cell responses in a healthy control and in the study patient before and after HCT. The expression of the activation markers CD25 and OX40 (lower panels) and the dilution of a cell dye during cell proliferation (upper panels) after T-cell stimulation with a peptide pool of the HPV19 E6 protein are shown. Normal T-cell activation results in the up-regulation of CD25 and OX40 and cell proliferation, as shown by dilution of a cell dye (healthy control, black rectangle). Such T-cell activation and proliferation is impaired in the study patient before HCT (red rectangle), whereas prominent T-cell activation and expansion of E6-specific CD4 T cells occurs after HCT (blue rectangle). **Panel D** shows the principal-component analysis (PCA) of the CD4 and CD8 T-cell transcriptome before and 36 hours after TCR stimulation with CD3/CD28 cross-linking antibodies, representing unstimulated or resting and stimulated or activated T cells, respectively. The PCA figures represent a two-dimensional scatterplot of the first two principal components (PC2) of the RNA sequencing transcriptional data from stimulated (squares) and unstimulated (circles) T cells from two healthy controls (black) and the study patient before HCT (red) and after HCT (blue). The study patient's stimulated T cells after HCT (blue squares) have more similarity to those from heathy controls (black squares) than do T cells from the study patient before HCT (red squares). Resting unstimulated T cells (circles) do not have substantial transcriptional differences between healthy controls and the study patient before and after HCT. **Panel E** shows hierarchical cluster analysis of the differentially regulated genes in CD4 and CD8 T cells before and 36 hours after TCR stimulation with CD3/CD28 cross-linking antibodies. The figures represent the factor change in the transcription of genes in T cells of two healthy controls (gray) and the study patient before HCT (red) and after HCT (blue) in unstimulated conditions (white bar at top of graph) and TCR-stimulated conditions (black bar at top of graph and boxed labels at bottom). Each row is a gene, and each column is a sample from one of the two healthy controls or the study patient. The study patient's stimulated CD4 and CD8 T cells after HCT (blue) cluster with those from healthy controls (black) as compared with T cells before HCT (red).

Discussion

Cutaneous SCC, a common cutaneous cancer, is caused primarily by ultraviolet-mediated somatic DNA mutations. However, the increased risk of cutaneous SCC in solid-organ transplantation, chronic lymphocytic leukemia, and other immunocompromising conditions — and the robust clinical response to immune-checkpoint inhibitors — indicate that impaired adaptive T-cell responses are associated with both the development and the progression of cutaneous SCC. Nonetheless, it remains unclear to what extent skin commensal β-HPVs, somatic neoantigens, or both are involved in generating and maintaining T-cell responses that can prevent or control skin carcinogenesis.

We found that a recurrent, invasive, treatment-resistant cutaneous SCC had high expression of β1-HPV19 viral oncogenes during host genome integration. This tumor lacked typical SCC-associated somatic driver mutations and had only modest ultraviolet-mediated and overall mutational burden. This patient's tumor showed β-HPV integration in cutaneous SCC, and we attribute the patient's benign and malignant HPV-related diseases to the specific immunologic context determined by a ZAP70–mediated impairment in HPV-specific T-cell responses. *ZAP70* hypomorphic variants, such as the ones identified in this patient, can be partially permissive for T-cell development but still impair TCR-mediated signal transduction. The precise genotype–phenotype correlation identified in this case allowed us to decipher the long-term clinical effect of altered TCR signaling on adaptive immunity against commensal HPV and consequent skin carcinogenesis.

The Washington Post
Democracy Dies in Darkness

Opinion

845,000 dead on U.S. highways. Why not address the main cause?

We need to ramp up the standards for road tests and train people to be better drivers.

But mostly, the problems lie with us. We aren't very good drivers. And there is a potential solution: better driver training. If we can fix bad driving, at least partially, we can save thousands of lives.

But here's what hasn't improved: the way we train drivers. All that's required is passing a written test, followed by a 15-minute road test that involves parallel parking, executing K-turns, signaling properly, obeying all signs and so forth.

Instead, I've seen my fellow drivers on the road eating, drinking, shaving, brushing their teeth, putting on makeup, playing air guitar, fighting, making out and, of course, texting. Despite laws prohibiting that last act while behind the wheel, one sees drivers on the phone every day on the highways.

Motor Vehicle Crash Prevention

The human toll of motor vehicle–related deaths in the United States is staggering: 42,939 people lost their lives on U.S. roadways in 2021 alone. Despite continued efforts to reduce the number of road fatalities, U.S. fatality rates (both per capita and per vehicle-mile traveled) are much higher than those observed in many other high-income nations. This crisis is not inevitable — analyses of naturalistic data from in situ driving provide us with an unprecedented understanding of the behaviors and circumstances that contribute to motor vehicle crashes, the leading cause of death for persons 5 to 29 years of age. These data, coupled with recent advances in technology, provide us with the tools necessary to reverse this preventable trend and make tangible progress toward a future with universally safe mobility.

In 2021, the U.S. Department of Transportation (USDOT) adopted the evidence-based Safe System Approach, which encompasses six principles: death and serious injuries on our roadways are unacceptable, humans make mistakes, humans are vulnerable, responsibility for safety is shared, safety is proactive, and redundancy is crucial.

Research Objectives and Principles of the Safe System Approach

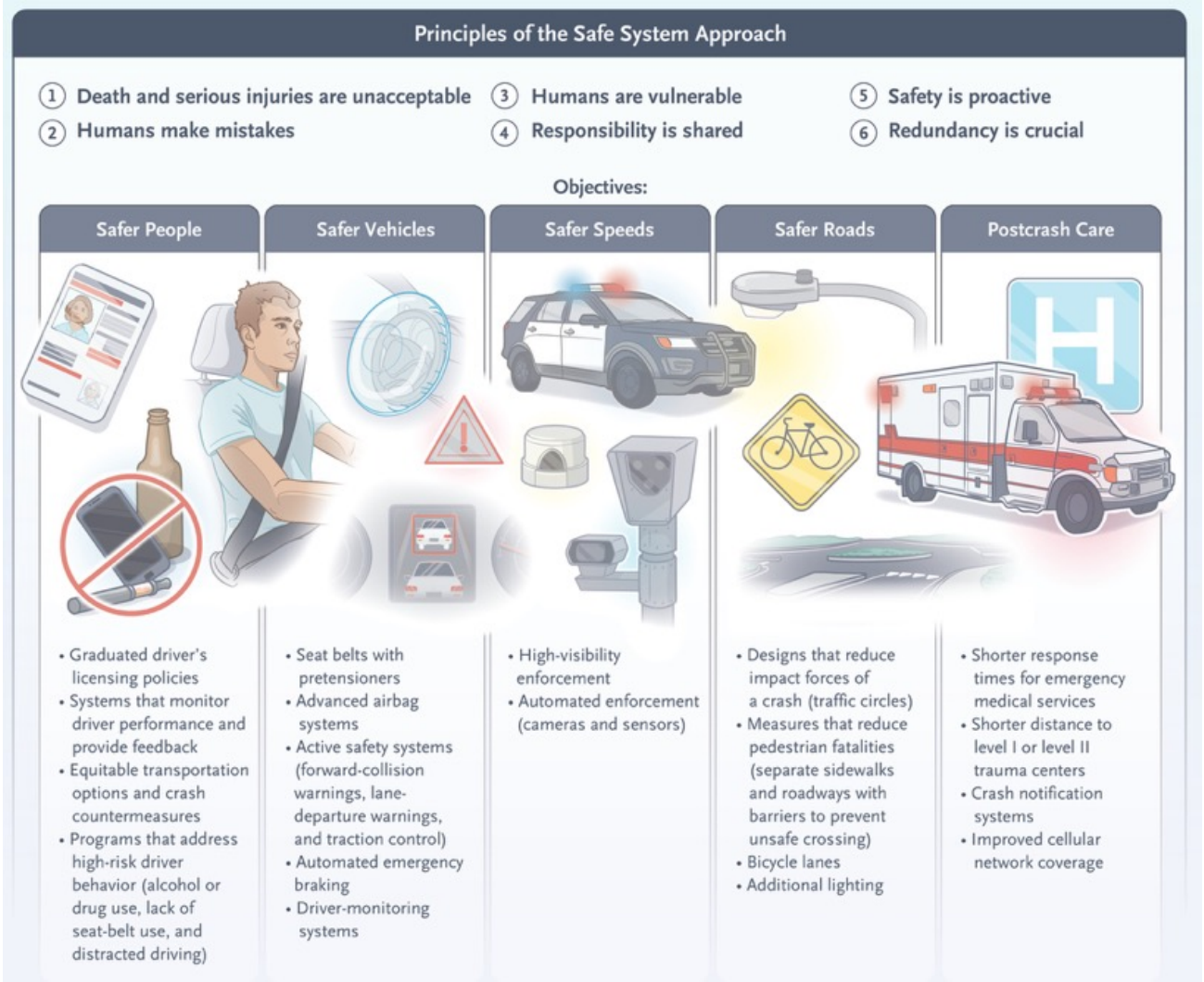

Motor Vehicle Crash Prevention

- More than 40,000 people died on U.S. roadways in 2021, a figure that represents a per capita rate that is much higher than those in many other high-income nations.
- The evidence-based Safe System Approach to reducing the incidence of traffic fatalities encompasses the following principles: roadway injuries are unacceptable, humans make mistakes and are vulnerable, safety is a shared responsibility and must be proactive, and redundancy is crucial.
- The responsibility for roadway safety is shared by users, designers, operators, policymakers, administrators, and health care professionals.
- Measures to improve safety include interventions to prevent high-risk behavior by drivers and passengers, road design to reduce the risk of crashes and to physically separate vehicles from pedestrians and cyclists, manufacture of vehicles with enhanced preventive features and crashworthiness, enforcement of safer traffic speeds, and improvements to postcrash medical care.

Haddon Matrix for Prevention of Motor Vehicle–Related Fatalities and Serious Injuries.

Stage	Vehicle Driver or Occupant	Vehicle	Roads and Infrastructure	Policy
Prevention	Effective training with regard to rules and norms, defensive driving, and appropriate use of vehicle features Alert and sober driver Driver judged fit to drive (on the basis of licensing and self-selection [mostly in the case of older drivers who choose to stop driving])	Driver-assistance systems (e.g., adaptive cruise control) Distraction-mitigating interfaces (e.g., voice control) Indirect visibility systems (e.g., backup cameras) Driver-monitoring systems (e.g., monitors of attention and sobriety status)	Positive guidance (roadway designed to provide drivers with clear, timely, and easily understandable information) Road diets (reductions in number and width of travel lanes) Marked pedestrian and bicycle lanes Effective traffic-control device strategies (motorist and nonmotorist) Road lighting	Enhanced graduated licensing of drivers Effective motor vehicle regulations (e.g., FMVSS) High-visibility presence of law enforcement Automated enforcement Meaningful penalties for violations
Precrash	Swift reaction to alerts and warnings and successful evasive maneuvering (indicate training and ability)	Active safety features (e.g., forward-collision warning, automatic electronic braking, lane-keep assistance)	Rumble strips High-friction surfaces Ample space on road shoulder Alerts about nonmotorists (e.g., protecting pedestrians)	Motor vehicle regulations (e.g., FMVSS) New Car Assessment Program and Insurance Institute for Highway Safety crash ratings
Crash	Body and seat position (indicates training)	Vehicle crashworthiness and passive safety devices (e.g., seat belts and airbags)	Obstacles (e.g., light poles) designed to break away; space adjacent to roadway is clear (e.g., no trees or obstacles); guardrails redirect or absorb energy	Motor vehicle regulations (e.g., FMVSS)
Postcrash	Rapid response and treatment by emergency medical services, quality of prehospital care, quality of emergency department care	Crash notification systems that automatically alert emergency response systems, access for extraction of victim, integrity of vehicle battery and fuel cells	Traffic management, monitoring, and strategy in vicinity of crash site Variable-message signage influencing routes and speeds by means of active traffic management when crashes occur	Proximity and capacity of emergency services, and protocols and policies in place to enable rapid response to crashes

Conclusions

As a society, we cannot accept an annual toll of 42,939 fatalities and 2,497,657 injuries (in 2021) on our nation's roadways· Worse yet, we are currently moving in the wrong direction, with the incidence of fatalities and injuries increasing on average over the past several years. The USDOT, in its Safe System Approach, shifts the blame for these fatalities and injuries from exclusively the road users (e.g., drivers and pedestrians) to all the stakeholders in our transportation system, including the engineers, policymakers, public health professionals, and medical professionals who design and affect all aspects of our transportation systems. The Safe System Approach is an evidenced-based framework that stands to improve safety for all, and its success depends on full participation by all stakeholders.

Spontaneous Intracranial Hypotension

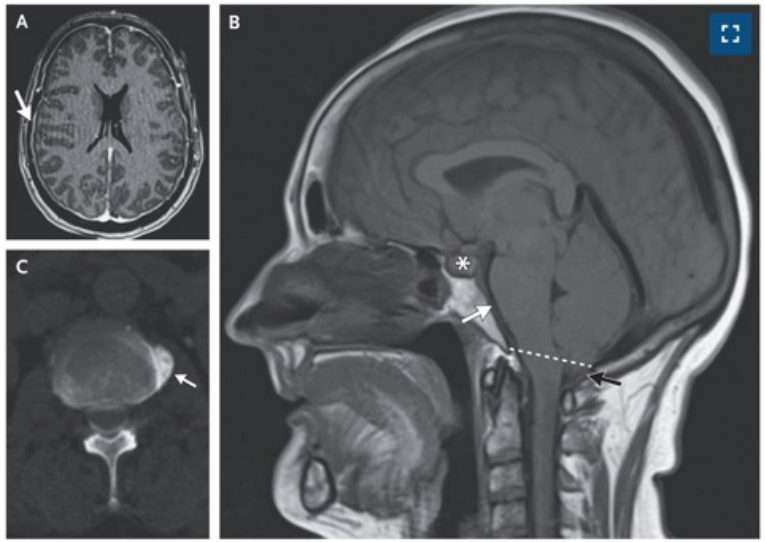

A 50-year-old woman presented to the emergency department with a 10-day history of a throbbing headache that had started suddenly after she felt a "pop" in her back. The headache worsened when she was upright and abated when she lay flat. A physical examination, including funduscopy, was normal. Magnetic resonance imaging (MRI) of the brain showed diffuse pachymeningeal enhancement (Panel A, arrow [axial view, T1 sequence with contrast material]). MRI also showed protrusion of the cerebellar tonsils (Panel B, black arrow and dashed line) into the foramen magnum (tonsillar ectopia), flattening of the pons with effacement of the prepontine cistern (Panel B, white arrow), and enlargement of the pituitary gland owing to increased blood flow (pituitary hyperemia; Panel B, asterisk [T1 sequence without contrast material]). Owing to concern about spontaneous intracranial hypotension, a computed tomographic myelogram was obtained to detect a cerebrospinal fluid (CSF) leak. An extradural leak was identified on the ventral surface of the spinal cord at the T12–L1 intervertebral space (Panel C, arrow) and attributed to an osteophyte at the same level. A diagnosis of spontaneous intracranial hypotension — a condition of postural headache that results from sagging of the brain owing to a noniatrogenic CSF leak — was made. Treatment with an epidural blood patch was administered, whereupon the patient's headache resolved.

Spiderweb-like Vessels in Retinopathy of Prematurity

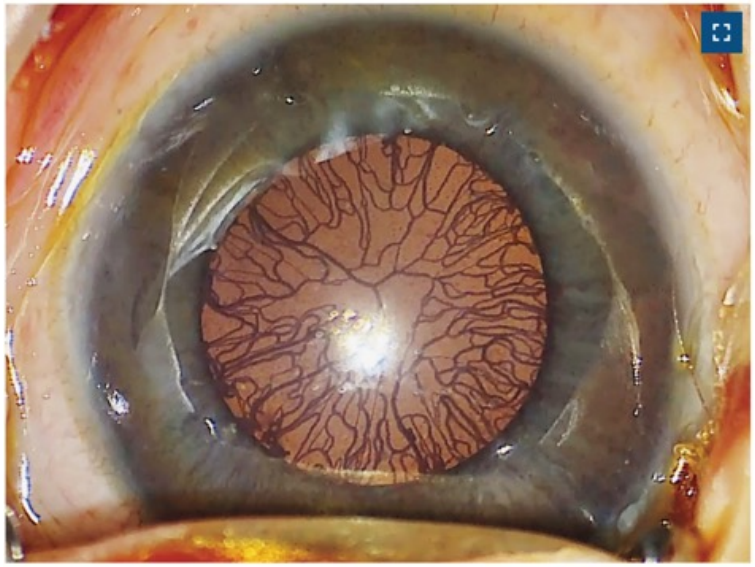

A baby boy was brought to an eye hospital at 8 weeks of age for evaluation and treatment of retinopathy of prematurity. The baby had been born at 25 weeks' gestation with a birth weight of 850 g and was hospitalized in a neonatal intensive care unit for neonatal respiratory distress syndrome. When the infant was 7 weeks old, an initial eye examination showed retinopathy of prematurity. On ophthalmologic examination at the current presentation, neovascularization of the iris was seen. There was also dilatation and tortuosity of the retinal vessels. Retinal perfusion extended to the posterior retina, indicating severe disease. Intraocular pressures were normal. A decision was made to inject an anti–vascular endothelial growth factor agent. A plastic surgical field and iodine were applied to the eye. The anterior chamber of both eyes was noted to have spiderweb-like vessels that densely covered the anterior lens capsule (as shown in the figure). Retinopathy of prematurity is characterized by delayed retinal vascular development followed by vasoproliferation. Risk factors include prematurity and low birth weight. Early screening and treatment are crucial to prevent blindness. After further treatment with laser therapy when the infant was 17 weeks old, the retinopathy stabilized.

Case 22-2025: A 19-Year-Old Woman with Seizurelike Activity and Odd Behaviors

A 19-year-old woman was admitted to this hospital because of episodes of shaking of the right arm and leg and odd behaviors.

The patient had been in her usual state of health until 10 days before the current presentation, when slowed speech developed, along with intermittent shaking and numbness of the right arm. Seven days before the current presentation, bystanders witnessed the patient collapse while she was standing on a subway platform; full-body shaking reportedly occurred. On arrival of emergency medical services, the patient was confused, drooling, and had bitten her tongue. During transport to the emergency department of another hospital by ambulance, she gradually became more alert.

In the emergency department, the patient did not recall the events at the subway station. The vital signs and physical examination were normal. The blood lactate level was 13.9 mmol per liter (125.2 mg per deciliter; reference range, 0.7 to 2.1 mmol per liter [6.3 to 18.9 mg per deciliter]), and the blood creatine kinase level was 84 U per liter (reference range, 30 to 135). Blood levels of electrolytes, glucose, alanine aminotransferase, and aspartate aminotransferase were normal, as were the results of tests of kidney function and the complete blood count. Computed tomography (CT) and magnetic resonance imaging (MRI) of the head, performed without the administration of intravenous contrast material, showed no abnormalities. The patient was admitted to the other hospital.

Additional history was obtained from the patient's parents. She had a history of depression and anxiety symptoms, for which she had seen a therapist briefly in the year before the current presentation; there were no previous psychiatric admissions. Medications since discharge from the other hospital included levetiracetam, lamotrigine, melatonin, and folic acid; she had been taking no medications before the admission to the other hospital. She had no known adverse reactions to medications. The patient was born and raised in an urban area of South Asia. One year before the current presentation, she moved to a suburban area of the Midwest United States, where she attended college and had two part-time jobs. Three weeks before the current presentation, she traveled with her parents to New England for vacation. The patient did not drink alcohol, smoke cigarettes, vape, use cannabis, or take illicit drugs. Her mother, father, and sibling were alive and well; her paternal grandmother had schizophrenia.

On the second hospital day, the patient was evaluated by the psychiatry consultant. During the interview, she had a sudden onset of extension and stiffening of the right arm, flexion and stiffening of the left arm, and turning of the head to the right, followed by full-body shaking. During the episode, the eyes stared but she blinked in response to threat. After approximately 60 seconds, the episode resolved. She described feeling that her "brain and mind were disconnected," and she did not think that she would be able to return to college. She did not have auditory or visual hallucinations or suicidal or homicidal thoughts.

Differential Diagnosis

This previously healthy young woman presented with neurologic symptoms and changes in behavior that were acute in onset and severe in nature.

Seizurelike Activity

This patient initially presented with collapse and episodes of full-body shaking, with subsequent amnesia and confusion. The blood lactate level was elevated; other laboratory test results were unremarkable, as was imaging of the head. This clinical picture is consistent with generalized seizure. During the admission to the first hospital, the patient had episodes of impaired speech, numbness of the right arm, and shaking of the right side, with an aura that was described as a feeling of dread.

Catatonia

On admission to this hospital, the patient began to have more bizarre and less consistent behaviors, such as variable and delayed speech with occasional mutism, as well as inconsistent oppositional behaviors and repetitive, purposeless movements. Routine laboratory test results continued to be unremarkable aside from elevated levels of creatine kinase.

Psychosis

The disorganized thought process and the sense of fragmentation reported by the patient are consistent with psychosis.

Common Disorders in Which Psychosis Is Typical

Toxidromes that result from substance use are common, and psychosis is a typical feature. Substance use may include recreational use of dextromethorphan or synthetic cannabinoids, which may not be detected on routine toxicology screening.

Common Disorders in Which Psychosis Is Atypical

Cancer, stroke, and severe traumatic brain injury are all unlikely causes of this patient's presentation, given the normal imaging studies. Most endocrine and metabolic considerations are ruled out on the basis of normal laboratory test results.

Rare Disorders in Which Psychosis Is Atypical

Genetic syndromes and neurodegenerative diseases rarely manifest in the second decade of life. Wilson's disease is unlikely in this patient without signs of liver disease, which are usually present by the time of onset of psychosis.

Rare Disorders in Which Psychosis Is Typical

Acute intermittent porphyria occurs in young women and is characterized not only by psychosis but also by seizure and changes in behavior. However, this patient had persistent symptoms over the course of weeks as opposed to the discrete episodes that usually characterize acute intermittent porphyria.

Diagnosis

Anti–NMDA receptor encephalitis.

Initial Management

Lumbar puncture was performed on hospital day 2. Gram's staining of the CSF revealed rare white cells and no bacteria. Analysis of the CSF showed 19 white cells per microliter (reference range, 0 to 5), of which 89% were lymphocytes, 8% were monocytes, and 3% were neutrophils. The CSF glucose and total protein levels were normal. Empirical treatment with intravenous acyclovir for a possible diagnosis of HSV infection was started.

In patients with presumed anti–NMDA receptor encephalitis, early treatment with immunosuppressive therapy aims to reduce circulating levels of antibodies that disrupt complex neuronal functions through interaction with glutamate NMDA receptors, which are widely distributed on cerebral neuronal membrane surfaces. Synergistic immunosuppressive regimens, including intravenous glucocorticoids and intravenous immune globulin (IVIG), are the mainstay of treatment based on clinical experience and expert opinion.

Approximately 50% of young women presenting with anti–NMDA receptor encephalitis will have an ovarian teratoma as the occult trigger of paraneoplastic disease. Pelvic imaging may provide additional early support for the diagnosis while awaiting results of antibody testing. If a teratoma is detected, prompt resection is critical. A transabdominal ultrasound image of the pelvis obtained on hospital day 5 revealed a heterogeneous mass, measuring 17 cm in diameter with mixed echogenicity, located in the right adnexa.

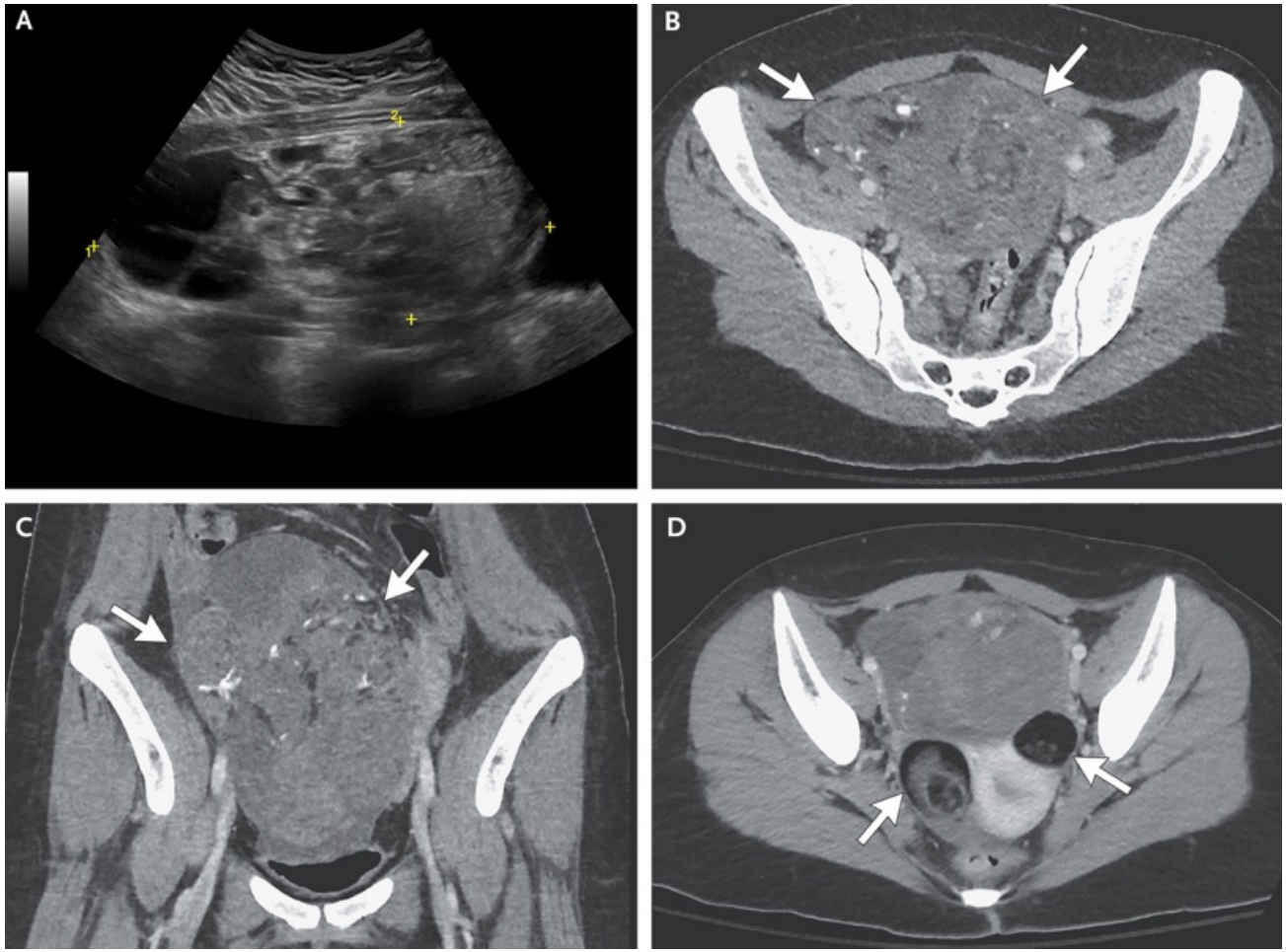

Imaging Studies of the Abdomen and Pelvis.

A transabdominal ultrasound image of the pelvis (Panel A) shows a 17-cm heterogeneous mass with mixed echogenicity in the right adnexa. Axial (Panel B) and coronal (Panel C) CT images of the abdomen and pelvis show a 17-cm heterogeneous mass in the midline of the pelvis containing fat, calcifications, and fluid and soft-tissue attenuation (arrows). An axial image of the pelvis (Panel D) taken at a more inferior level shows bilateral adnexal masses that contain fat and soft-tissue elements (arrows) and are more homogeneous than the larger mass.

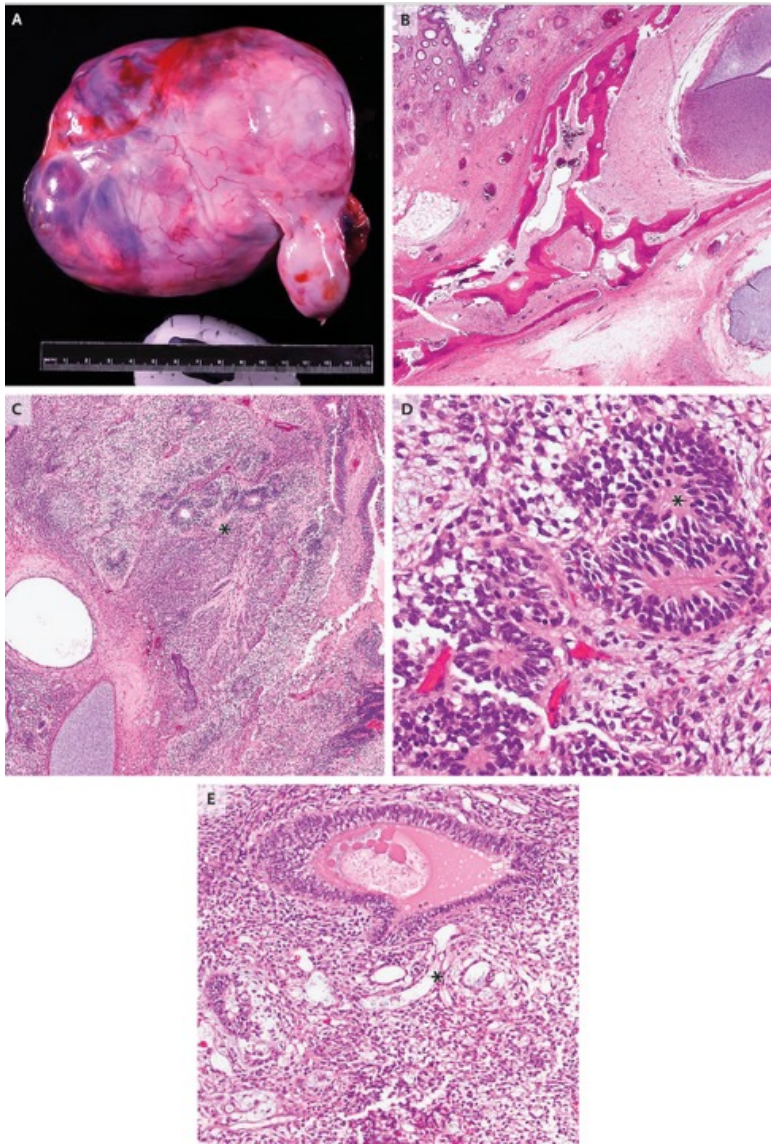

Left Salpingo-Oophorectomy Specimen.

A photograph of the left ovarian mass shows a tan-white and diffusely nodular external surface (Panel A). Hematoxylin and eosin staining of a section of a mature teratoma specimen obtained from the left ovary (Panel B) shows tissue composition derived from all three germ layers, including the ectoderm (keratinizing squamous epithelium and skin adnexal structures), mesoderm (bone and adipose tissue), and endoderm (intestinal epithelium). Hematoxylin and eosin staining of a specimen of the immature teratoma from the left ovary (Panel C) shows tissue composed of diffuse sheets, primitive tubules, and pseudorosettes and rosettes of immature neuroepithelium (Panel C, asterisk); high-grade cytologic atypia with brisk mitotic activity within immature neuroepithelium (Panel D, asterisk) was present, as was a yolk-sac tumor component comprising anastomosing channels and variably sized cysts lined by primitive-appearing cells (Panel E, asterisk). The immature teratoma was approximately 70% of the overall tumor volume, and the yolk-sac tumor was approximately 30% of the overall tumor volume.

This patient received additional immunosuppression in the context of worsening symptoms 2 weeks after first-line therapy. Therapeutic plasma exchange was initiated in addition to induction doses of rituximab, a combination that is often used in patients who do not have a response to first-line therapy. After the patient received additional immunosuppressive therapy and therapeutic plasma exchange, her condition improved substantially, and she showed remarkable insight into her illness without any further evidence of psychosis. After a 6-week inpatient hospitalization, she was transferred to a rehabilitation facility for ongoing speech and language therapy, occupational therapy, physical therapy, and monitoring of catatonia while lorazepam was tapered.

During the first 24 months of treatment for anti–NMDA receptor encephalitis, the risk of relapse is 12%. Relapses are most likely to manifest with isolated psychiatric symptoms and can occur up to 13 years after initial diagnosis.

In patients with anti–NMDA receptor encephalitis, immunosuppression is maintained for many months. One regimen with a favorable safety profile is administration of intravenous methylprednisolone, initially with weekly infusions, followed by infusions at 2-week intervals and then at 4-week intervals over the course of 6 to 12 weeks. At her last follow-up with the neurology consultant 7 months after discharge, the patient had completed treatment with methylprednisolone. She continues to receive rituximab infusions every 6 months, and there have been no signs of relapse.

Final Diagnosis

Malignant mixed germ-cell tumor and anti–NMDA receptor encephalitis.

Anti-NMDA receptor encephalitis is a rare autoimmune disease where the body's immune system mistakenly attacks NMDA receptors in the brain, causing inflammation and various neurological and psychiatric symptoms. It is characterized by a range of symptoms including psychosis, memory deficits, seizures, and movement disorders. Treatment often involves immunosuppressants and tumor removal if a germ cell tumor is present, with a generally good prognosis when treatment is initiated early.

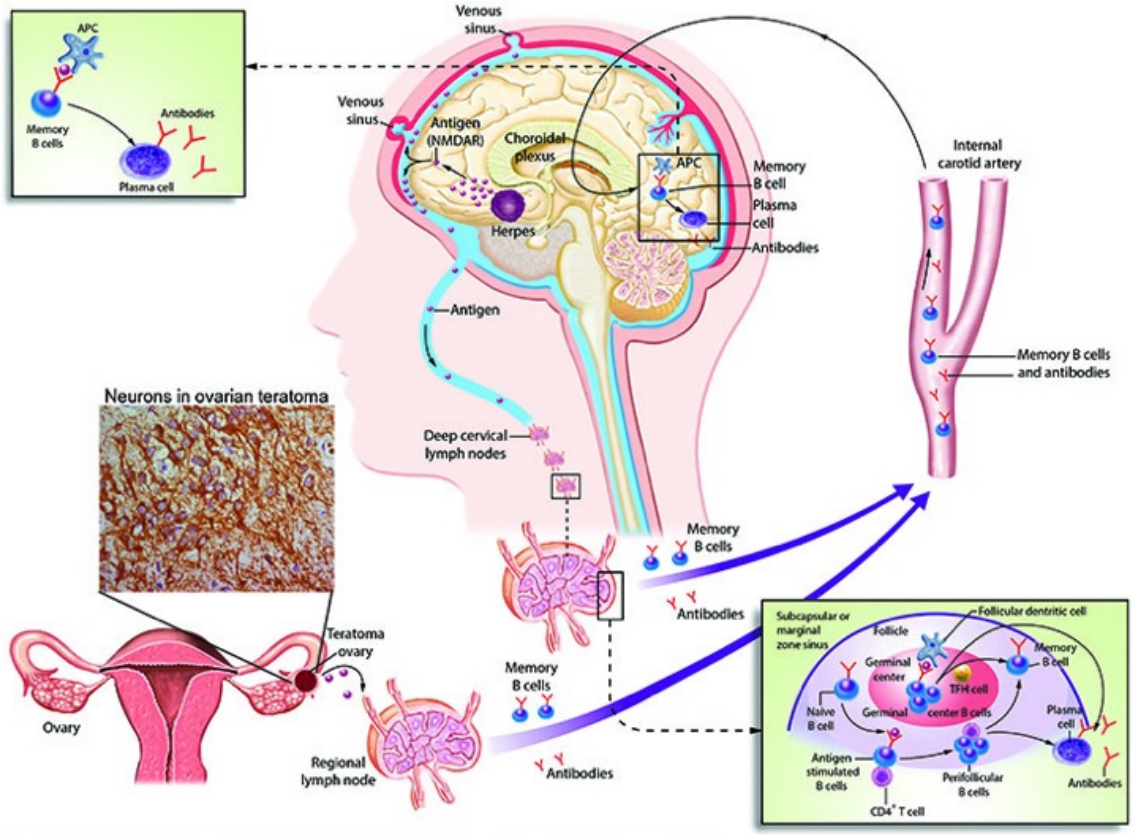

THE LANCET

Enzalutamid ist ein Medikament, das zur Behandlung von Prostatakrebs eingesetzt wird. Es ist ein Androgenrezeptor-Inhibitor und wird bei fortgeschrittenem Prostatakrebs, der nicht mehr auf eine Standard-Hormontherapie anspricht (kastrationsresistenter Prostatakrebs), oder bei metastasiertem Prostatakrebs eingesetzt.

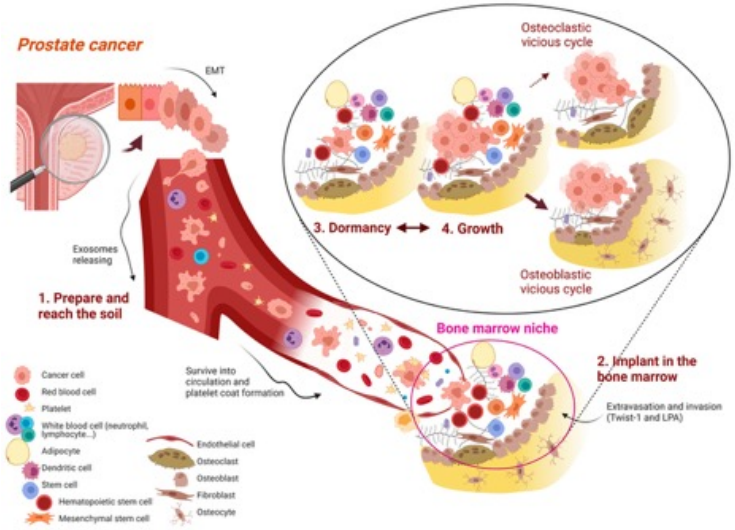

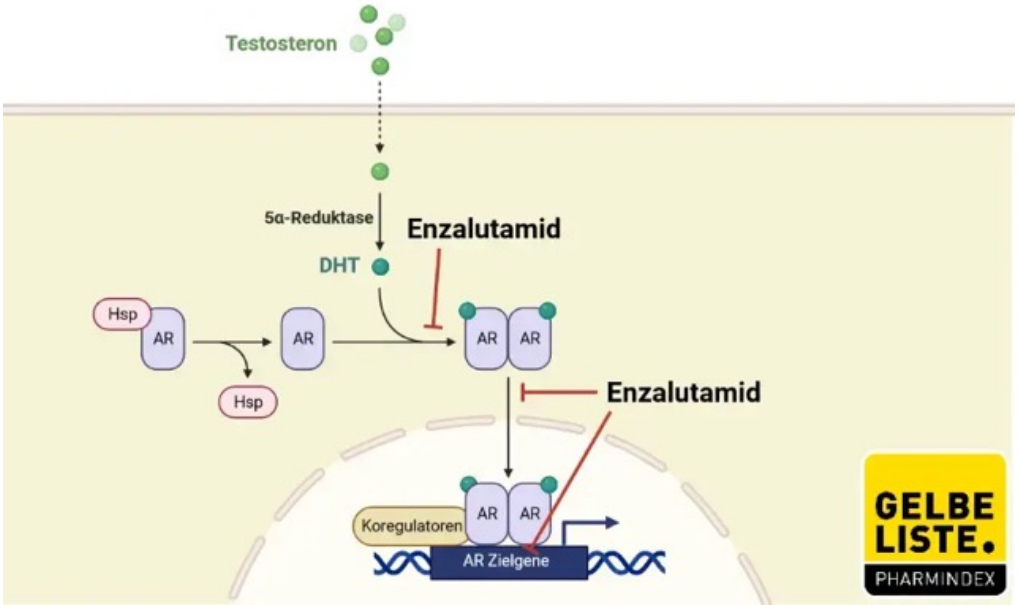

PARP ist die Abkürzung für Poly(ADP-Ribose)-Polymerase. Es handelt sich um Enzyme, die an der DNA-Reparatur beteiligt sind. PARP-Inhibitoren sind Medikamente, die diese Enzyme hemmen und somit die Reparatur von DNA-Schäden in Krebszellen verhindern, was zu deren Absterben führen kann.

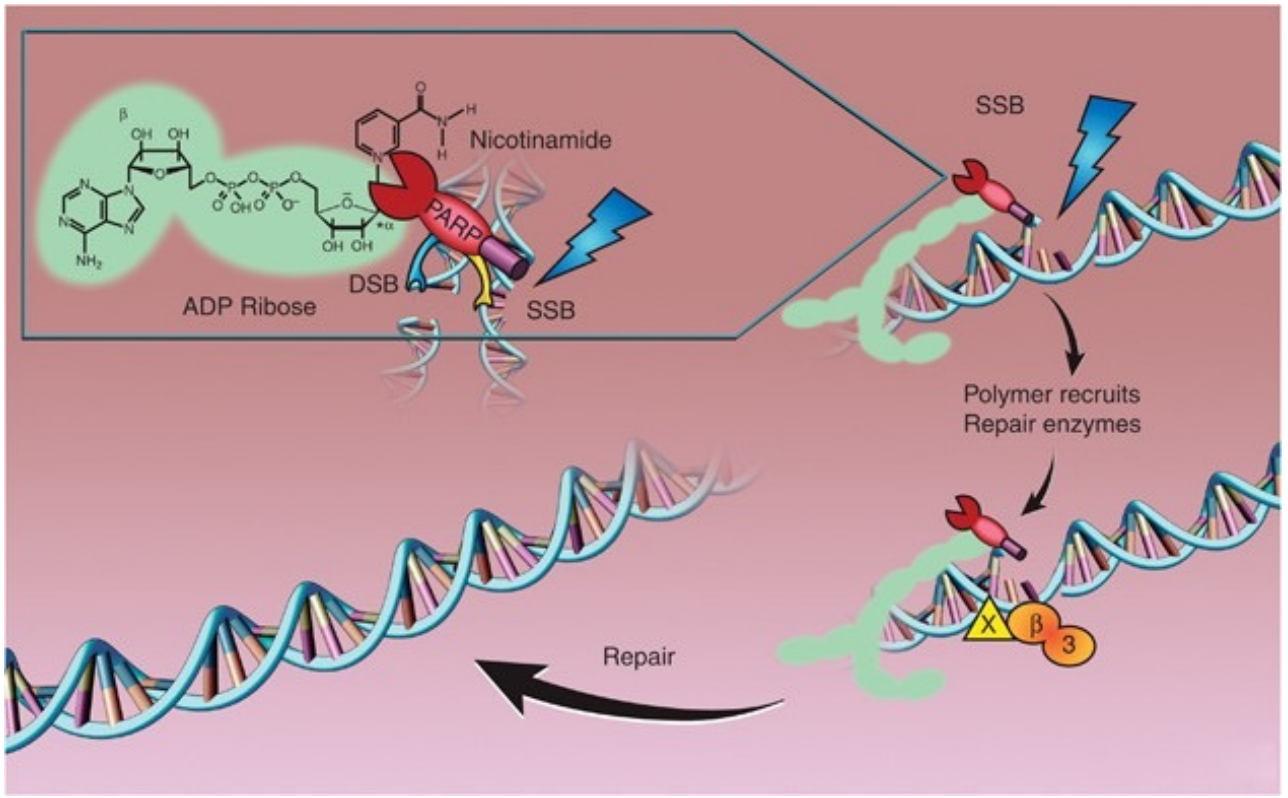

Talazoparib, ist ein Medikament, das zur Behandlung bestimmter Krebsarten eingesetzt wird. Es gehört zur Gruppe der PARP-Inhibitoren und wird oral in Form von Hartkapseln verabreicht.

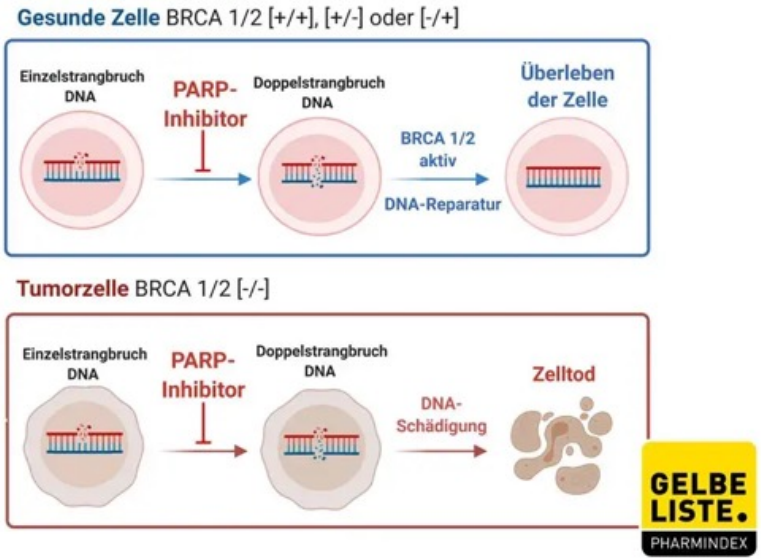

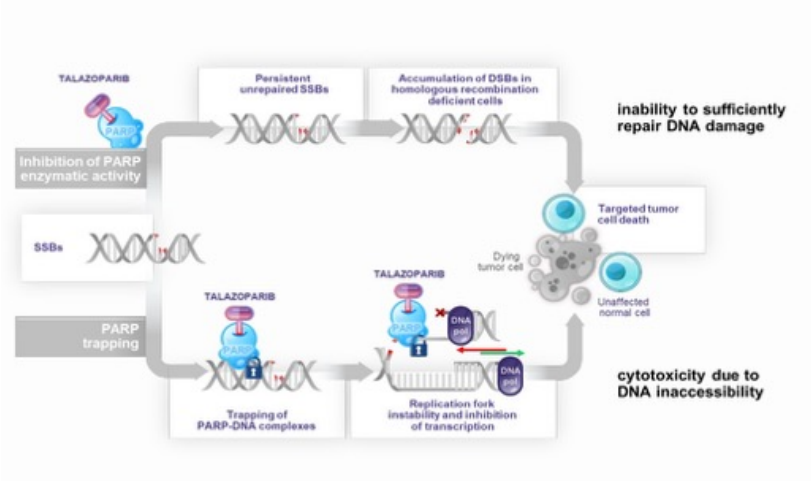

Talazoparib plus enzalutamide in men with metastatic castration-resistant prostate cancer: final overall survival results from the randomised, placebo-controlled, phase 3 TALAPRO-2 trial

Summary

Background The primary analysis of this phase 3 trial combining talazoparib with enzalutamide demonstrated significantly improved radiographic progression-free survival (rPFS) versus enzalutamide plus placebo in patients with metastatic castration-resistant prostate cancer unselected for homologous recombination repair (HRR) gene alterations. Overall survival data were immature at that time. Here we report the final prespecified overall survival analysis, an updated descriptive analysis of rPFS, and safety in the cohort unselected for HRR gene alterations.

Methods TALAPRO-2 was a randomised, double-blind, placebo-controlled, phase 3 trial. In the genetically unselected cohort, patients were randomly assigned from 200 centres, including hospitals, cancer centres, and medical centres, in 26 countries in North America, Europe, Israel, South America, South Africa, and the Asia–Pacific region. Adult men (aged ≥18 years [≥20 years in Japan]) with asymptomatic or mildly symptomatic metastatic castration-resistant prostate cancer receiving ongoing androgen deprivation therapy, and with no previous life-prolonging systemic therapy for castration-resistant prostate cancer, were randomly assigned (1:1) to talazoparib 0·5 mg plus enzalutamide 160 mg or enzalutamide plus placebo, administered orally once daily as initial treatment for metastatic castration-resistant prostate cancer, stratified by HRR gene alteration status (HRR-deficient *vs* HRR-non-deficient or unknown) and previous treatment for castration-sensitive disease (yes *vs* no). The sponsor, patients, and investigators were masked to talazoparib or placebo, and enzalutamide was open label. The primary endpoint was rPFS by blinded independent central review, and overall survival (time from randomisation to death due to any cause) was an event-based α-protected key secondary endpoint (α-threshold at final overall survival analysis was 0·022 [two-sided])—both assessed in the intention-to-treat population. Follow-up for overall survival was intended to continue until the planned final analysis. Safety was assessed in patients who received at least one dose of a study drug. This study is registered with ClinicalTrials.gov, NCT03395197, and is ongoing.

Findings Between Jan 7, 2019, and Sept 17, 2020, 993 patients were assessed for eligibility, of whom 188 (19%) patients were excluded and 805 (81%) patients were enrolled and randomly assigned (402 [50%] to talazoparib plus enzalutamide, 403 [50%] to enzalutamide plus placebo). At a median follow-up of 52·5 months (IQR 48·6–56·0), overall survival was significantly improved with talazoparib plus enzalutamide compared with enzalutamide plus placebo (hazard ratio [HR] 0·80 [95% CI 0·66–0·96]; p=0·016); median overall survival was 45·8 months (95% CI 39·4–50·8) in the talazoparib group compared with 37·0 months (34·1–40·4) in the control group. Overall survival favoured talazoparib plus enzalutamide over enzalutamide plus placebo in HRR-deficient patients (n=169; HR 0·55 [0·36–0·83]; p=0·0035) and to a lesser extent in HRR-non-deficient or unknown patients (n=636; HR 0·88 [0·71–1·08]; p=0·22). Updated rPFS also favoured talazoparib plus enzalutamide (HR 0·67 [0·55–0·81]; p<0·0001); median rPFS was 33·1 months for talazoparib plus enzalutamide versus 19·5 months for enzalutamide plus placebo. Safety was consistent with the known profile of talazoparib; common grade 3 or higher adverse events with talazoparib plus enzalutamide were anaemia (195 [49%] *vs* 18 [4%] patients with enzalutamide plus placebo) and neutropenia (77 [19%] *vs* six [1%] patients with enzalutamide plus placebo).

Interpretation Combining talazoparib with enzalutamide significantly improved overall survival in patients with metastatic castration-resistant prostate cancer, supporting this combination as a standard-of-care initial treatment option for these patients.

Funding Pfizer.

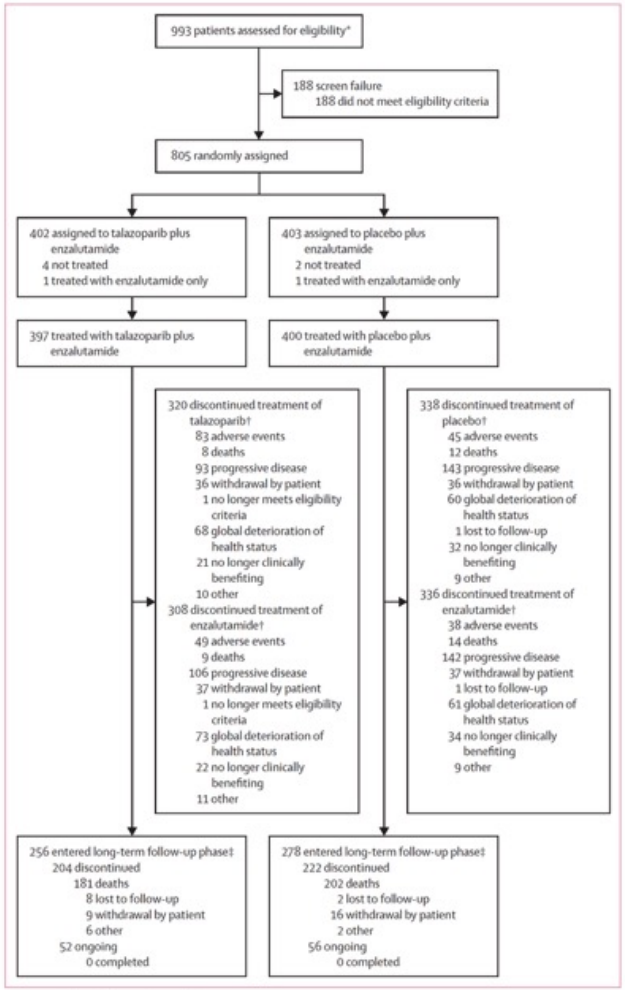

Figure 1: **Trial profile (unselected cohort)**

*Two patients previously reported as other at the primary data cutoff were later confirmed to have completed screening and then determined to have failed screening. †308 patients in the talazoparib plus enzalutamide group discontinued treatment of both talazoparib and enzalutamide. 336 patients in the placebo plus enzalutamide group discontinued treatment of both placebo and enzalutamide. ‡Long-term follow-up began after safety follow-up and occurred every 8 weeks until week 25 and every 12 weeks thereafter until death, patient withdrawal of consent for follow-up, or study termination.

	Talazoparib plus enzalutamide (n=402)	Placebo plus enzalutamide (n=403)
Age, years	71 (66–76)	71 (65–76)
Race		
White	243 (60%)	255 (63%)
Black or African American	11 (3%)	5 (1%)
Asian	127 (32%)	120 (30%)
Multiracial	0	1 (<1%)
Other*	2 (<1%)	1 (<1%)
Not reported	19 (5%)	21 (5%)
Renal impairment†‡		
None or mild	344 (86%)	347 (86%)
Moderate	42 (10%)	41 (10%)
Baseline serum PSA, µg/L	18·2 (6·9–59·4)	16·2 (6·4–53·4)
Baseline circulating tumour cell count, cells per 7·5 mL of blood	1 (0–7)	1 (0–6)
Gleason score†		
<8	117 (29%)	113 (28%)
≥8	281 (70%)	283 (70%)
Disease site		
Bone (including with soft tissue component)	349 (87%)	342 (85%)
Lymph node	147 (37%)	167 (41%)
Visceral (lung)	45 (11%)	61 (15%)
Visceral (liver)	12 (3%)	16 (4%)
Other soft tissue	37 (9%)	33 (8%)
ECOG performance status		
0	259 (64%)	271 (67%)
1	143 (36%)	132 (33%)
Previous taxane-based chemotherapy§	86 (21%)	93 (23%)
Previous treatment with a second-generation ARPI	23 (6%)	27 (7%)
Abiraterone	21 (5%)	25 (6%)
Orteronel	2 (<1%)	2 (<1%)
HRR gene alteration status by randomisation stratification		
Deficient	85 (21%)	84 (21%)
Non-deficient or unknown	317 (79%)	319 (79%)
HRR gene alteration status by prospective tumour tissue and ctDNA testing¶		
Deficient	85 (21%)	82 (20%)
Non-deficient	207 (51%)	219 (54%)
Unknown	110 (27%)	102 (25%)
BRCA1/2 alteration	27 (7%)	32 (8%)

Data are n (%) or median (IQR). Reprinted from Agarwal et al.[18] ARPI=androgen receptor pathway inhibitor. ctDNA=circulating tumour DNA. ECOG=Eastern Cooperative Oncology Group. HRR=homologous recombination repair. PSA=prostate-specific antigen. *American Indian, Alaska Native, Native Hawaiian, or Other Pacific Islander. †Not reported for the remaining patients. ‡Moderate renal impairment defined as 30–59 mL/min per 1·73 m^2. §All received docetaxel. ¶Prespecified exploratory endpoint analysis by prospective tumour tissue and ctDNA testing to separate unknown from non-deficient HRR gene alteration status. Prospective unknown status for HRR gene alteration status primarily reflects the sample or samples submitted to Foundation Medicine not being analysed (typically because of failed quality control metrics) or test results not being reported (due to limitations in sample quality or purity).

Table 1: Summary of baseline characteristics (unselected intention-to-treat population; data cutoff Aug 16, 2022)

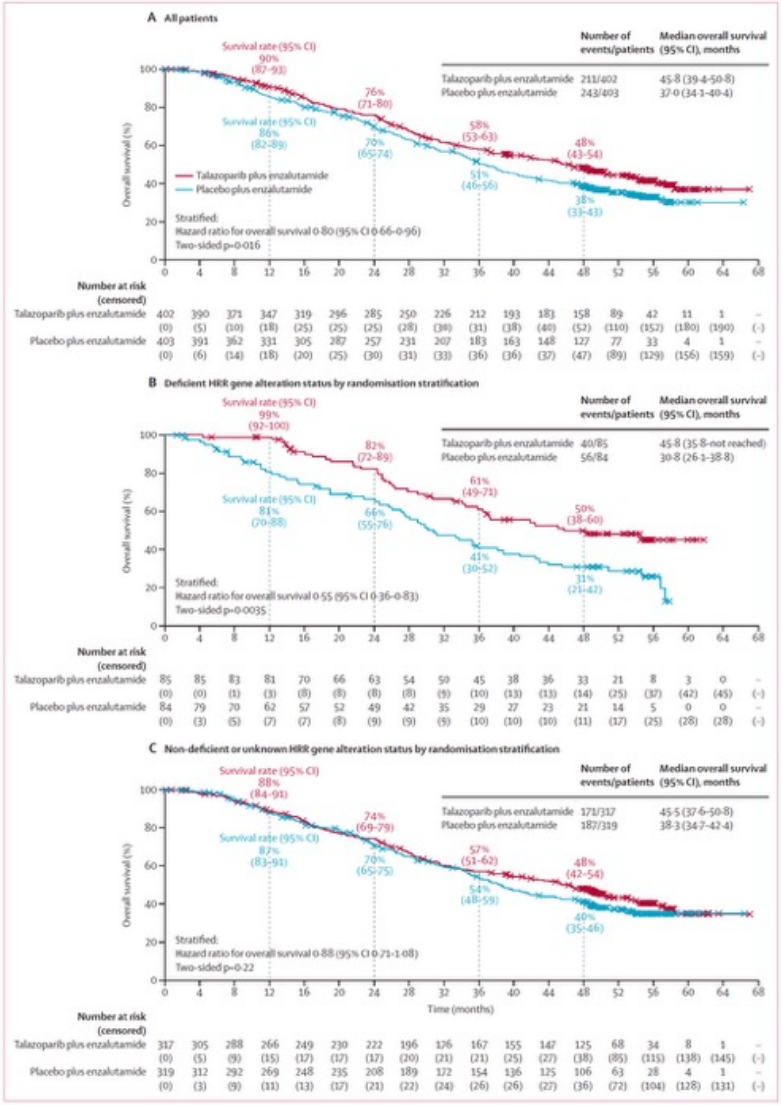

(Figure 2 continues on next page)

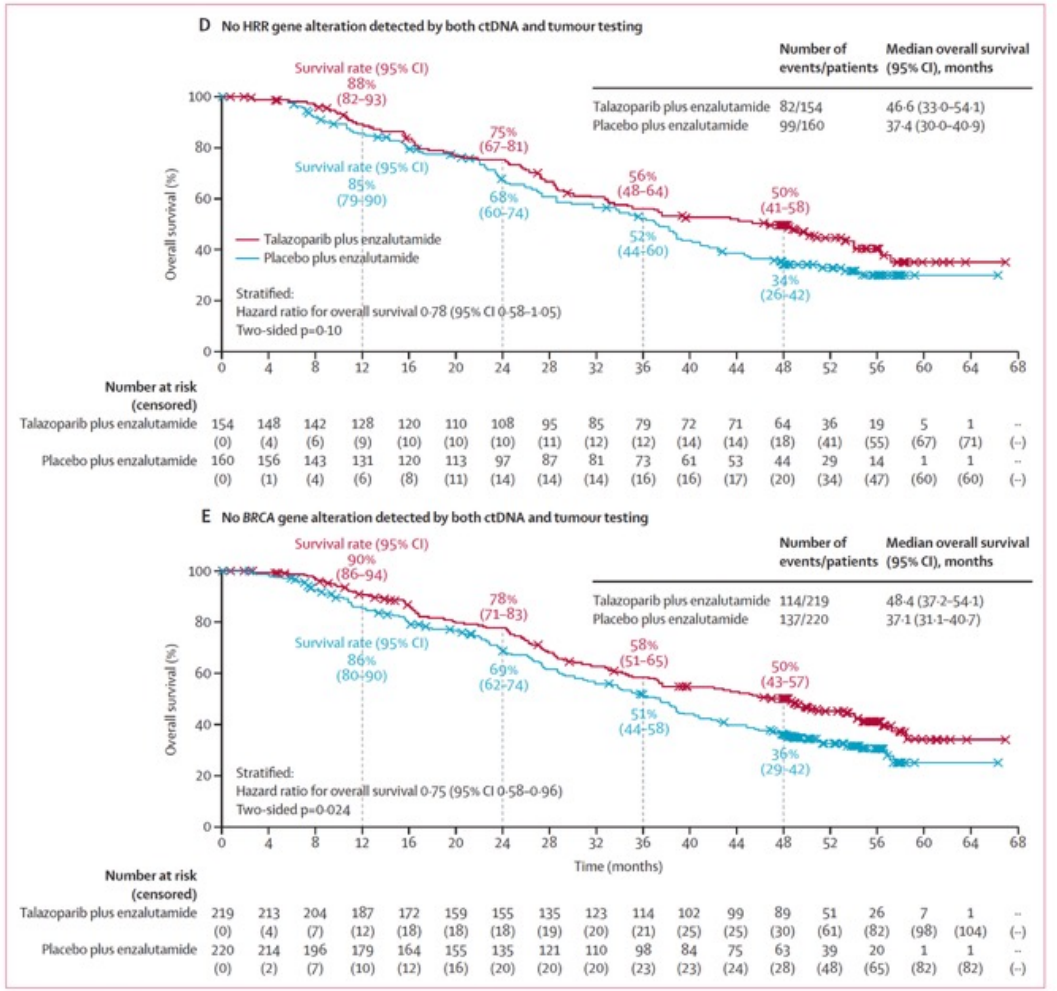

Figure 2: **Overall survival in trial populations (unselected intention-to-treat population)**
Panels A–C show prespecified analyses for all patients (A) and for subgroups of patients with either deficient HRR gene alteration status (B) or non-deficient or unknown HRR gene alteration status (C), by randomisation stratification. Panels D and E show post-hoc analyses for subgroups of patients with no HRR gene alteration detected (D) and with no *BRCA* gene alteration detected (E), by both ctDNA and tumour tissue, using all available test results of pre-screening and screening samples including both prospective and retrospective analyses. Not all patients had blood samples for ctDNA analysis. ctDNA=circulating tumour DNA. HRR=homologous recombination repair.

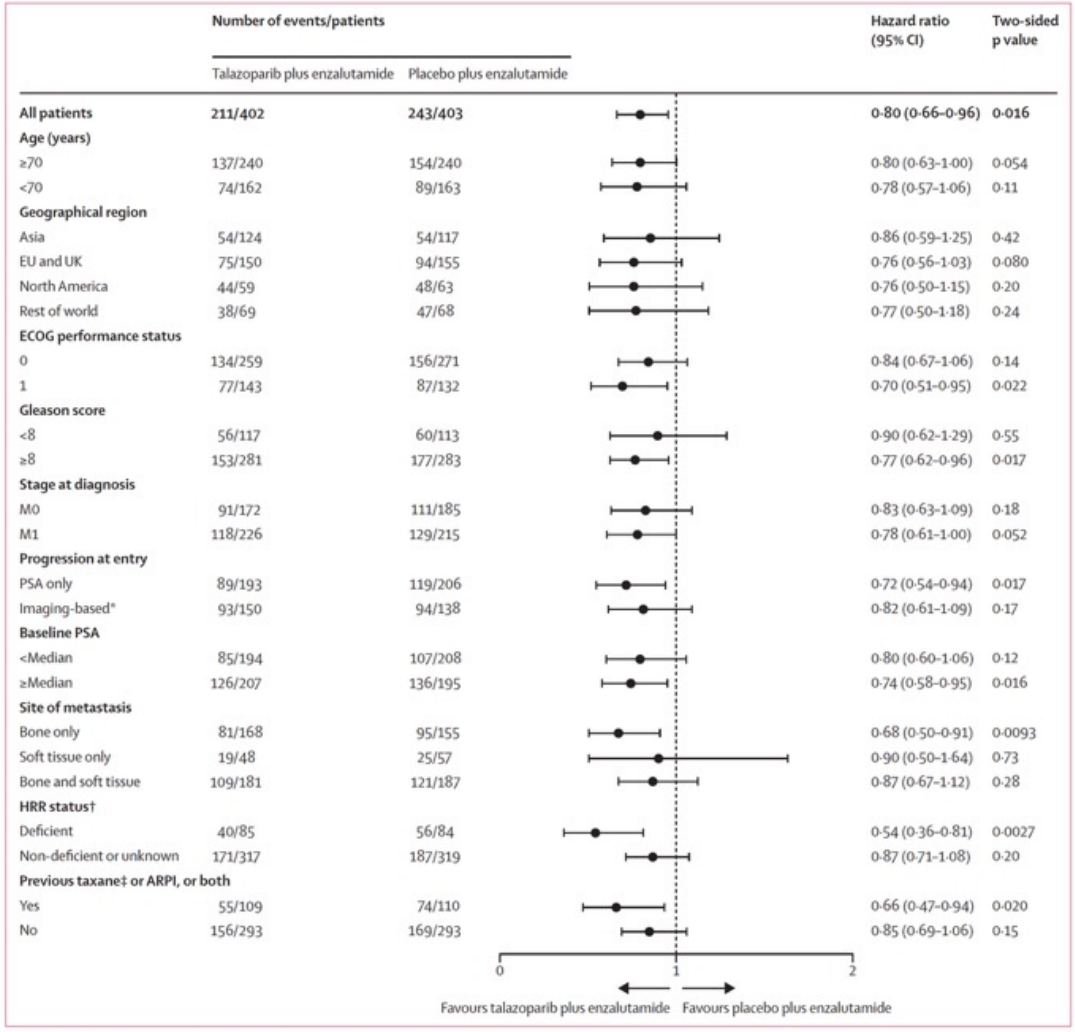

Figure 3: **Subgroup analysis of overall survival by baseline characteristics (unselected intention-to-treat population)**
The overall hazard ratio for all patients was based on a Cox model stratified by the randomisation stratification factors. For all subgroups, the hazard ratio was based on an unstratified Cox model with treatment as the only covariate. ARPI=androgen receptor pathway inhibitor. ECOG=Eastern Cooperative Oncology Group. HRR=homologous recombination repair. PSA=prostate-specific antigen. *With or without PSA progression. †Per randomisation stratification. ‡All received docetaxel.

	Talazoparib plus enzalutamide (n=398)		Placebo plus enzalutamide (n=401)	
	All grades	Grade ≥3	All grades	Grade ≥3
Any adverse event	394 (99%)	316 (79%)	384 (96%)	199 (50%)
Treatment-related adverse event	360 (90%)	244 (61%)	286 (71%)	75 (19%)
Serious adverse event	182 (46%)	168 (42%)	126 (31%)	113 (28%)
Grade 5 adverse event	14 (4%)*	..	20 (5%)†	..
Adverse event resulting in dose interruption of:				
Talazoparib or placebo‡	260 (65%)	..	99 (25%)	..
Enzalutamide§	175 (44%)	..	91 (23%)	..
Adverse event resulting in dose reduction of:				
Talazoparib or placebo‡	217 (55%)	..	29 (7%)	..
Enzalutamide§	61 (15%)	..	33 (8%)	..
Adverse event resulting in permanent drug discontinuation of:				
Talazoparib or placebo‡	86 (22%)	..	52 (13%)	..
Enzalutamide§	53 (13%)	..	48 (12%)	..
Most common adverse events (all grades in ≥10% of patients)¶				
Anaemia	270 (68%)	195 (49%)	80 (20%)	18 (4%)
Neutropenia	150 (38%)	77 (19%)	29 (7%)	6 (1%)
Fatigue	139 (35%)	17 (4%)	121 (30%)	8 (2%)
Back pain	107 (27%)	13 (3%)	83 (21%)	4 (1%)
Thrombocytopenia	102 (26%)	29 (7%)	16 (4%)	4 (1%)
Leukopenia	96 (24%)	27 (7%)	19 (5%)	0
Decreased appetite	89 (22%)	6 (2%)	67 (17%)	4 (1%)
Fall	89 (22%)	11 (3%)	68 (17%)	8 (2%)
Nausea	85 (21%)	2 (<1%)	53 (13%)	3 (<1%)
Constipation	78 (20%)	1 (<1%)	73 (18%)	2 (<1%)
Arthralgia	69 (17%)	2 (<1%)	87 (22%)	2 (<1%)
Diarrhoea	63 (16%)	1 (<1%)	60 (15%)	1 (<1%)
Asthenia	61 (15%)	12 (3%)	38 (9%)	4 (1%)
Hypertension	61 (15%)	25 (6%)	68 (17%)	33 (8%)
Dizziness	55 (14%)	4 (1%)	25 (6%)	2 (<1%)
Decreased weight	53 (13%)	4 (1%)	43 (11%)	3 (<1%)
Hot flush	51 (13%)	0	56 (14%)	0
Lymphopenia	51 (13%)	25 (6%)	23 (6%)	4 (1%)
Oedema peripheral	47 (12%)	0	27 (7%)‖	0
Dyspnoea	45 (11%)	2 (<1%)	25 (6%)	2 (<1%)
Pain in extremity	43 (11%)	1 (<1%)	35 (9%)	1 (<1%)
Headache	40 (10%)	1 (<1%)	39 (10%)	1 (<1%)

Data are n (%). Shown are adverse events that occurred from the time of the first dose of study treatment until 28 days after permanent discontinuation of all study treatments or before initiation of a new antineoplastic or any investigational therapy, whichever occurred first. Adverse events were graded according to the National Cancer Institute Common Terminology Criteria for Adverse Events version 4.03. *One was considered treatment-related and was attributed to disease progression. †Two were considered treatment-related, of which one was due to COVID-19. ‡Includes permanent discontinuation, dose reduction, or dose interruption of talazoparib or placebo only plus permanent discontinuation, dose reduction, or dose interruption of both talazoparib or placebo and enzalutamide. §Includes permanent discontinuation, dose reduction, or dose interruption of enzalutamide only plus permanent discontinuation, dose reduction, or dose interruption of both talazoparib or placebo and enzalutamide. ¶None of these events were recorded as grade 5. ‖One additional patient had a missing or unknown grade.

Table 2: **Summary of adverse events (unselected safety population)**

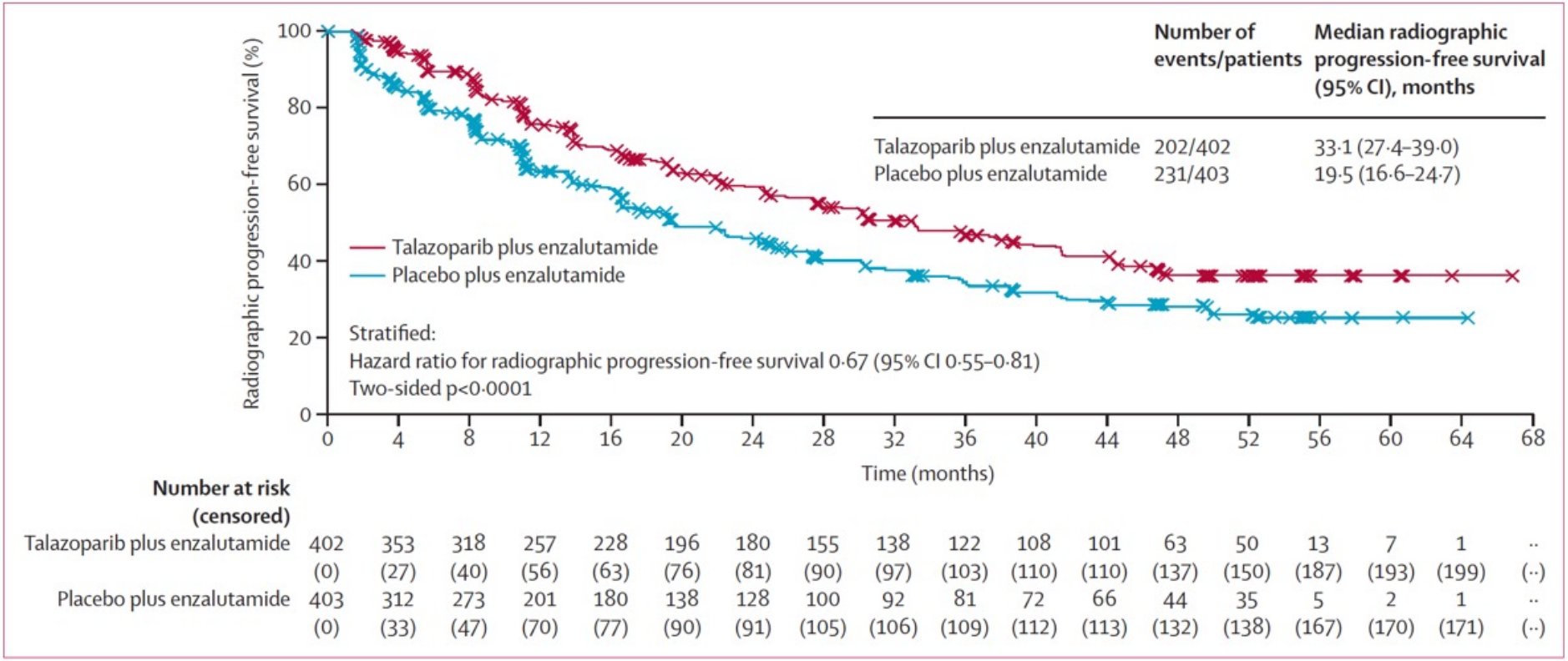

Figure 4: **Radiographic progression-free survival by blinded independent central review (unselected intention-to-treat population)**

Research in context

Evidence before this study

Before the TALAPRO-2 trial was started in December, 2017, we searched PubMed for relevant preclinical or clinical research published on DNA damage repair, homologous recombination repair (HRR), so-called BRCAness, novel hormonal therapies or androgen receptor pathway inhibitors (ARPIs), androgen receptor signalling inhibition, poly(ADP-ribose) polymerase (PARP) inhibitors, and advanced prostate cancer to help determine the most appropriate study design for a trial in metastatic castration-resistant prostate cancer. These searches found that (1) prostate cancer is a common cause of cancer-related death in men worldwide, (2) metastatic castration-resistant prostate cancer remains a lethal disease despite current therapies, (3) therapies targeting androgen receptor signalling together with androgen deprivation therapy were a mainstay of standard of care for initial treatment of metastatic castration-resistant prostate cancer, and (4) there remained an unmet need to prolong benefit of initial metastatic castration-resistant prostate cancer treatment as resistance invariably developed in these patients. Based on the literature and emerging evidence, we theorised that co-inhibition of the androgen receptor pathway and PARP might result in enhanced benefit with the potential to extend efficacy of PARP inhibitors to prostate cancer tumours without HRR gene alterations. Besides TALAPRO-2, two additional studies, PROpel and MAGNITUDE, have investigated the combination of PARP inhibitors (olaparib and niraparib, respectively) with the androgen biosynthesis inhibitor abiraterone acetate plus prednisone (or prednisolone in PROpel; AAP) as initial treatment of metastatic castration-resistant prostate cancer versus AAP. In an unselected population (ie, regardless of HRR gene alteration status), results from the primary analysis of the PROpel trial showed improved radiographic progression-free survival (rPFS) with olaparib plus AAP versus placebo plus AAP. Results from the final overall survival analysis of PROpel have also been reported for the unselected population, but statistical significance was not reached for olaparib plus abiraterone versus placebo plus abiraterone. In the MAGNITUDE trial, patients were enrolled into HRR-deficient or HRR-non-deficient cohorts based on HRR gene alterations status. In the HRR-deficient cohort, treatment with niraparib plus AAP resulted in significantly longer rPFS than with placebo plus AAP, whereas futility was declared in the HRR-non-deficient cohort based on prespecified criteria.

Added value of this study

TALAPRO-2 is the first phase 3 study investigating the novel combination of the potent PARP inhibitor talazoparib and the ARPI enzalutamide versus a standard of care (enzalutamide) in patients with metastatic castration-resistant prostate cancer. The previously reported primary analysis of TALAPRO-2 showed statistically significant improvement in rPFS with talazoparib plus enzalutamide versus enzalutamide plus placebo in the unselected cohort as well as in the HRR-deficient cohort. This analysis presents data from the key alpha-protected secondary endpoint of overall survival in the unselected cohort. The reported statistically significant and clinically meaningful improvement in overall survival with talazoparib plus enzalutamide versus enzalutamide plus placebo expands on the evidence for clinical efficacy of talazoparib plus enzalutamide as initial treatment in the unselected population of patients with metastatic castration-resistant prostate cancer.

Implications of all the available evidence

Together with the results from the HRR-deficient cohort (reported separately), and to our knowledge, TALAPRO-2 is the first trial to date to show a statistically significant and clinically meaningful improvement in overall survival for a PARP inhibitor plus ARPI combination versus an active standard-of-care ARPI, and this improvement was shown in both the HRR-deficient population as well as in this unselected population. The results in the unselected cohort of TALAPRO-2 further support the combination of talazoparib plus enzalutamide as a standard-of-care initial treatment option for metastatic castration-resistant prostate cancer.

Homologous recombination repair (HRR) is a crucial DNA repair pathway that accurately fixes DNA double-strand breaks (DSBs) by using an undamaged homologous DNA sequence, often the sister chromatid, as a template. This process is vital for maintaining genomic stability and preventing mutations that can lead to cancer.

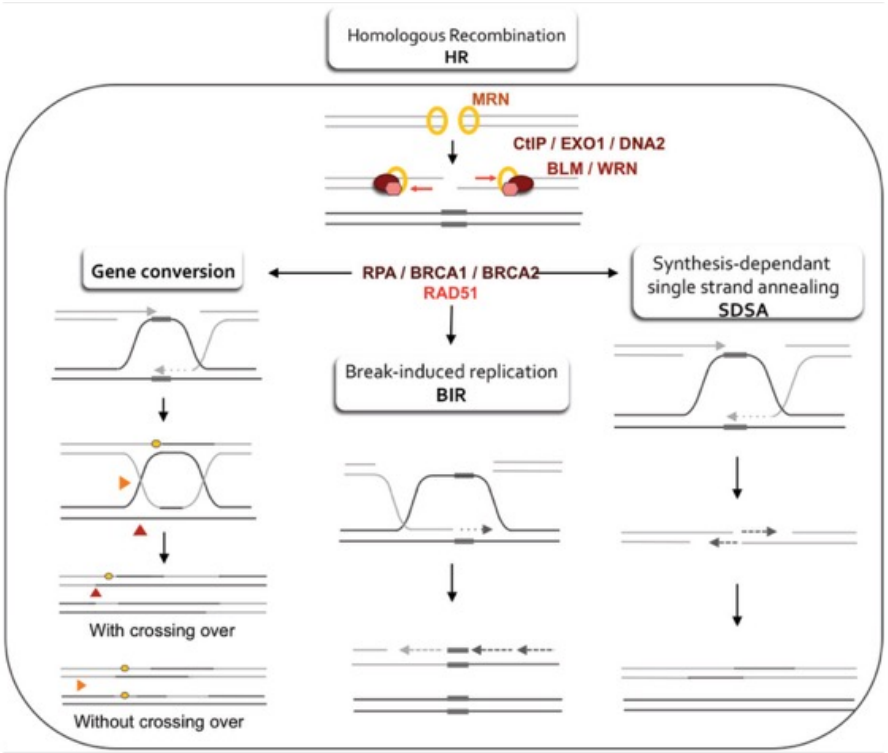

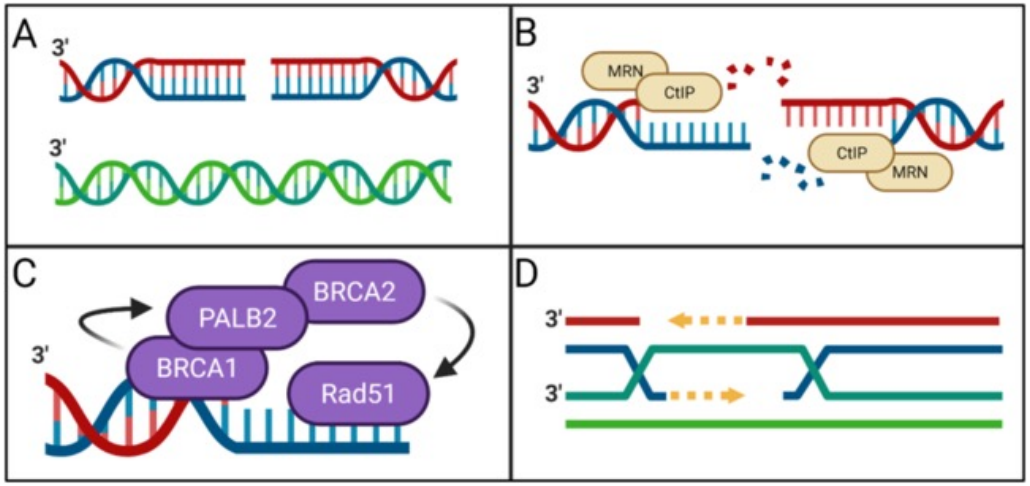

Talazoparib plus enzalutamide in men with HRR-deficient metastatic castration-resistant prostate cancer: final overall survival results from the randomised, placebo-controlled, phase 3 TALAPRO-2 trial

Homologous recombination repair (HRR)

Summary

Background Metastatic castration-resistant prostate cancer remains incurable and is particularly aggressive in patients with alterations in DNA damage repair genes involved directly or indirectly in homologous recombination repair (HRR). In the primary analysis of TALAPRO-2, talazoparib plus enzalutamide significantly improved radiographic progression-free survival (rPFS) versus enzalutamide plus placebo in patients with metastatic castration-resistant prostate cancer harbouring HRR gene alterations. At primary analysis, overall survival was immature. Here we report final prespecified overall survival analysis, updated rPFS, safety, and patient-reported outcomes in the HRR-deficient cohort of TALAPRO-2.

Methods TALAPRO-2 is an ongoing international, randomised, double-blind, placebo-controlled phase 3 trial. The HRR-deficient cohort included randomly assigned patients from 142 hospitals, cancer centres, and medical centres in 26 countries; the study included men aged at least 18 years (≥20 years in Japan) with asymptomatic or mildly symptomatic metastatic castration-resistant prostate cancer, progressive disease at study entry, and no previous life-prolonging systemic therapy for castration-resistant prostate cancer, but were receiving ongoing androgen deprivation therapy. Patients were prospectively assessed for tumour HRR gene alterations and randomly assigned (1:1) to once-daily oral talazoparib 0·5 mg plus enzalutamide 160 mg or enzalutamide plus placebo stratified by prior treatment (yes *vs* no) for castration-sensitive disease. The sponsor, patients, and investigators were masked to talazoparib or placebo, whereas enzalutamide was open label. The primary endpoint was rPFS (time from randomisation to radiographic progression or death, whichever occurred first) by blinded independent central review, and overall survival (time from randomisation to death due to any cause) was a key alpha-protected secondary endpoint, both assessed in the intention-to-treat population. Follow-up for overall survival was intended to continue until the planned final analysis. For statistical significance at the final overall survival analysis, the two-sided p value from the stratified log-rank test needed to be 0·024 or less based on a group sequential design with O'Brien–Fleming spending function. Safety was assessed in patients who had received at least one study drug dose. The trial is registered with ClinicalTrials.gov, NCT03395197.

Findings Between Dec 18, 2018, and Jan 20, 2022, 399 patients with HRR-deficient metastatic castration-resistant prostate cancer were randomly assigned (200 [50%] to talazoparib plus enzalutamide and 199 [50%] to enzalutamide plus placebo). At a median follow-up of 44·2 months (IQR 36·0–50·8), treatment with talazoparib plus enzalutamide resulted in a statistically significant improvement in overall survival versus enzalutamide (hazard ratio [HR] 0·62 [95% CI 0·48–0·81]; two-sided p=0·0005); median overall survival 45·1 months (95% CI 35·4–not reached) in the talazoparib group versus 31·1 months (27·3–35·4) in the control group. In the subgroup of patients with *BRCA1/2* alterations (n=155 [39%]), median overall survival was not reached for talazoparib plus enzalutamide versus 28·5 months for enzalutamide (HR 0·50 [95% CI 0·32–0·78]; p=0·0017); 4-year overall survival rates were 53% in the talazoparib group versus 23% in the control group. In patients without *BRCA1/2* alterations (n=244 [61%]), median overall survival was 42·4 months for talazoparib plus enzalutamide versus 32·6 months for enzalutamide (HR 0·73 [95% CI 0·52–1·02]; p=0·066). Updated rPFS favoured talazoparib plus enzalutamide versus enzalutamide (HR 0·47 [95% CI 0·36–0·61]; p<0·0001; median rPFS 30·7 *vs* 12·3 months). No new safety signals were identified; most common adverse events of grade 3 or higher with talazoparib plus enzalutamide were anaemia (86 [43%] patients) and neutropenia (39 [20%] patients).

Interpretation Talazoparib plus enzalutamide resulted in statistically significant and clinically meaningful improvement in survival versus enzalutamide plus placebo, further supporting this combination as a standard of care in HRR-deficient metastatic castration-resistant prostate cancer.

Funding Pfizer.

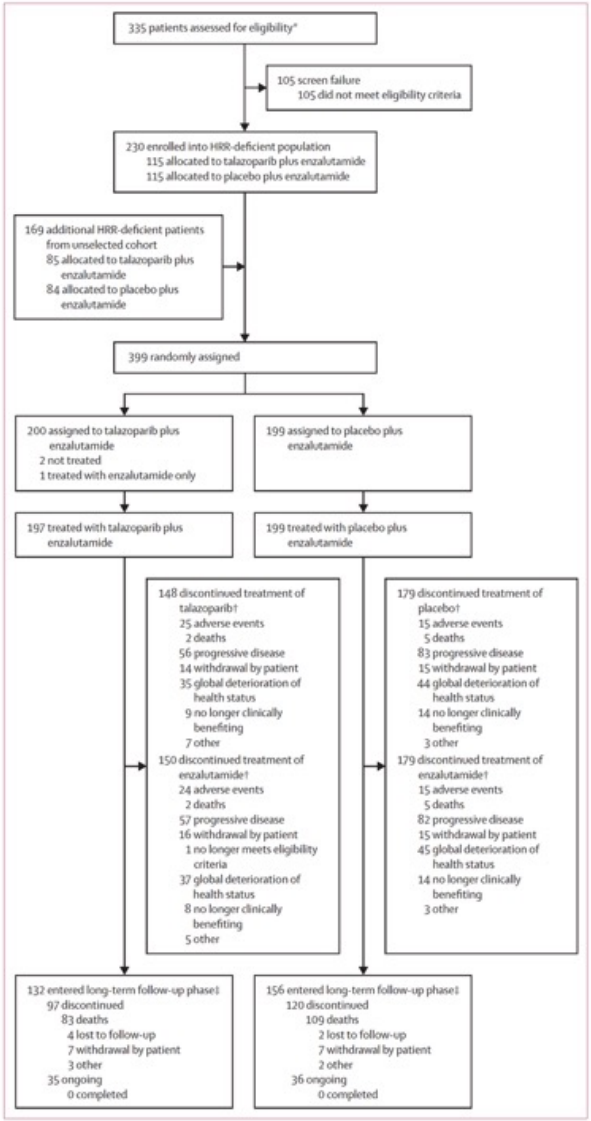

Figure 1: **Trial profile**
HRR=homologous recombination repair. *The number of patients has been updated from the primary analysis to address a programming error in which 19 patients from the China extension cohort had been included in the clinical study report. †148 patients in the talazoparib plus enzalutamide group discontinued treatment of both talazoparib and enzalutamide. 179 patients in the placebo plus enzalutamide arm discontinued treatment of both placebo and enzalutamide. ‡Long-term follow-up began after safety follow-up and occurred every 8 weeks until week 25 and every 12 weeks thereafter until death, patient withdrawal of consent for follow-up, or study termination.

	Talazoparib plus enzalutamide (n=200)	Placebo plus enzalutamide (n=199)
Age, years	70 (65-76)	71 (64-76)
Race		
White	137 (68%)	136 (68%)
Black or African American	6 (3%)	5 (3%)
Asian	45 (22%)	39 (20%)
Multiracial	0	1 (<1%)
Other*	1 (<1%)	1 (<1%)
Not reported or unknown	11 (6%)	17 (9%)
Baseline serum PSA, µg/L	19·6 (6·7-62·8)	18·0 (7·1-57·4)
Gleason score†		
<8	42 (21%)	52 (26%)
≥8	152 (76%)	143 (72%)
Disease site		
Bone (including with soft tissue component)	175 (88%)	158 (79%)
Lymph node	82 (41%)	94 (47%)
Visceral (lung)	23 (12%)	26 (13%)
Visceral (liver)	9 (4%)	6 (3%)
Other soft tissue	23 (12%)	20 (10%)
ECOG performance status		
0	128 (64%)	118 (59%)
1	72 (36%)	81 (41%)
Previous treatment with a second-generation androgen receptor pathway inhibitor	17 (9%)	17 (9%)
Abiraterone	16 (8%)	16 (8%)
Orteronel	1 (<1%)	1 (<1%)
Previous taxane-based chemotherapy‡	57 (28%)	60 (30%)
Patients with at least one alteration in corresponding HRR gene§	198 (99%)	197 (99%)
ATM	47 (24%)	39 (20%)
ATR	3 (2%)	12 (6%)
BRCA1	11 (6%)	12 (6%)
BRCA2	62 (31%)	73 (37%)
CDK12	36 (18%)	39 (20%)
CHEK2	34 (17%)	37 (19%)
FANCA	4 (2%)	5 (3%)
MLH1	9 (4%)	1 (<1%)
MRE11A	1 (<1%)	2 (1%)
NBN	8 (4%)	3 (2%)
PALB2	9 (4%)	8 (4%)
RAD51C	2 (1%)	2 (1%)

Data are n (%) or median (IQR). Reprinted from Fizazi K, Azad AA, Matsubara N, et al.[48] ARPI=androgen receptor pathway inhibitor, ECOG=Eastern Cooperative Oncology Group. HRR=homologous recombination repair. PSA=prostate-specific antigen. *American Indian, Alaska Native, Native Hawaiian, or other Pacific Islander. †Not reported for the remaining patients. ‡All received docetaxel; HRR-deficient safety population. §Three patients (one in the talazoparib plus enzalutamide group and two in the placebo plus enzalutamide group) did not have HRR gene alterations, and one patient in the talazoparib group was of unknown HRR gene alteration status.

Table 1: Summary of baseline characteristics (HRR-deficient intention-to-treat population)

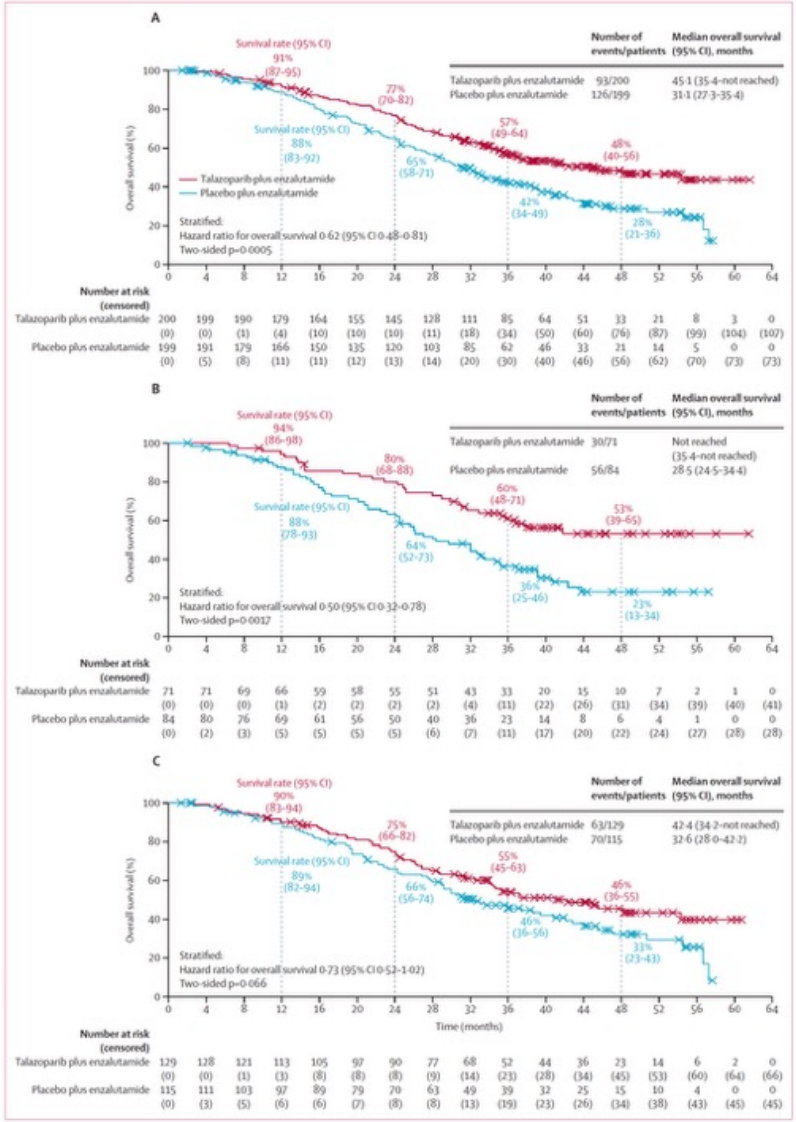

Figure 2: **Overall survival**
Overall survival in patients with (A) any HRR gene alteration; (B) *BRCA1/2* gene alterations; and (C) non-*BRCA1/2* HRR gene alterations (HRR-deficient intention-to-treat population). HRR=homologous recombination repair.

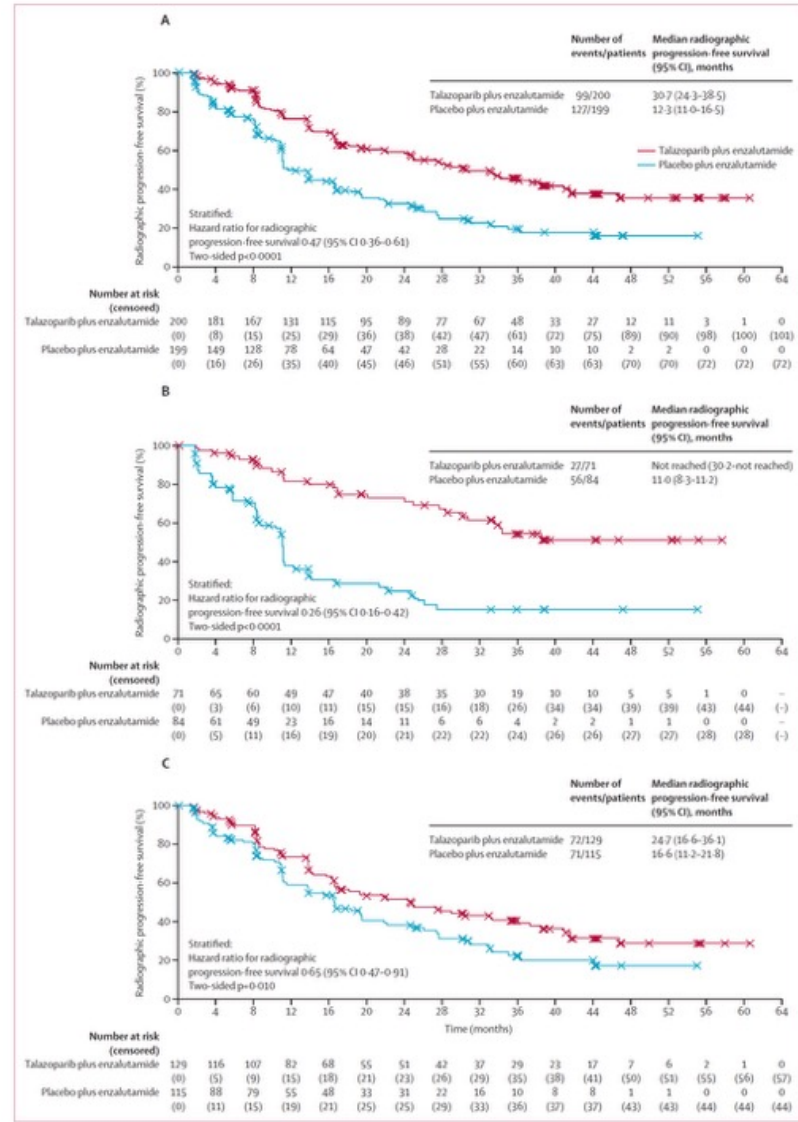

Figure 3: **Radiographic progression-free survival**
Radiographic progression-free survival in patients with (A) any HRR gene alteration; (B) *BRCA1/2* gene alterations; and (C) non-*BRCA1/2* HRR gene alterations (assessed by BICR; HRR-deficient intention-to-treat population). BICR=blinded-independent central review. HRR=homologous recombination repair.

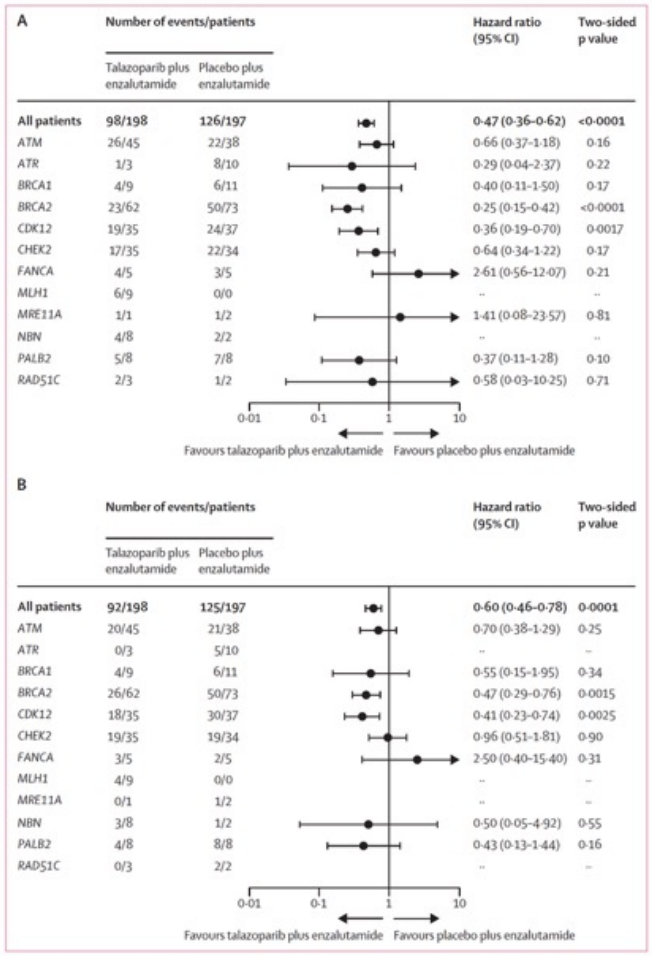

Figure 4: **Radiographic progression-free survival assessed by BICR (A) and overall survival by HRR gene alteration subgroups (B)**

Figure shows results in the HRR-deficient intention-to-treat population and uses all available tumour and pre-screening or screening circulating tumour DNA records, including records generated after randomisation date. For the subgroups of patients with non-*BRCA* alterations, patients with co-occurring *BRCA1* or *BRCA2* alterations are excluded. For the subgroup of patients with *BRCA1* alterations, patients with co-occurring *BRCA2* alterations are excluded. Patients with co-alterations in multiple genes not including *BRCA1/2* are counted under each individual corresponding gene subgroup. All patients category is based on prospective test results. BICR=blinded independent central review. HRR=homologous recombination repair.

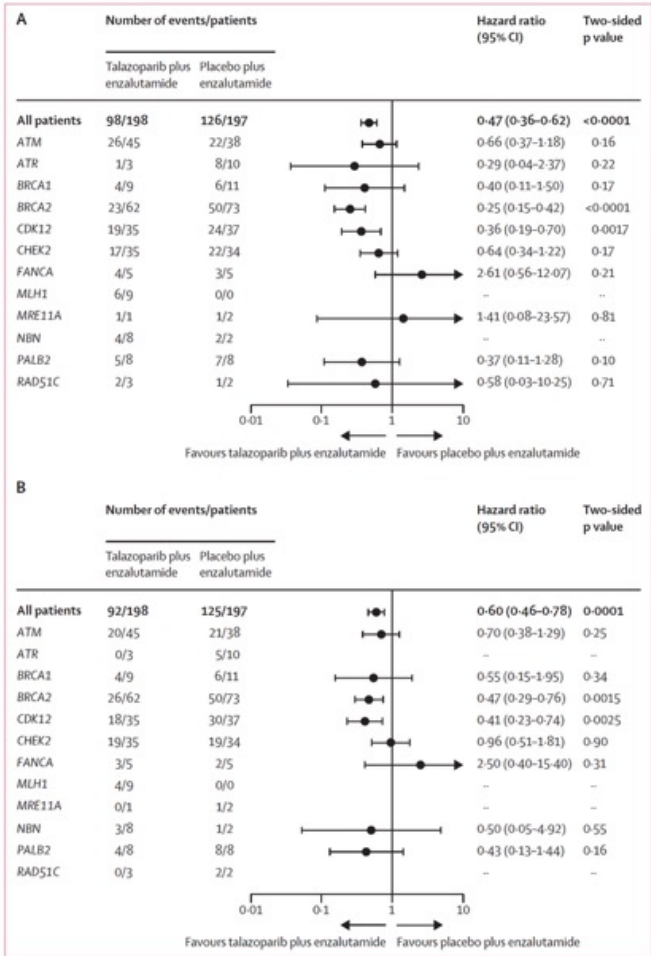

Figure 4: **Radiographic progression-free survival assessed by BICR (A) and overall survival by HRR gene alteration subgroups (B)**

Figure shows results in the HRR-deficient intention-to-treat population and uses all available tumour and pre-screening or screening circulating tumour DNA records, including records generated after randomisation date. For the subgroups of patients with non-*BRCA* alterations, patients with co-occurring *BRCA1* or *BRCA2* alterations are excluded. For the subgroup of patients with *BRCA1* alterations, patients with co-occurring *BRCA2* alterations are excluded. Patients with co-alterations in multiple genes not including *BRCA1/2* are counted under each individual corresponding gene subgroup. All patients category is based on prospective test results. BICR=blinded independent central review. HRR=homologous recombination repair.

	Talazoparib plus enzalutamide (n=198)		Placebo plus enzalutamide (n=199)	
	All grades	Grade ≥3	All grades	Grade ≥3
Any adverse event	197 (99%)	149 (75%)	194 (97%)	88 (44%)
Treatment-related adverse event	182 (92%)	116 (59%)	150 (75%)	28 (14%)
Serious adverse event	79 (40%)	71 (36%)	47 (24%)	39 (20%)
Serious and treatment-related adverse event	32 (16%)	..	1 (<1%)	..
Adverse event resulting in dose interruption of				
Talazoparib or placebo*	123 (62%)	..	42 (21%)	..
Enzalutamide†	80 (40%)	..	38 (19%)	..
Adverse event resulting in dose reduction of				
Talazoparib or placebo*	109 (55%)	..	10 (5%)	..
Enzalutamide†	33 (17%)	..	12 (6%)	..
Adverse event resulting in permanent drug discontinuation of				
Talazoparib or placebo*	26 (13%)	..	19 (10%)	..
Enzalutamide†	25 (13%)	..	19 (10%)	..
Grade 5 adverse event‡	5 (3%)‡	..	6 (3%)‡	..
Most common adverse events (all grades in ≥10% of patients)§				
Anaemia	132 (67%)	86 (43%)	37 (19%)	9 (5%)
Fatigue	69 (35%)	3 (2%)	56 (28%)	2 (1%)
Neutropenia	69 (35%)	39 (20%)	14 (7%)	2 (1%)
Thrombocytopenia	51 (26%)	15 (8%)	5 (3%)	1 (<1%)
Back pain	48 (24%)	3 (2%)	46 (23%)	3 (2%)
Decreased appetite	46 (23%)	2 (1%)	31 (16%)	2 (1%)
Hypertension	44 (22%)	22 (11%)	39 (20%)	16 (8%)
Nausea	43 (22%)	3 (2%)	36 (18%)	1 (<1%)
Leukopenia	43 (22%)	14 (7%)	15 (8%)	0
Fall	39 (20%)	5 (3%)	28 (14%)	3 (2%)
Asthenia	34 (17%)	5 (3%)	33 (17%)	0
Arthralgia	33 (17%)	1 (<1%)	49 (25%)	0
Constipation	32 (16%)	0	41 (21%)	0
Diarrhoea	27 (14%)	0	24 (12%)	0
Hot flush	24 (12%)	0	33 (17%)	0
Pyrexia	22 (11%)	1 (<1%)	4 (2%)	0
Dizziness	21 (11%)	1 (<1%)	16 (8%)	2 (1%)
Weight decreased	21 (11%)	4 (2%)	18 (9%)	1 (<1%)
Dyspnoea	20 (10%)	1 (<1%)	11 (6%)	0
Headache	14 (7%)	0	24 (12%)	1 (<1%)

Data are n (%). HRR=homologous recombination repair. Shown are adverse events that occurred from the time of the first dose of study treatment until 28 days after permanent discontinuation of all study treatments or before initiation of a new antineoplastic or any investigational therapy, whichever occured first. Adverse events were graded according to National Cancer Institute Common Terminology Criteria for Adverse Events version 4.03. All data are reported per the safety population defined as all patients who were treated with at least one dose of study treatment, including one patient who was randomly assigned to talazoparib plus enzalutamide but received enzalutamide only (197 patients in the talazoparib plus enzalutamide group and 199 patients in the placebo plus enzalutamide group treated with both study treatments). *Includes permanent discontinuation, dose reduction, or dose interruption of talazoparib or placebo only plus permanent discontinuation, dose reduction, or dose interruption of both talazoparib or placebo and enzalutamide. †Includes permanent discontinuation, dose reduction, or dose interruption of enzalutamide only plus permanent discontinuation, dose reduction, or dose interruption of both talazoparib or placebo and enzalutamide. ‡One death occurred in the talazoparib group due to disease progression and was reported by the investigator as having a reasonable possibility that the event was treatment-related, with study medications contributing to the immediate cause of death, which was reported as septic shock. No events in the placebo group were considered treatment related. §None of these events were recorded as grade 5.

Table 2: **Summary of adverse events (HRR-deficient safety population)**

Research in context

Evidence before this study

Before the TALAPRO-2 trial was started in December, 2017, we searched PubMed for relevant preclinical or clinical research published on DNA damage repair, homologous recombination repair (HRR), so-called BRCAness, novel hormonal therapies or androgen receptor pathway inhibitors (ARPIs), androgen receptor signalling inhibition, poly(ADP) ribose polymerase (PARP) inhibitors, and advanced prostate cancer. The worldwide incidence of prostate cancer is rising, and metastatic castration-resistant prostate cancer remains a lethal disease despite approvals of new agents. Therapies targeting androgen receptor signalling together with androgen deprivation therapy are the mainstay of standard of care for first-line treatment of metastatic castration-resistant prostate cancer. The prognosis is particularly poor for patients with metastatic castration-resistant prostate cancer harbouring HRR gene alterations. Since 2017, results from phase 2/3 investigational trials of PARP inhibitor monotherapy (olaparib, rucaparib, and talazoparib) have indicated efficacy of these agents in patients with *BRCA*-altered or HRR-altered (including *BRCA*) metastatic castration-resistant prostate cancer who had previously received treatment for metastatic castration-resistant prostate cancer. Two randomised phase 3 trials, PROpel (NCT03732820) and MAGNITUDE (NCT03748641), which were conducted in parallel with the current study, investigated the combination of a PARP inhibitor (olaparib and niraparib, respectively) with the androgen biosynthesis inhibitor abiraterone acetate plus prednisone (or prednisolone in PROpel; AAP) as first-line treatment for metastatic castration-resistant prostate cancer versus AAP plus placebo. Results from the primary analysis of MAGNITUDE showed improved radiographic progression-free survival (rPFS) with niraparib plus AAP versus AAP plus placebo in patients with HRR-altered metastatic castration-resistant prostate cancer. In exploratory subgroup analysis of PROpel, rPFS benefit was noted with olaparib plus AAP versus AAP plus placebo in patients with HRR-altered metastatic castration-resistant prostate cancer. Results from the final overall survival analysis of PROpel and the interim and final analyses of MAGNITUDE showed differences in overall survival benefits for the combination versus AAP alone. In the subgroup of patients with HRR gene alterations in PROpel, olaparib plus AAP showed overall survival benefit versus AAP alone, although these analyses were not powered for statistical significance. The second interim analysis of the HRR-deficient cohort in MAGNITUDE showed no overall survival benefit for niraparib plus AAP versus AAP alone in patients with HRR gene alterations.

Added value of this study

The previously reported primary analysis of the prospectively assessed HRR-deficient cohort of TALAPRO-2 showed a statistically significant improvement in rPFS with talazoparib plus enzalutamide compared with enzalutamide plus placebo, as well as improvements in other secondary endpoints. In this prespecified analysis of the key alpha-protected secondary endpoint of overall survival of TALAPRO-2, talazoparib plus enzalutamide resulted in a statistically significant and clinically meaningful improvement in overall survival versus enzalutamide plus placebo in patients with metastatic castration-resistant prostate cancer harbouring tumour HRR gene alterations. Additionally, exploratory analyses indicated benefit of the talazoparib plus enzalutamide combination in subgroups of patients with or without tumour *BRCA1/2* alterations, which extends the evidence of PARP inhibitor plus ARPI efficacy beyond *BRCA1/2* alterations to non-*BRCA1/2* HRR gene alterations. Exploratory post-hoc analyses reveal efficacy benefits across multiple individual HRR gene alteration subgroups, including among patients with tumour *CDK12*m, for whom PARP inhibitors had previously shown little benefit. No new safety signals were reported with long-term follow-up. These results add to our understanding of the efficacy of talazoparib plus enzalutamide in patients with metastatic castration-resistant prostate cancer harbouring tumour HRR gene alterations.

Implications of all the available evidence

As described previously, the overall survival results from the PROpel and MAGNITUDE trials differ from those reported in TALAPRO-2, the reasons for which are yet to be understood but might be related to differences in the characteristics of the individual PARP inhibitors (eg, PARP trapping ability) or the ARPI partner, the trial design (retrospectively or prospectively assessed HRR gene alterations), or differences in the dosing of these agents. Together with the results from the unselected cohort (reported separately), these data indicate that TALAPRO-2 is the only phase 3 trial to date to show statistically significant overall survival improvement with a PARP inhibitor plus ARPI combination versus an ARPI alone in patients with metastatic castration-resistant prostate cancer harbouring prospectively assessed tumour HRR gene alterations, as well as in unselected patients with metastatic castration-resistant prostate cancer. These data further establish the combination of talazoparib plus enzalutamide as a standard of care for patients with metastatic castration-resistant prostate cancer harbouring tumour HRR gene alterations.

Necator americanus gehört zur Familie der Nematoden und lebt im Dünndarm von Menschen, Hunden und Katzen. Mit seinem Artverwandten Ancylostoma duodenale ist er der humanpathogene Auslöser der Ancylostomatidose.
Dieser Parasit unterscheidet sich von seinem Artverwandten - Ancylostoma duodenale - durch die geografische Verbreitung, unterschiedlicher Mundapparate und seine relative Größe. Er besitzt zwei dorsale und zwei ventrale Schneideplatten im vorderen Rand seiner Mundkapsel. Zudem hat er je ein paar subdorsale sowie subventrale Zähne nahe des Hinterleibes. Die männlichen Tiere werden zwischen 7-9 mm lang, die weiblichen 9-11 mm. Sie leben etwa 3 bis 5 Jahre. Fertilisierte Weibchen legt 5000 bis 10.000 Eier täglich.

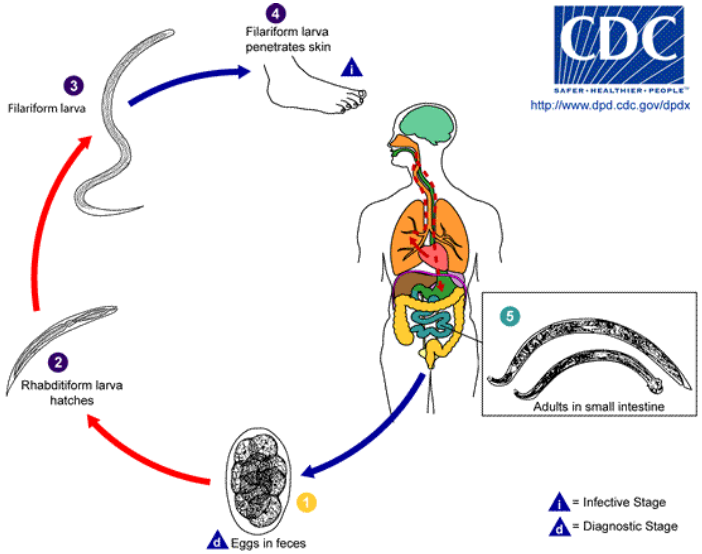

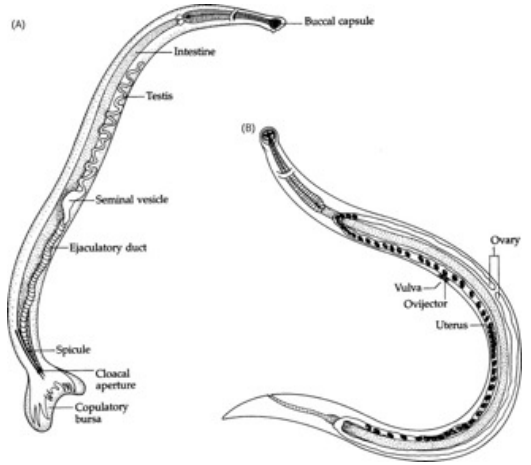

Albendazol ist ein Arzneistoff aus der Gruppe der Benzimidazole und wird als Anthelminthikum zur Behandlung verschiedener Wurminfektionen eingesetzt. Es wirkt, indem es die Glukoseaufnahme und den Stoffwechsel von Helminthen (Würmern) stört, was zum Absterben der Parasiten führt. Albendazol ist sowohl in der Human- als auch in der Veterinärmedizin gebräuchlich.

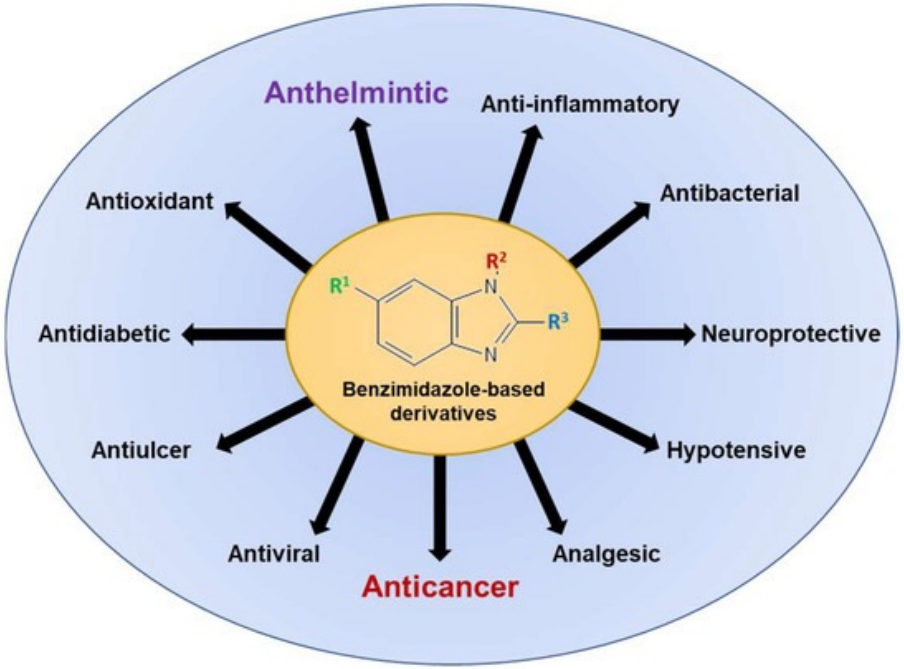

Feasibility of interrupting the transmission of soil-transmitted helminths: the DeWorm3 community cluster-randomised controlled trial in Benin, India, and Malawi

Summary

Background Soil-transmitted helminths are targeted for elimination as a public health problem. This study assessed whether, with high coverage, community-wide mass drug administration (MDA) could lead to transmission interruption.

Methods DeWorm3 is an open-label, community cluster-randomised controlled trial in Benin, India, and Malawi. In each country, a single governmental administrative unit (population ≥80 000 individuals) with soil-transmitted helminth endemicity and participation in at least five rounds of community-wide MDA for lymphatic filariasis, was divided into 40 clusters (population ≥1650 individuals), which were randomly assigned (1:1) to community-wide MDA versus school-based deworming. Laboratory personnel were masked to exposure status and all investigators were masked to post-baseline outcome data until unmasking. In all clusters, preschool-aged and school-aged children received school-based deworming as per national guidelines for 3 years. In intervention clusters, door-to-door community-wide MDA (a single oral dose of 400 mg albendazole) was delivered to all eligible individuals biannually by community drug distributors for 3 years. All individuals aged 12 months and older in India and Benin and aged 24 months and older in Malawi were eligible for treatment, except women in the first trimester of pregnancy, those with adverse reactions to benzimidazoles, those who were acutely ill or intoxicated, or those reporting treatment within the previous 2 weeks. The co-primary outcomes were individual-level prevalence and cluster-level transmission interruption (ie, weighted prevalence of predominant species of ≤2%) of the predominant soil-transmitted helminth species, assessed by quantitative PCR (qPCR) 24 months after the last round of MDA. The analysis set contained a subset of randomly selected participants per cluster who enrolled in the endline assessment, provided a stool sample, and had a qPCR result. All individuals who received treatment were eligible for inclusion in the safety population. This trial is registered with ClinicalTrials.gov (NCT03014167), and is active but not recruiting.

Findings Between Oct 10, 2017, and Feb 17, 2023, 120 clusters (40 clusters per country, comprising 357 716 individuals) were randomly assigned, 60 to community-wide MDA and 60 to school-based deworming. 184 030 (51·4%) individuals in the clusters at baseline were female, 173 663 (48·5%) were male, and 23 (<0·1%) were other. The analysis set consisted of 58 827 individuals in the control group and 58 554 in the intervention group 24 months after the cessation of all deworming, *Necator americanus* prevalence (the predominant species at all sites) in the community-wide MDA group was lower than the school-based deworming group in Benin (adjusted prevalence ratio [aPR] 0·44 [95% CI 0·34–0·58]), India (0·41 [0·32–0·52]), and Malawi (0·40 [0·34–0·46]). Transmission interruption was achieved for *N americanus* in 11 (55%) of 20 intervention clusters versus six (30%) of 20 control clusters in Benin (p=0·20), in one (5%) intervention cluster versus no control clusters in India (p=1·00), and in no clusters in either group in Malawi (p=1·00). 984 adverse events were reported among 487 participants over the study, of which 32 among 13 participants resulted in hospitalisation and were classified as serious adverse events (three of which were related to study procedures).

Interpretation Soil-transmitted helminth transmission interruption might be possible in focal geographies but does not appear to be programmatically feasible within the evaluated timeframe. Community-wide MDA should be considered as an alternative strategy to school-based deworming programmes to improve equity and outcomes in helminth-endemic areas.

Funding The Gates Foundation.

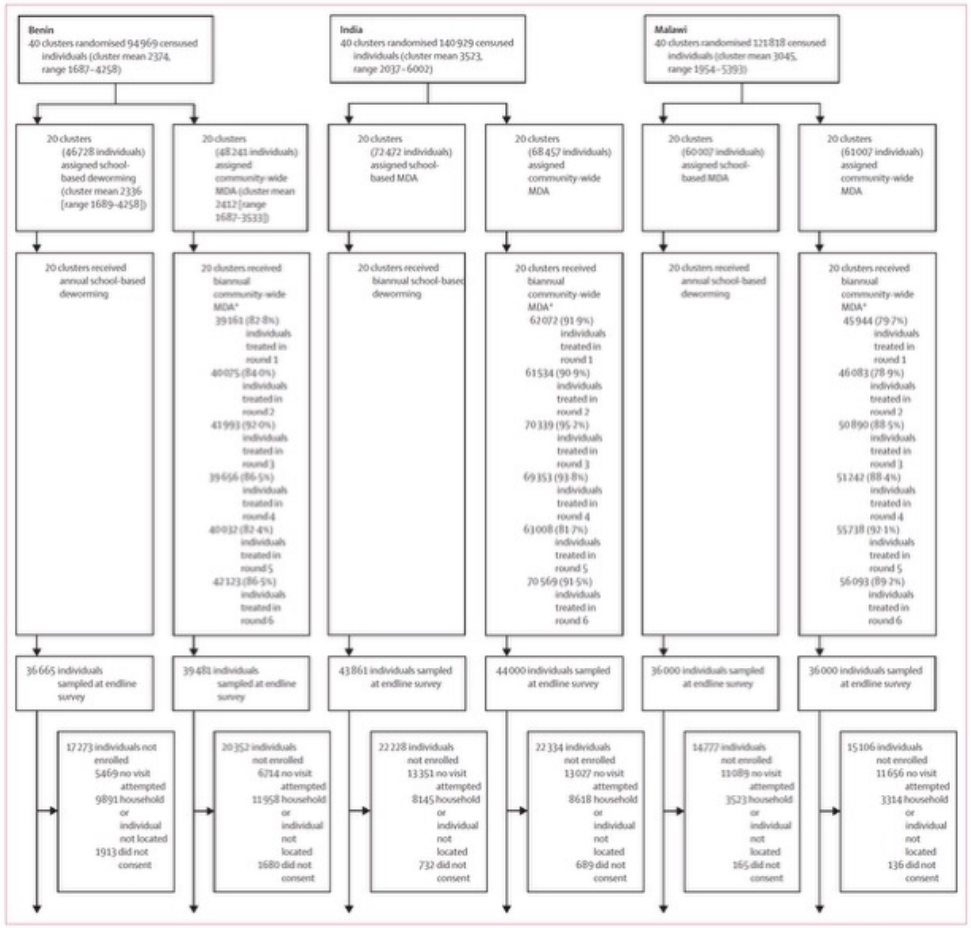

(Figure 1 continues on next page)

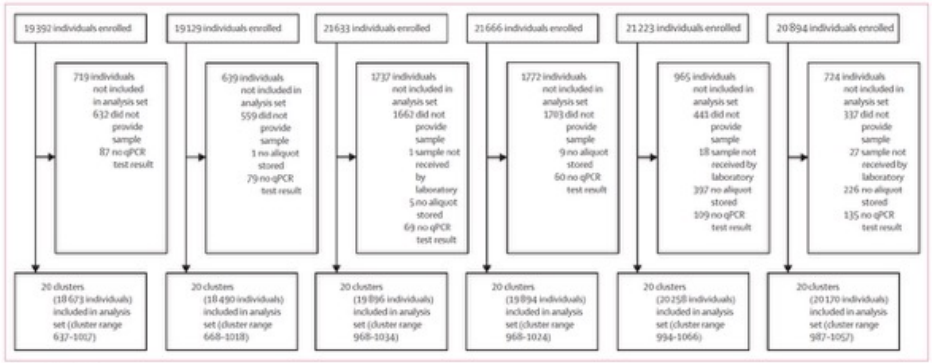

Figure 1: **Trial profile**
MDA=mass drug administration. qPCR=quantitative PCR. *Denominators vary because MDA depends on the national guidelines in each country, with exclusions of anyone younger than 1 year, anyone in their first trimester of pregnancy, and anyone who died between the time of the census and treatment delivery.

	Benin		India		Malawi	
	School-based deworming	Community-wide MDA	School-based deworming	Community-wide MDA	School-based deworming	Community-wide MDA
Study site characteristics						
Geographical area of study site, km²	84·5	63·8	285·2	289·5	140·3	148·3
Urbanicity in study clusters*						
Rural	9 (45·0%)	9 (45·0%)	17 (85·0%)	16 (80·0%)	16 (80·0%)	15 (75·0%)
Peri-urban	4 (20·0%)	4 (20·0%)	3 (15·0%)	4 (20·0%)	4 (20·0%)	5 (25·0%)
Urban	7 (35·0%)	7 (35·0%)	0	0	0	0
Household characteristics						
Households enumerated	11 905	12 473	18 716	17 819	13 762	13 988
Household residents†	4 (2–5)	4 (2–5)	4 (3–5)	4 (3–5)	4 (3–6)	4 (3–6)
Population density within 0·5 km of the household						
<1000 people per km²	2098 (17·6%)	2650 (21·2%)	9729 (52·0%)	8694 (48·8%)	5848 (42·5%)	4098 (29·3%)
1000–4999 people per km²	6733 (56·6%)	5003 (40·1%)	8084 (43·2%)	8715 (48·9%)	7914 (57·5%)	9890 (70·7%)
≥5000 people per km²	3074 (25·8%)	4820 (38·6%)	903 (4·8%)	410 (2·3%)	0	0
Owner-occupied dwelling	7369 (61·9%)	7720 (61·9%)	16 703 (89·2%)	15 928 (89·4%)	11 769 (85·5%)	12 195 (87·2%)
Flooring material						
Natural	2086 (17·5%)	2213 (17·7%)	2413 (12·9%)	2151 (12·1%)	10 847 (78·8%)	11 229 (80·3%)
Manmade	9784 (82·2%)	10 192 (81·7%)	16 284 (87·0%)	15 647 (87·8%)	2905 (21·1%)	2751 (19·7%)
Other or unknown	35 (0·3%)	68 (0·5%)	19 (0·1%)	21 (0·1%)	10 (0·1%)	8 (0·1%)
Sanitation‡						
Basic facilities	2835 (23·8%)	2838 (22·8%)	6200 (33·1%)	5473 (30·7%)	9367 (68·1%)	9515 (68·0%)
Limited facilities	3297 (27·7%)	3430 (27·5%)	359 (1·9%)	294 (1·6%)	3492 (25·4%)	3478 (24·9%)
Unimproved facilities	1142 (9·6%)	1300 (10·4%)	186 (1·0%)	254 (1·4%)	534 (3·9%)	659 (4·7%)
No facilities (open defecation)	4388 (36·9%)	4636 (37·2%)	11 954 (63·9%)	11 792 (66·2%)	352 (2·6%)	305 (2·2%)
Other or unknown	243 (2·0%)	269 (2·2%)	17 (0·1%)	6 (<0·1%)	17 (0·1%)	31 (0·2%)
Drinking water source‡						
Basic	9967 (83·7%)	10 197 (81·8%)	17 328 (92·6%)	16 553 (92·9%)	10 524 (76·5%)	10 271 (73·4%)
Limited	688 (5·8%)	865 (6·9%)	631 (3·4%)	512 (2·9%)	2970 (21·6%)	3513 (25·1%)
Unimproved	1196 (10·0%)	1357 (10·9%)	616 (3·3%)	634 (3·6%)	241 (1·8%)	170 (1·2%)
Surface water	20 (0·2%)	17 (0·1%)	49 (0·3%)	30 (0·2%)	26 (0·2%)	27 (0·2%)
Other or unknown	34 (0·3%)	37 (0·3%)	92 (0·5%)	90 (0·5%)	1 (<0·1%)	7 (0·1%)
Household has electricity	5253 (44·1%)	5493 (44·0%)	17 581 (93·9%)	16 615 (93·2%)	786 (5·7%)	541 (3·9%)
Household has livestock	1687 (14·2%)	1488 (11·9%)	7580 (40·5%)	6872 (38·6%)	4871 (35·4%)	4858 (34·7%)
Household has a mobile phone	8889 (74·7%)	9012 (72·3%)	15 688 (83·8%)	15 004 (84·2%)	6032 (43·8%)	5965 (42·6%)
Study population						
Enumerated	46 728	48 241	72 472	68 457	60 811	61 007
Sex						
Male	22 700 (48·6%)	23 188 (48·1%)	36 141 (49·9%)	34 153 (49·9%)	28 589 (47·0%)	28 892 (47·4%)
Female	24 028 (51·4%)	25 052 (51·9%)	36 318 (50·1%)	34 300 (50·1%)	32 218 (53·0%)	32 114 (52·6%)
Other	0	1 (<0·1%)	13 (<0·1%)	4 (<0·1%)	4 (<0·1%)	1 (<0·1%)
Age distribution						
Infants (<1 year)	1297 (2·8%)	1319 (2·7%)	900 (1·2%)	850 (1·2%)	2199 (3·6%)	2168 (3·6%)
Preschool-age children (1–4 years)	5413 (11·6%)	5775 (12·0%)	4453 (6·1%)	4029 (5·9%)	8768 (14·4%)	8687 (14·2%)
School-age children (5–14 years)	12 897 (27·6%)	13 146 (27·3%)	11 260 (15·5%)	10 578 (15·5%)	18 905 (31·1%)	18 747 (30·7%)
Adults (≥15 years)	26 919 (57·6%)	27 963 (58·0%)	55 859 (77·1%)	53 000 (77·4%)	30 840 (50·7%)	31 321 (51·3%)
Women of reproductive age (15–49 years)	10 388 (22·2%)	10 876 (22·5%)	20 180 (27·8%)	19 098 (27·9%)	13 720 (22·6%)	13 702 (22·5%)
Age unknown	202 (0·4%)	38 (0·1%)	0	0	99 (0·2%)	84 (0·1%)

(Table 1 continues on next page)

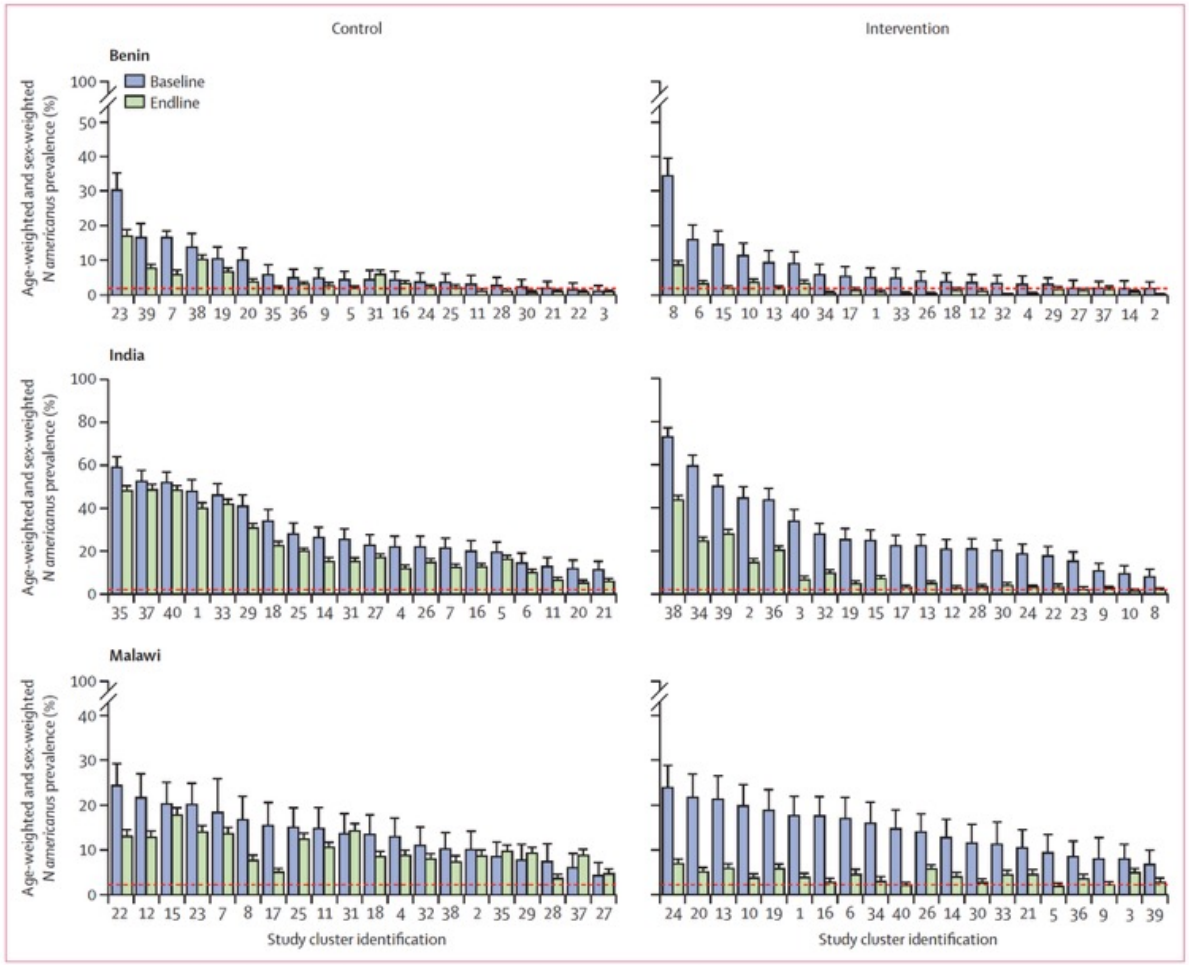

Figure 2: **Baseline and endline individual-level *N americanus* qPCR prevalence for each cluster, by treatment group and country**

N americanus qPCR prevalence was computed for each study cluster at baseline (mean 403 [SD 34] samples per cluster) and endline (978 [80] samples per cluster) weighted to the age distribution and sex distribution of the most recent census at the time of survey. Clusters have been ordered by prevalence at baseline (highest to lowest). Error bars represent one-sided binomial 95% CIs and prevalences are displayed separated by site and study treatment group with an overlaid transmission interruption threshold (≤2%). The y axes are presented to different scales per country to enable better visualisation of the data. *N americanus*=*Necator americanus*. qPCR=quantitative PCR.

	Benin			India			Malawi			Pooled		
	Control (n=18 673)	Intervention (n=18 490)	p value*	Control (n=19 896)	Intervention (n=19 894)	p value*	Control (n=20 258)	Intervention (n=20 170)	p value*	Control (n=58 827)	Intervention (n=58 554)	p value*
N americanus												
Endline prevalence†	748 (4·0%)	322 (1·7%)	..	4310 (21·7%)	1906 (9·8%)	..	1989 (9·8%)	827 (4·1%)	..	7047 (12·0%)	3055 (5·2%)	..
Treatment effect	1 (ref)	0·43 (0·23–0·83)	0·011	1 (ref)	0·44 (0·25–0·79)	0·0061	1 (ref)	0·42 (0·34–0·52)	<0·001	1 (ref)	0·43 (0·30–0·63)	<0·001
Adjusted treatment effect‡	1 (ref)	0·44 (0·34–0·58)	<0·001	1 (ref)	0·41 (0·32–0·52)	<0·001	1 (ref)	0·40 (0·34–0·46)	<0·001	1 (ref)	0·41 (0·36–0·48)	<0·001
A duodenale												
Endline prevalence†	11 (0·1%)	11 (0·1%)	..	3 (<0·1%)	3 (<0·1%)	..	15 (0·1%)	6 (<0·1%)	..	29 (0·1%)	20 (<0·1%)	..
Treatment effect	1 (ref)	1·02 (0·37–2·83)	0·97	1 (ref)	1·00 (0·23–4·39)	>0·99	1 (ref)	0·41 (0·09–1·75)	0·23	1 (ref)	0·70 (0·34–1·45)	0·34
Adjusted treatment effect‡	1 (ref)	0·83 (0·27–2·57)	0·75	1 (ref)	0·92 (0·17–4·94)	0·92	1 (ref)	0·31 (0·07–1·40)	0·13	1 (ref)	0·70 (0·33–1·51)	0·37
A lumbricoides												
Endline prevalence†	59 (0·3%)	123 (0·7%)	..	7 (<0·1%)	17 (0·1%)	..	15 (0·1%)	12 (0·1%)	..	81 (0·1%)	152 (0·3%)	..
Treatment effect	1 (ref)	2·08 (0·49–8·87)	0·32	1 (ref)	2·44 (0·83–7·14)	0·10	1 (ref)	0·80 (0·39–1·67)	0·56	1 (ref)	1·88 (0·59–6·00)	0·28
Adjusted treatment effect‡	1 (ref)	1·50 (0·83–2·72)	0·18	1 (ref)	2·07 (0·81–5·29)	0·13	1 (ref)	0·71 (0·37–1·38)	0·31	1 (ref)	1·40 (0·89–2·18)	0·14
T trichiura												
Endline prevalence†	6 (<0·1%)	13 (0·1%)	..	5 (<0·%1)	7 (<0·1%)	..	4 (<0·1%)	2 (<0·1%)	..	15 (<0·1%)	22 (<0·1%)	..
Treatment effect	1 (ref)	2·20 (0·88–5·51)	0·093	1 (ref)	1·40 (0·38–5·18)	0·61	1 (ref)	0·50 (0·09–2·81)	0·43	1 (ref)	1·48 (0·75–2·91)	0·26
Adjusted treatment effect‡	1 (ref)	2·26 (0·85–6·02)	0·10	1 (ref)	0·95 (0·34–2·67)	0·93	1 (ref)	0·28 (0·03–2·63)	0·27	1 (ref)	1·54 (0·76–3·12)	0·23
Any soil-transmitted helminth species												
Endline prevalence†	819 (4·4%)	467 (2·5%)	..	4318 (21·7%)	1930 (9·7%)	..	2016 (10·0%)	846 (4·2%)	..	7153 (12·2%)	3243 (5·5%)	..
Treatment effect	1 (ref)	0·57 (0·31–1·05)	0·073	1 (ref)	0·45 (0·25–0·80)	0·0061	1 (ref)	0·42 (0·34–0·52)	<0·001	1 (ref)	0·46 (0·32–0·65)	<0·001
Adjusted treatment effect‡	1 (ref)	0·52 (0·38–0·71)	<0·001	1 (ref)	0·41 (0·33–0·52)	<0·001	1 (ref)	0·40 (0·35–0·47)	<0·001	1 (ref)	0·42 (0·37–0·49)	<0·001

Data are prevalence ratio (95% CI) or n (%) unless otherwise specified. For Benin, sample sizes are 37 163 (unadjusted) and 37 058 (adjusted). For India, sample sizes are 39 790 (unadjusted) and 39 598 (adjusted). For Malawi, sample sizes are 40 428 (unadjusted) and 40 294 (adjusted). For pooled countries, sample sizes are 117 381 (unadjusted) and 116 950 (adjusted). *A duodenal=Ancylostoma duodenale. A lumbricoides=Ascaris lumbricoides. N americanus=Necator americanus. T Trichiura=Trichuris trichuria.* *Assessed by estimating prevalence ratios using modified Poisson regression with robust SEs. The primary analysis is the adjusted analysis. †Unweighted; soil-transmitted helminth positivity by quantitative PCR defined as a cycle threshold <34·43980 for *N americanus*, <28·57587 for *A lumbricoides*, and <40·00 for *A duodenale* and *T trichiura* . ‡Adjusted for baseline study cluster-specific age-weighted and sex-weighted prevalence, age distribution, sex, individual migration status, household size, population density per 1000 individuals within 0·5 km of the household, socioeconomic status as measured by an asset index divided into quintiles, and water and sanitation access as measured by WHO–UNICEF Joint Monitoring Programme for Water Supply, Sanitation, and Hygiene indicators.

Table 2: **Comparison of the individual-level soil-transmitted helminth species-specific endline quantitative PCR prevalence**

	Transmission interrupted (N=11 clusters)	Transmission not interrupted (N=9 clusters)	RR (95% CI)*	p value
Baseline prevalence of *N americanus*†	3·5% (1·4)	11·6% (9·8)	0·80 (0·71–0·90)	0·0003
Population density‡	4761·4 (1652·3)	2493·4 (2021·9)	1·27 (1·10–1·47)	0·0011
Households with open defecation§	24·0% (32·5)	49·4% (32·4)	0·92 (0·83–1·03)	0·17
Individual MDA treatment coverage in rounds 1–6	84·4% (4·2)	86·5% (5·0)	0·95 (0·86–1·05)	0·30
Clusters that achieved mean 90% coverage in rounds 1–6	1/11 (9·1%)	2/9 (22·2%)	0·57 (0·11–2·95)	0·50
Individual MDA treatment acceptance¶	57·6% (9·8)	63·7% (10·6)	0·97 (0·92–1·02)	0·24
Migration of individuals‖	5·0% (2·8)	4·1% (1·9)	1·07 (0·94–1·22)	0·32
Households with earthen household floor materials**	9·9% (7·1)	23·4% (10·0)	0·70 (0·57–0·86)	0·0007

Data are mean (SD) or n/N (%) unless specified. *N americanus*=*Necator americanus*. RR=risk ratio. *All models were modified Poisson regression with robust SEs. †Study cluster-specific *N americanus* prevalence was weighted to the age and sex distribution of the baseline census population. *N americanus* positivity by quantitative PCR was defined as a cycle threshold <34·43980. RR is expressed per 1% increase. ‡The number of study residents living within 0·5 km of each household expressed per km^2. RR is expressed per 1000 individuals. §RR is expressed per 5% change in open defecation. ¶The percentage of cluster residents who were treated at all MDA rounds in which they were eligible. RR is expressed per 1% increase. ‖Defined as the percentage of cluster residents who reported living in the household less than 6 months in the previous year during the endline census. RR is expressed per 1% increase. **Defined as the percentage of cluster residents who lived in a household with floor materials made from earth, sand, mud, clay, or dung during the endline census. RR is expressed per 5% change in floor material.

Table 3: **Cluster-level factors associated with transmission interruption of *N americanus* in the intervention group in Benin**

Research in context

Evidence before this study

The current WHO target for soil-transmitted helminths is elimination as a public health problem, delivered through annual and biannual school-based deworming of at-risk groups, including preschool-aged and school-aged children. Previously developed mathematical models indicate that interruption of soil-transmitted helminth transmission might be feasible with intensified deworming. A 2024 systematic review and meta-analysis by Ugwu and colleagues provides further evidence that community-wide deworming interventions lead to greater reductions in soil-transmitted helminth prevalence than school-based deworming. It included studies that overlapped with the timeframe of the DeWorm3 study, but were limited by smaller sample sizes, shorter duration, and restricted geographical representativeness.

Added value of this study

DeWorm3 was done in three different countries in Africa and Asia to ensure geographical representativeness. The overall population included in the study was large and the sample size of individuals who received the intervention and were evaluated for study outcomes allowed for robust estimation of the study objectives. In addition, the rigorous design of the study—as a cluster-randomised trial—allowed for assessment of the contribution of each intervention while limiting potential bias. Although transmission interruption was not achieved across all clusters, community-wide MDA led to substantially greater reductions in the prevalence of the predominant species of soil-transmitted helminth at all sites compared with school-based deworming.To our knowledge, this is the first large randomised controlled trial to assess the feasibility of interrupting the transmission of soil-transmitted helminths and is by far the largest trial to evaluate the impact of community-wide MDA.

Implications of all the available evidence

Due to the reductions in soil-transmitted helminth prevalence shown (driven by the predominant species *Necator americanus*) both in our trial and in others, community-wide MDA should be considered as a strategy to achieve the stated WHO goal of elimination as a public health problem, particularly in areas with high baseline prevalence (as lower prevalence reduced morbidity at the population level). However, transmission interruption using community-wide MDA was not achieved at programmatically relevant scale within the 3-year timeframe of the study, which was the first trial to look at this endpoint. The data from this large, rigorous, and geographically representative study adds to the previous evidence, to directly inform policy and programmes in soil-transmitted helminth-endemic areas. The study adds evidence to support policy development as countries transition donor financing and assess the role of community-wide MDA in achieving global targets for addressing neglected tropical diseases. Our data can also be used to reparametrise existing models to better inform prevalence thresholds and treatment duration and frequency to inform future efforts to interrupt soil-transmitted helminths transmission. In addition, our trial showed the feasibility of using high-throughput molecular assays as an alternative to existing coproscopic methods to provide robust estimates of soil-transmitted helminth prevalence and intensity. Given the improved diagnostic performance of quantitative PCR over traditional microscopy, quantitative PCR should be used in research and programmatic settings in which prevalence and intensity are low to improve estimates.

ASTER 70s - Adjuvant Systemic Treatment for (ER)-Positive HER2-negative Breast Carcinoma in Women Over 70 According to Genomic Grade (GG): Chemotherapy + Endocrine Treatment Versus Endocrine Treatment

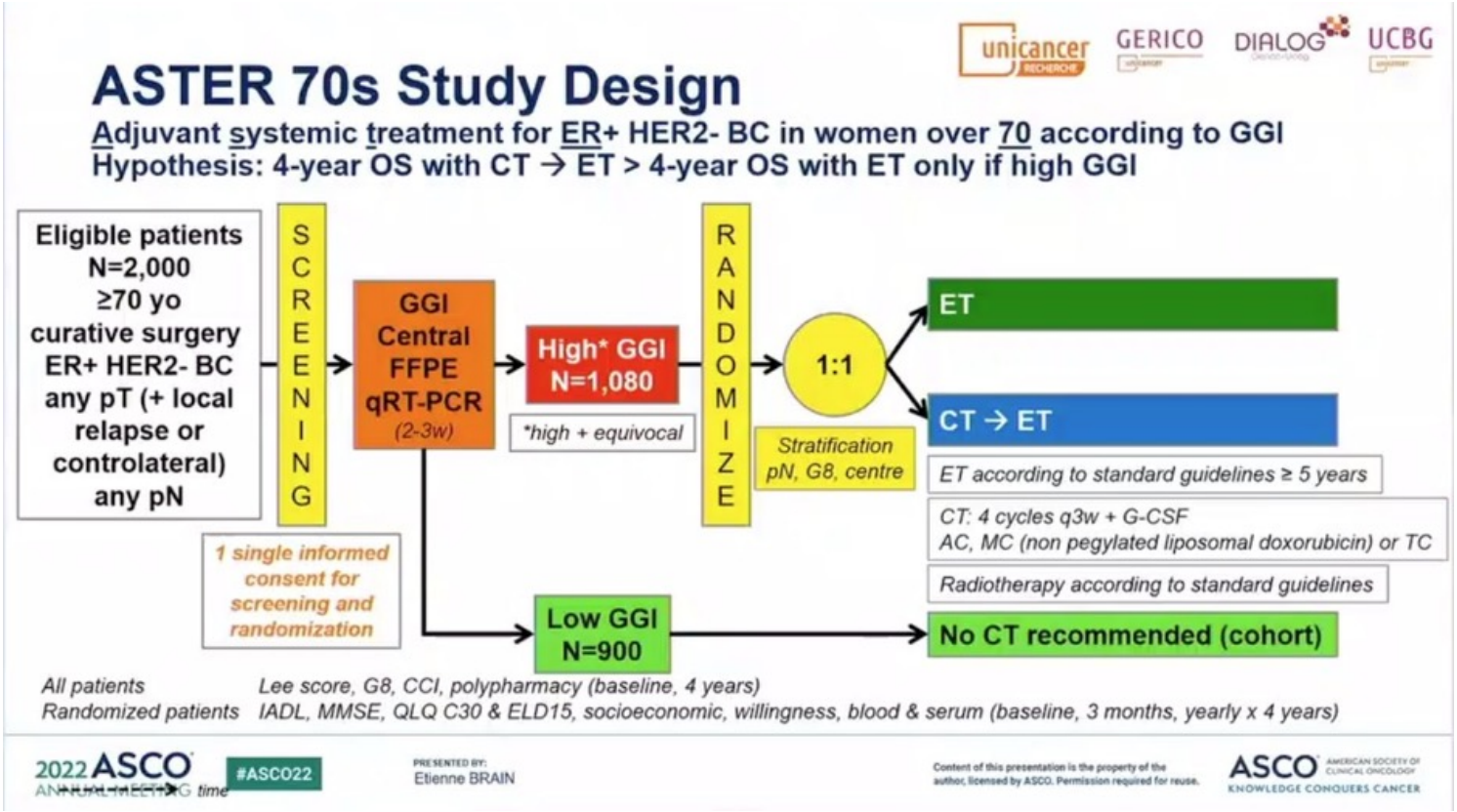

Adjuvant chemotherapy and hormonotherapy versus adjuvant hormonotherapy alone for women aged 70 years and older with high-risk breast cancer based on the genomic grade index (ASTER 70s): a randomised phase 3 trial

Summary

Background For women aged 70 years or older with oestrogen receptor-positive HER2-negative invasive breast cancer, hormonotherapy is a standard adjuvant treatment, while the role of chemotherapy is debated. We aimed to assess the effect of adjuvant chemotherapy on overall survival in these older patients with high-risk tumours according to a prognostic genomic signature.

Methods This phase 3, randomised, superiority study was conducted at 84 clinical sites in France and Belgium in women aged 70 years and older with oestrogen receptor-positive and HER2-negative primary breast cancer or isolated local recurrence before any systemic treatment and after complete surgery. Genomic grade index (GGI) testing was done with a reverse-transcriptase PCR assay of eight genes on paraffin-embedded tumour tissue in a central laboratory. Patients with a GGI high-risk tumour were randomly allocated (1:1) to receive either four cycles of postoperative taxane-based or anthracycline-based chemotherapy given every 3 weeks followed by hormonotherapy (chemotherapy group) or hormonotherapy alone (no chemotherapy group). Randomisation was stratified according to the G8 screening tool score for geriatric frailty, nodal status, and centre. The primary endpoint was overall survival. This study is registered with ClinicalTrials.gov (NCT01564056) and is under active follow-up.

Findings Between April 12, 2012 and April 14, 2016, 1969 patients were screened for GGI, of whom 1089 had a GGI high-risk tumour and were randomly allocated to the chemotherapy group (n=541) or the no chemotherapy group (n=548). Median age was 75·1 years (IQR 72·5 to 78·7) and geriatric frailty (G8 score ≤14) was identified in 437 patients (40%) patients. With a median follow-up time of 7·8 years (95% CI 7·5 to 7·8), overall survival rates were 90·5% (95% CI 87·6 to 92·8) at 4 years and 72·7% (67·8 to 77·0) at 8 years in the chemotherapy group, and 89·3% (86·2 to 91·6) at 4 years and 68·3% (63·3 to 72·7) at 8 years in the no chemotherapy group (stratified log-rank p=0·2100; hazard ratio 0·83 [95% CI 0·63 to 1·11]), yielding statistically non-significant absolute differences in survival probability of 1·3 percentage points (95% CI −2·4 to 5·0) at 4 years and 4·5% (95% CI −2·1 to 11·1) at 8 years. Safety analysis favoured the no chemotherapy group: at least one grade 3 or higher adverse event occurred in 52 (9%) of 548 patients in the no chemotherapy group (including one death not related to treatment), compared with 183 (34%) of 541 patients in the chemotherapy group (including three deaths, of which one was related to treatment).

Interpretation The addition of adjuvant chemotherapy to hormonotherapy conferred no survival benefit in women aged 70 years and above with a GGI high-risk oestrogen receptor-positive HER2-negative breast cancer, and was associated with more adverse events, providing important data on the benefit–risk balance of adding adjuvant chemotherapy to adjuvant hormonotherapy in this older age group.

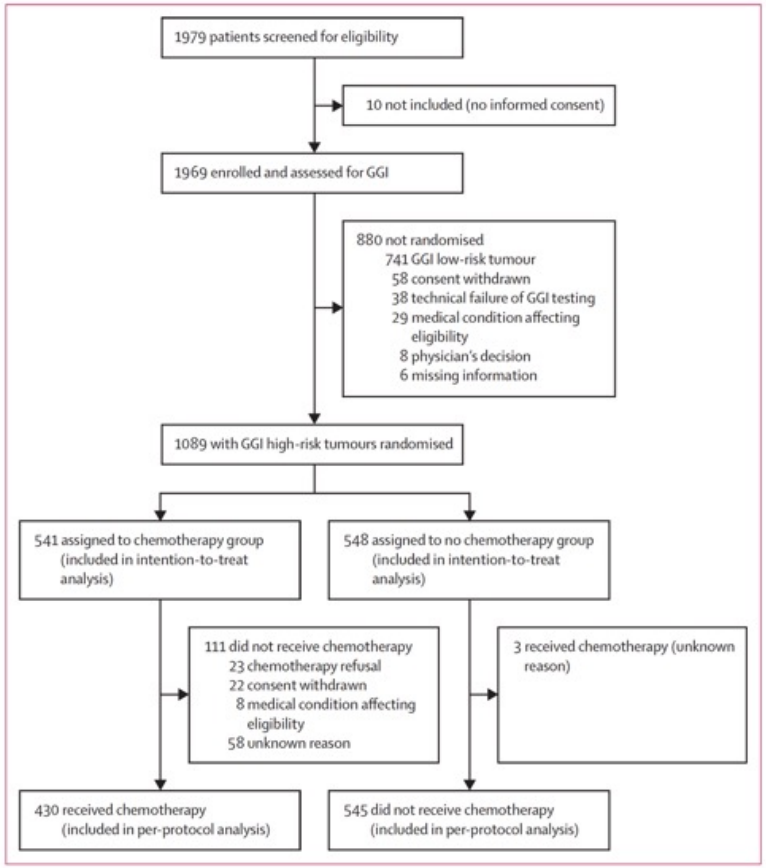

Figure 1: **Trial profile**
GGI=genomic grade index.

	Chemotherapy group (n=541)	No chemotherapy group (n=548)
Age, years	75·2 (72·7–79·0)	74·9 (72·4–78·6)
ECOG performance status		
0	340 (63%)	374 (69%)
1	190 (35%)	160 (29%)
2	11 (2%)	11 (2%)
Missing data	0	3
G8 geriatric frailty score*		
>14	318 (59%)	334 (61%)
≤14	223 (41%)	214 (39%)
Lee's prognostic index score†		
<6	108 (20%)	116 (22%)
6–9	371 (69%)	372 (69%)
>9	55 (10%)	50 (9%)
Missing data	7	10
Age-adjusted Charlson comorbidity index		
5	262 (49%)	280 (52%)
6	173 (32%)	166 (31%)
>6	98 (18%)	94 (17%)
Missing data	8	8
Instrumental activities of daily living	8 (8–8)	8 (8–8)
Minimal mental status examination	28 (26–29)	28 (26–30)
History of non-breast cancer	37 (7%)	56 (10%)
Breast cancer local relapse or contralateral tumour	65 (12%)	76 (14%)
pT stage		
1	234 (44%)	238 (44%)
2	270 (50%)	270 (50%)
3	31 (6%)	35 (6%)
4	2 (<1%)	1 (<1%)
Missing data	4	4
pN stage		
0	300 (55%)	300 (55%)
1	179 (33%)	186 (34%)
2	59 (11%)	59 (11%)
pN+ unspecified	3 (1%)	3 (1%)
Histological subtype		
Ductal invasive	389 (72%)	373 (68%)
Lobular invasive	88 (16%)	99 (18%)
Mixed	21 (4%)	25 (5%)
Other	42 (8%)	50 (9%)
Missing data	1	1
Bilateral tumour	23 (4%)	24 (4%)
Multifocal tumour	103 (19%)	106 (19%)
Oestrogen receptor status		
Positive	541 (100%)	547 (100%)
Missing data	0	1
Progesterone receptor status		
Positive	421 (78%)	432 (79%)
Negative	119 (22%)	115 (21%)
Missing data	1	1
Ki67 index, %	20 (15–30)	25 (15–35)

(Table 1 continues on next page)

(Continued from previous page)

	Chemotherapy group (n=541)	No chemotherapy group (n=548)
HER2 status		
Negative (IHC 0, 1+, or 2+ and FISH–)	534 (>99%)	535 (>99%)
Positive (IHC 3+, or IHC 2+ and FISH+)	1 (<1%)	2 (<1%)
Missing data	6	11
Histological grade		
I	26 (5%)	37 (7%)
II	300 (55%)	302 (56%)
III	215 (40%)	202 (37%)
Missing data	0	7
Genomic grade index		
–0·277 to 0·278	190 (35%)	194 (35%)
>0·278	351 (65%)	354 (65%)
Type of surgery		
Breast-conserving surgery	325 (60%)	335 (61%)
Mastectomy	216 (40%)	211 (39%)
Missing data	0	2

Data are median (IQR) or n (%); percentages are based on non-missing data. ECOG=Eastern Cooperative Oncology Group. FISH=fluorescence in situ hybridisation. IHC=immunohistochemistry. *Screening tool for geriatric frailty; scores ≤14 suggest the presence of frailty and recommend a full geriatric assessment. †Prognostic index for 4-year mortality risk; scores <6 indicate a less than 4% risk, scores of 6–9 indicate a 15% risk, and scores >9 indicate a more than 42% risk.

Table 1: **Baseline and tumour characteristics of randomly allocated patients (n=1089)**

	Chemotherapy group (n=541)	No chemotherapy group (n=548)
Chemotherapy choice		
Taxane*	281 (52%)	2 (<1%)
Anthracycline†	148 (27%)	1 (<1%)
Other	1 (<1%)	0
None	111 (21%)	545 (99%)
Treatment completion		
Chemotherapy discontinued before cycle 4	44 (8%)	0
Chemotherapy discontinued for toxicity	35 (6%)	0
Hormonotherapy discontinued for toxicity at least once during follow-up	114 (21%)	124 (23%)
Adverse event		
At least one any-grade adverse event	503 (93%)	445 (81%)
At least one grade ≥3 adverse event	183 (34%)	52 (9%)
At least one serious adverse event	88 (16%)	17 (3%)
Death	3 (1%)	1 (<1%)

*Docetaxel plus cyclophosphamide. †Doxorubicin plus cyclophosphamide; or non-pegylated liposomal doxorubicin plus cyclophosphamide.

Table 2: **Treatment and adverse events in randomly allocated patients**

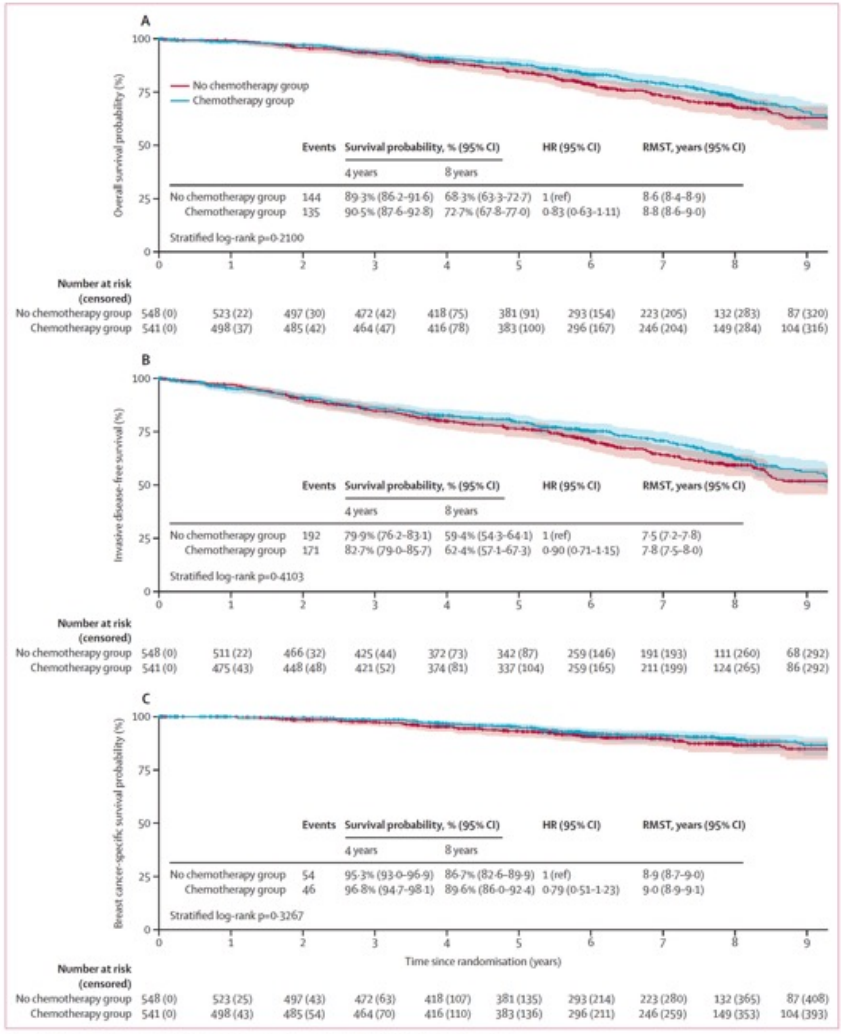

Figure 2: **Kaplan–Meier survival estimates by treatment group in the intention-to-treat population**
(A) Overall survival; events were defined as death due to any cause. (B) Invasive disease-free survival; events were defined as invasive breast cancer relapse (including contralateral tumour), any second invasive cancer (breast or other), or death from any cause. (C) Breast cancer-specific survival; events were defined as death due to breast cancer. Dashed lines indicate 95% CIs. HRs were estimated with Cox regression stratified on pN stage, G8 score, and centre. RMST was estimated until 10 years of follow-up and adjusted for pN stage and G8 score. HR=hazard ratio. RMST=restricted mean survival time.

	Deaths/total patients, n/N		8-year overall survival probability, % (95% CI)		HR (95%CI)	$P_{interaction}$
	No chemotherapy group	Chemotherapy group	No chemotherapy group	Chemotherapy group		
Age (years)						0·9223
≤75	65/323	57/294	76·0% (70·0–81·0)	79·5% (73·2–84·4)	0·74 (0·46–1·19)	
>75	79/223	78/247	56·3% (47·7–64·0)	63·9% (55·8–70·9)	0·65 (0·41–1·02)	
G8 frailty score						0·6918
>14	72/334	64/318	74·8% (68·7–79·9)	79·6% (73·7–84·3)	0·88 (0·60–1·30)	
≤14	72/214	71/223	57·2% (48·5–64·9)	62·3% (53·6–69·8)	0·78 (0·52–1·19)	
Lee's prognostic index score						0·7149
<6	20/116	17/108	81·1% (71·8–87·6)	86·1% (76·6–91·9)	0·91 (0·35–2·35)	
6–9	97/372	87/371	68·1% (61·8–73·6)	73·1% (66·9–78·3)	0·72 (0·49–1·05)	
>9	26/50	27/55	35·8% (20·6–51·4)	41·8% (24·9–57·9)	1·54 (0·45–5·24)	
pN stage (0 *vs* +)						0·6425
0	63/300	60/300	74·9% (68·5–80·1)	77·1% (70·4–82·4)	0·90 (0·59–1·37)	
+	81/248	75/241	60·2% (52·3–67·3)	67·7% (60·1–74·2)	0·79 (0·54–1·15)	
pN stage (0 *vs* 1 *vs* 2)						0·6596
0	63/300	60/300	74·9% (68·5–80·1)	77·1% (70·4–82·4)	0·90 (0·59–1·37)	
1	51/186	48/179	65·8% (56·5–73·6)	72·9% (64·2–79·9)	0·81 (0·48–1·36)	
2	30/59	26/59	41·0% (26·0–55·5)	49·5% (33·4–63·7)	0·82 (0·34–2·00)	
pT stage						0·2618
1	45/238	36/234	76·7% (69·4–82·4)	84·5% (77·9–89·3)	0·51 (0·27–0·96)	
2–4	99/306	97/303	61·5% (54·5–67·7)	64·2% (57·1–70·4)	0·83 (0·57–1·21)	
Genomic grade index						0·7941
−0·277 to 0·278	37/194	39/190	77·1% (69·0–83·3)	76·2% (67·7–82·8)	0·86 (0·40–1·87)	
>0·278	107/354	96/351	63·7% (57·3–69·4)	70·9% (64·6–76·2)	0·82 (0·57–1·16)	
Overall	**144/548**	**135/541**	**68·3% (63·3–72·7)**	**72·7% (67·8–77·0)**	**0·83 (0·63–1·11)**	

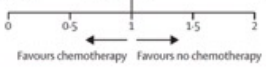

***Figure 3*: Forest plot for overall survival among prespecified subgroups in the intention-to-treat population**
HRs were estimated with Cox regression stratified on pN stage, G8 score, and centre. p values are for interaction in the Cox model. HR=hazard ratio.

	Chemotherapy group (n=135)	No chemotherapy group (n=144)
Breast cancer	46 (40%)	54 (41%)
Comorbidities	55 (48%)	55 (42%)
Second cancer	12 (11%)	22 (17%)
Toxicity	1 (1%)	1 (1%)
Unknown	21	12

Percentages are based on patients with known causes of death (n=114 in the chemotherapy group and n=132 in the no chemotherapy group).

***Table 3*: Causes of death among randomly allocated patients who died during follow-up**

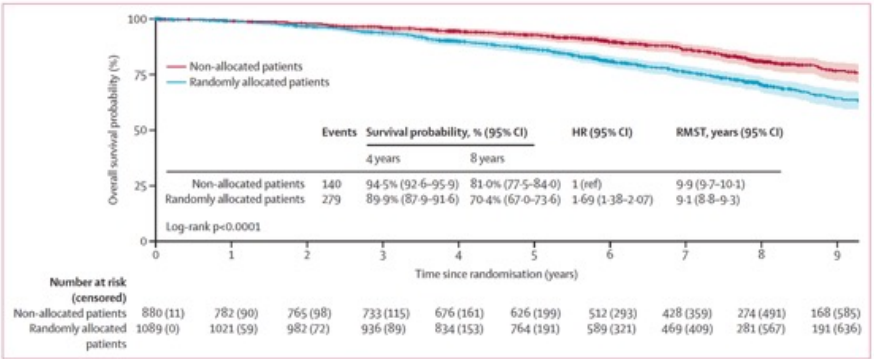

***Figure 4*: Kaplan-Meier estimates of overall survival in randomly allocated versus non-allocated patients**
Events were defined as death due to any cause. Dashed lines indicate 95% CIs. RMST was estimated until 10 years of follow-up. HR=hazard ratio. RMST=restricted mean survival time.

Research in context

Evidence before this study

Adjuvant chemotherapy has been shown to improve survival in women with early-stage breast cancer. However, less than 5% of the women included in a 2005 meta-analysis of trials comparing chemotherapy with no chemotherapy were 70 years of age or older. Furthermore, older women included in trials are generally selected based on stringent criteria, such as having few comorbidities or no previous primary cancer, making them poorly representative of the general population of older patients with breast cancer. The Société Internationale d'OncoGériatrie (SIOG) and the European Society of Breast Cancer Specialists (EUSOMA) periodically review the literature (PubMed and Embase) on the management of older patients with breast cancer and publish recommendations. In 2012, the two societies concluded that most of the evidence on the benefit of adjuvant chemotherapy concerned patients with oestrogen receptor-negative breast cancer. Genomic signatures might help to refine the assessment of the prognosis of oestrogen receptor-positive tumours and thus identify patients at high risk.

Added value of this study

To our knowledge, ASTER 70s is the first phase 3 superiority trial investigating the benefit of chemotherapy versus no chemotherapy in the adjuvant setting specifically in women aged 70 years or older with oestrogen receptor-positive breast cancer and at high risk according to a genomic signature (the genomic grade index). Using a pragmatic design, we did not identify any statistically significant increase in overall survival when adding four cycles of chemotherapy to hormonotherapy for these patients.

Implications of all the available evidence

The ASTER 70s trial provides important information to improve shared decision making between doctor and patient when discussing adjuvant breast cancer treatment. The results show the ongoing challenge of identifying older patients with oestrogen receptor-positive HER2-negative breast cancer who are suitable candidates for adjuvant chemotherapy in addition to hormonotherapy, consolidating the SIOG and EUSOMA recommendations updated in 2021 on the management of older patients with breast cancer. The results also highlight the risk of extrapolating to this population the results obtained using similar strategies on younger populations, distancing research from defining the right and optimal treatment, which is traditionally still based on achieving its highest intensity, whereas increasing frailty with age calls for frequent de-escalation. Further research is needed into tumour and ageing biomarkers to identify women aged 70 years or older who could benefit from adjuvant chemotherapy. Further, this study demonstrates that pragmatic trials can be conducted to improve the representation of older patients in clinical research, with a view to establishing appropriate guidelines.

The *Lancet* One Health Commission: harnessing our interconnectedness for equitable, sustainable, and healthy socioecological systems

Executive summary

Industrialisation, urbanisation, and globalisation have substantially improved human life expectancy over the past century. In tandem, an expanding array of interlinked threats to humans, other animals, plants, and a myriad of other biotic and abiotic elements in our shared ecosystems has been generated. These threats include emerging and re-emerging infectious diseases, antimicrobial resistance (AMR), non-communicable diseases (NCDs), jeopardised food safety and security, freshwater scarcity, climate change, pollution, and biodiversity loss. These pressing health and sustainability challenges exceed the scope of any single discipline, government ministry, or societal sector, underscoring the need for interdisciplinary, transdisciplinary, and multisectoral collaboration, as well as for a socioecologically oriented systems perspective that appreciates the fundamental interconnections between humans, other animals, and the wider ecosystem.

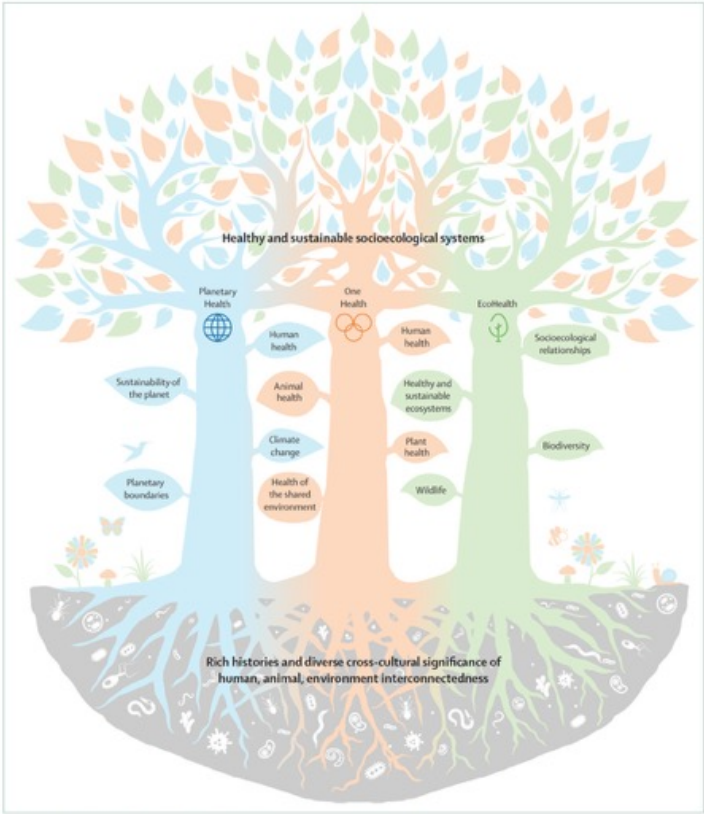

Figure 1: **Integrated approaches to achieving healthy and sustainable socioecological systems**
Planetary Health focuses on the relationship between humans and the natural systems on which human health depends, as regulated by the nine planetary boundaries.[66] Planetary Health is premised on the proposal that we have entered a new planetary epoch, known as the Anthropocene,[67] in which these life-sustaining systems have been fundamentally altered by human activity, with such rapidity that human health and wellbeing are potentially threatened. EcoHealth seeks to understand health in the context of socioecological relationships, with the aim of achieving sustainable health throughout the ecosystem. Biodiversity and equity are core values.[68,69] Although multiple perspectives coexist within and between each of these fields, and although each has evolved and diversified, this figure depicts some of the conventional foci of Planetary Health, One Health, and EcoHealth, which all advance a holistic perspective on socioecological health interdependencies, generate insight into socioecological interconnection, and contribute to a shared ambition of healthy and sustainable socioecological systems.

Trump brings back presidential physical fitness test canceled by Obama

Trump signed an executive order resurrecting the test, which for decades pushed children across the country to do 40 push-ups, 10 pull-ups and a 6.5-minute mile.

The Donald Trump workout

President Donald Trump signed an executive order on Thursday alongside a coterie of current and retired professional athletes to bring the presidential fitness test back to U.S. schools — a national test of physical performance that had been administered inside school gyms across the country for decades.

"I'm pleased to announce that we're officially restoring the presidential fitness test and the presidential fitness award," Trump said at a White House signing ceremony. "From the late 1950s until ... 2013 ... scholars all across our country competed against each other in the presidential fitness test, and it was a big deal. This was a wonderful tradition, and we're bringing it back."

A version of the test was first deployed during Dwight D. Eisenhower's presidential administration. For decades, it pushed children across the country to do 40 push-ups, 10 pull-ups and a 6½-minute mile. The Obama administration disbanded the test in 2012, replacing it with a program focused on overall health instead of athleticism.

Mile = 1500 M

How rare is a 6/30 mile?

Average mile time

	17–21 years
Top 1% of males	6:30
Top 50% of males	8:18
Top 1% of females	7:48
Top 50% of females	9:51

Eine 1500-Meter-Zeit von 6 Minuten ist eine sehr gute Zeit und deutet auf eine hohe Fitness hin. Es entspricht einer Pace von 4 Minuten pro Kilometer, was für viele Läufer ein ambitioniertes Ziel ist.

Heavy water, specifically doubly labeled water (DLW), is used to measure metabolism in humans and animals by tracking the elimination rates of deuterium (^{2}H) and oxygen-18 (^{18}O) from the body. Since deuterium leaves the body only through water loss, while oxygen-18 is lost through both water and carbon dioxide (CO2), the difference in their elimination rates allows for the calculation of CO2 production, which is directly related to energy expenditure. This method is particularly useful for determining energy expenditure in free-living conditions over extended periods.

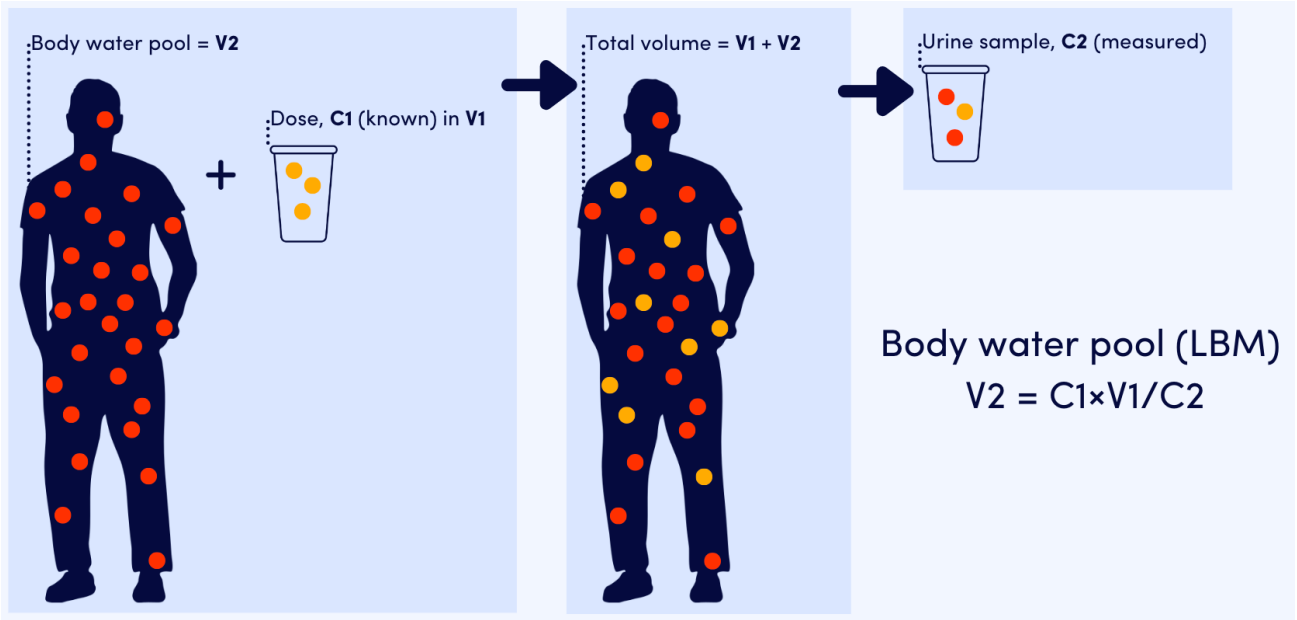

Not radioactive

Measured with mass spec.

PNAS RESEARCH ARTICLE | ANTHROPOLOGY OPEN ACCESS

Energy expenditure and obesity across the economic spectrum

Global economic development has been associated with an increased prevalence of obesity and related health problems. Increased caloric intake and reduced energy expenditure are both cited as development-related contributors to the obesity crisis, but their relative importance remains unresolved. Here, we examine energy expenditure and two measures of obesity (body fat percentage and body mass index, BMI) for 4,213 adults from 34 populations across six continents and a wide range of lifestyles and economies, including hunter-gatherer, pastoralist, farming, and industrialized populations. Economic development was positively associated with greater body mass, BMI, and body fat, but also with greater total, basal, and activity energy expenditure. Body size–adjusted total and basal energy expenditures both decreased approximately 6 to 11% with increasing economic development, but were highly variable among populations and did not correspond closely with lifestyle. Body size–adjusted total energy expenditure was negatively, but weakly, associated with measures of obesity, accounting for roughly one-tenth of the elevated body fat percentage and BMI associated with economic development. In contrast, estimated energy intake was greater in economically developed populations, and in populations with available data (n = 25), the percentage of ultraprocessed food in the diet was associated with body fat percentage, suggesting that dietary intake plays a far greater role than reduced energy expenditure in obesity related to economic development.

Significance

Economic development is associated with increased prevalence of obesity and related health problems, but the relative importance of increased caloric intake and reduced energy expenditure remains unresolved. We show that daily energy expenditures are greater in developed populations, and activity energy expenditures are not reduced in more industrialized populations, challenging the hypothesis that decreased physical activity contributes to rises in obesity with economic development. Instead, our results suggest that dietary intake plays a far greater role than reduced expenditure in the elevated prevalence of obesity associated with economic development.

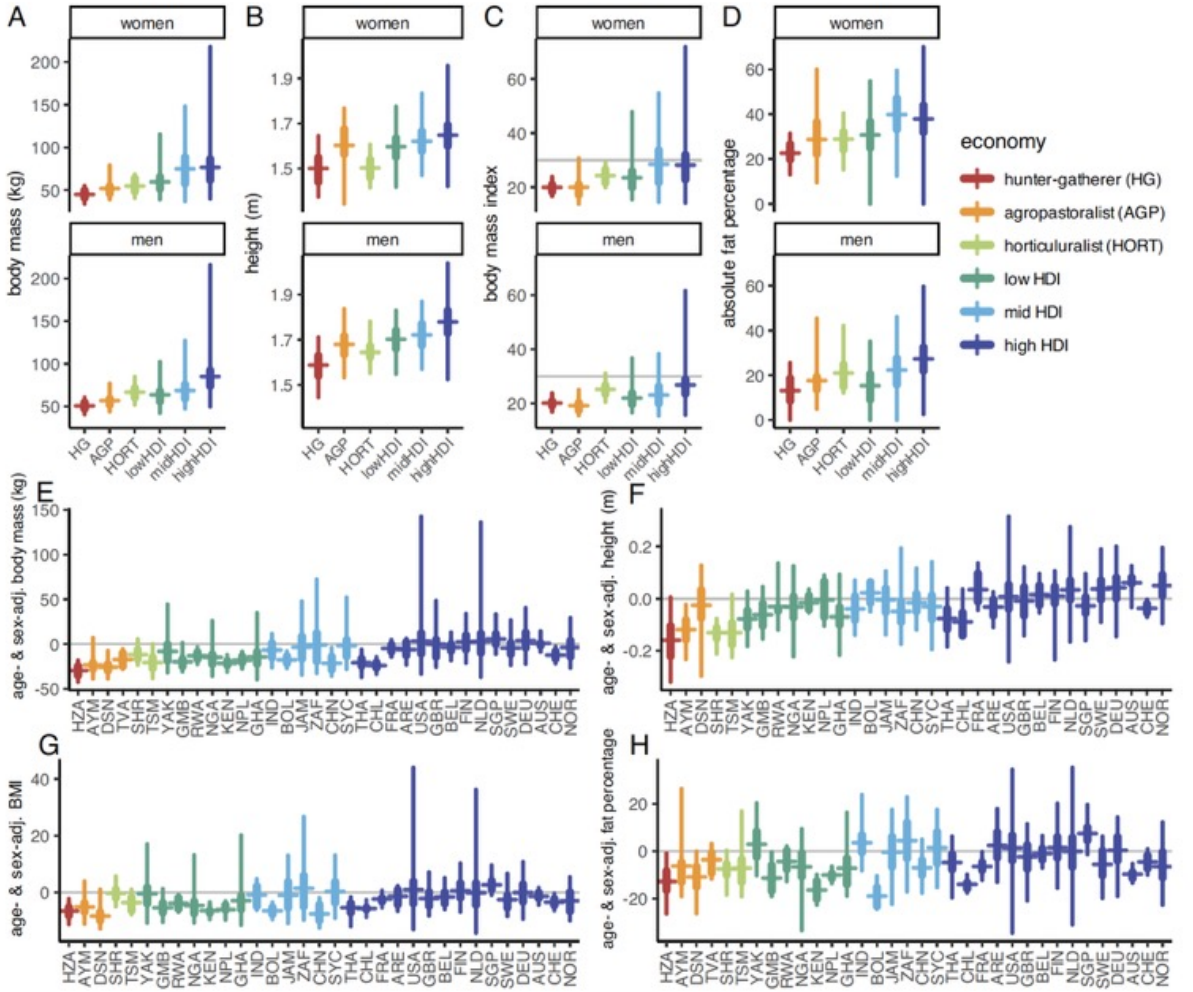

Fig. 1. Body size and composition across economies. Cohorts are ordered from lowest to highest HDI score. Bars indicate mean and quartiles. (*A–D*) Body mass, height, BMI, and body fat percentage increase with economic development in both women and men. Substantial portions of the BMI distribution fall above the criterion for obesity (BMI ≥ 30 kg/m^2) in Low, Mid, and High HDI populations. (*E–H*) There is considerable variability within and between populations in age- and sex-adjusted body mass, height, BMI, and body fat percentage. See *SI Appendix*, Table S8 for population measures and abbreviations.

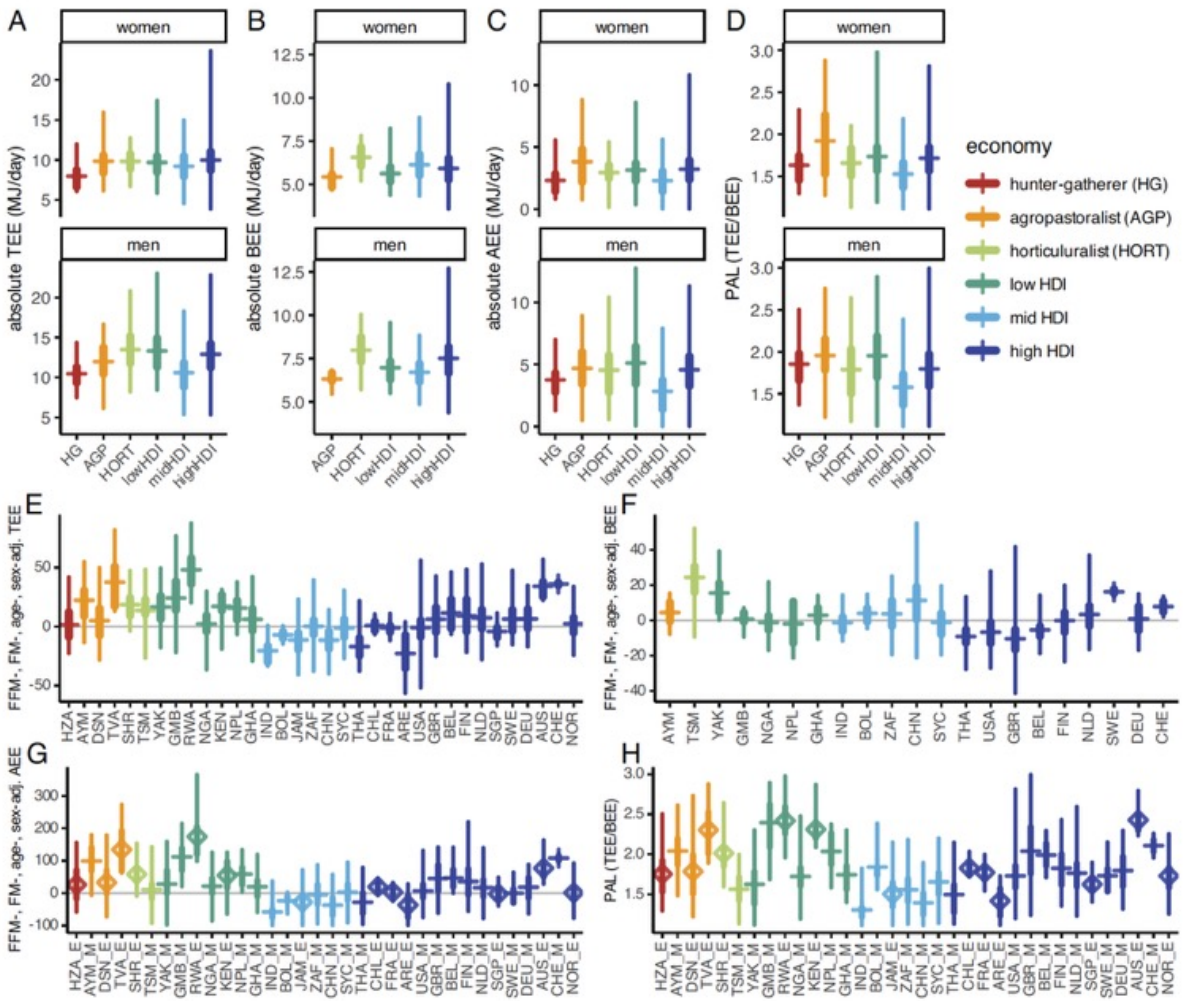

Fig. 2. Energy expenditure across economies. (*A–D*) TEE, BEE, and AEE increase with economic development. Bars indicate mean and quartiles. (*E–H*) Adjusted expenditures, calculated from residuals from multiple regression with FFM, FM, age, and sex varied considerably within and between populations. Size-adjusted TEE and BEE (residuals from regression with FFM, FM, sex, and age) decreased weakly with economic development. PAL and size-adjusted AEE were unrelated to economic development. Populations with measured basal expenditures are indicated with _M, estimated with _E.

HG move about
10 km/day

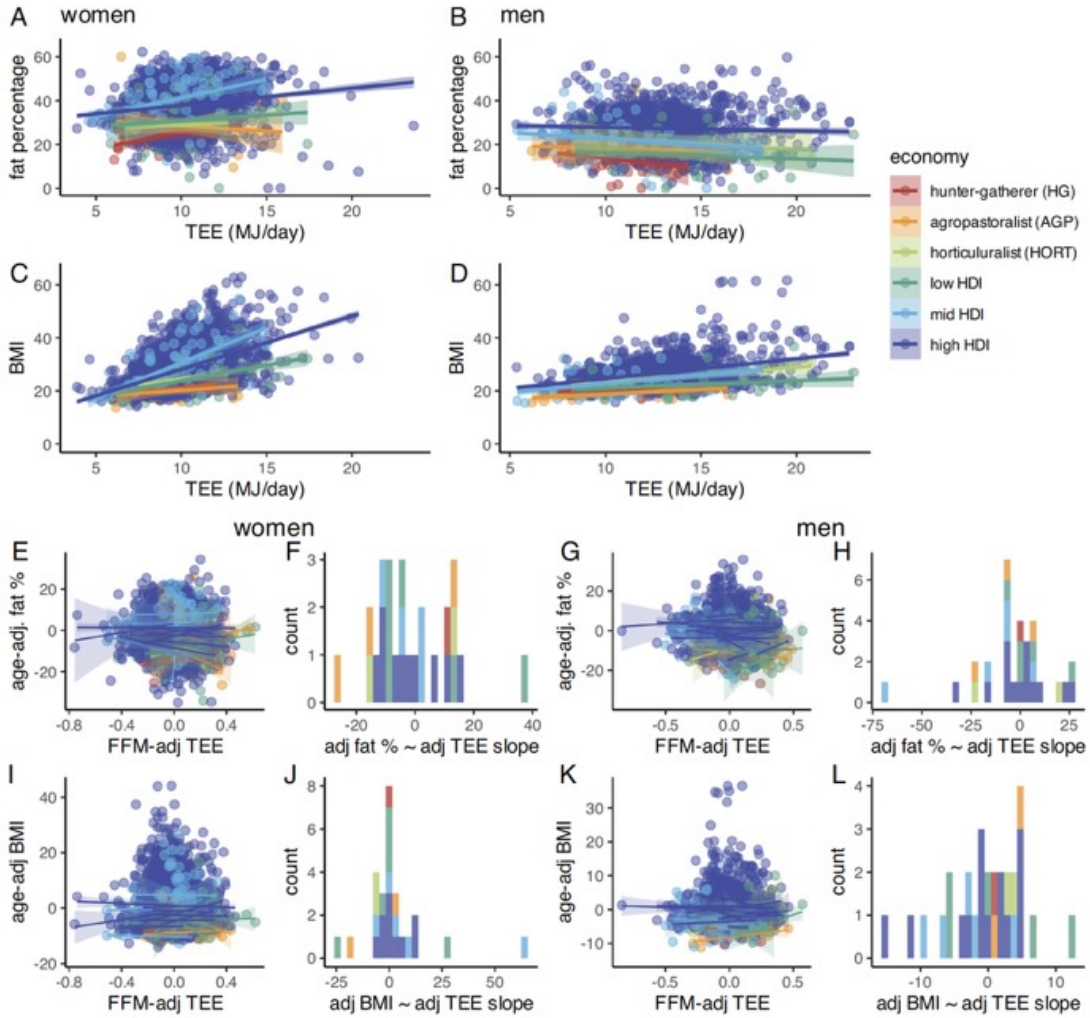

Fig. 3. The relationship between energy expenditure, adiposity, and BMI. The relationship between TEE and body fat percentage (*A* and *B*) and BMI (*C* and *D*) differed between women and men. The relationship between FFM-adjusted TEE and body fat percentage (*E*–*H*) and BMI (*I*–*L*) was weak, highly variable, and distributed about 0 among populations (*SI Appendix*, Tables S4 and S5).

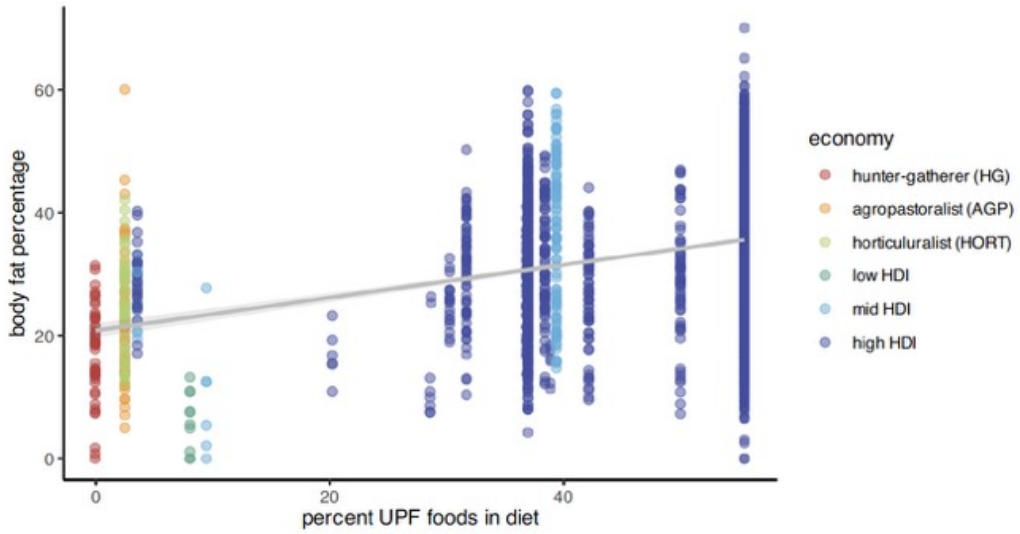

Fig. 4. UPF and adiposity. The percentage of daily calorie intake from UPF was positively associated with body fat percentage in bivariate analyses and in multiple regression including FFM-adjusted total expenditure, age, sex, and HDI rank (*SI Appendix*, Table S5).

Results here highlight the need to identify the factors that make foods in developed countries obesogenic. Not all impacts of economic development and the adoption of the modern food system have been negative. Current global networks of production and supply ensure that affordable foods and food components are available to almost every population on earth (38). Much of the additional energy provided by modern food systems appears to be channeled into healthy growth, as both adult stature and FFM are considerably greater among industrialized populations (Fig. 1 and *SI Appendix*, Tables S1 and S2). Indeed, in the present sample, the increase in BMI with economic development was largely attributable to greater FFM (*SI Appendix*, Table S2). Efforts to track and prevent obesity will be improved by utilizing measures of body fat rather than BMI, and by focusing on dietary intake rather than expenditure. Regulating food environments to maximize the benefits of increased calorie availability without promoting a nutrient-poor, obesogenic diet remains a crucial challenge in public health that will only become more acute as economic development continues globally.

Prisoner can be executed without turning off pacemaker, Tennessee high court rules

A lower court had ruled that Byron Black's implanted combination pacemaker-defibrillator could prolong his suffering by shocking his heart after lethal injection.

A death row prisoner in Tennessee can be executed despite having an implanted heart device that his lawyers say is likely to prolong his suffering, the state Supreme Court ruled Thursday in a first-of-its-kind legal battle.

A lower court had ruled that Byron Black could not be executed while his cardiac implantable electronic device — which acts as a pacemaker and a defibrillator — was on, because it could deliver painful shocks to his heart to try to revive him during a lethal injection. The Thursday ruling overturns that decision and allows Black's scheduled execution Tuesday to proceed.

Black, 68, suffers from several illnesses, including heart failure and dementia, underscoring the complexities of executing an aging death row population.

"This issue hasn't come up before, but it's likely to repeat in the future," said Kelley Henry, Black's federal public defender.